



HAL
open science

Conceptual design, simulation and experimental validation of divided wall column : application for non-reactive and reactive mixture

Trung Dung Nguyen

► **To cite this version:**

Trung Dung Nguyen. Conceptual design, simulation and experimental validation of divided wall column : application for non-reactive and reactive mixture. Chemical and Process Engineering. Institut National Polytechnique de Toulouse - INPT, 2015. English. NNT : 2015INPT0012 . tel-04230582

HAL Id: tel-04230582

<https://theses.hal.science/tel-04230582>

Submitted on 6 Oct 2023

HAL is a multi-disciplinary open access archive for the deposit and dissemination of scientific research documents, whether they are published or not. The documents may come from teaching and research institutions in France or abroad, or from public or private research centers.

L'archive ouverte pluridisciplinaire **HAL**, est destinée au dépôt et à la diffusion de documents scientifiques de niveau recherche, publiés ou non, émanant des établissements d'enseignement et de recherche français ou étrangers, des laboratoires publics ou privés.



Université
de Toulouse

THÈSE

En vue de l'obtention du

DOCTORAT DE L'UNIVERSITÉ DE TOULOUSE

Délivré par :

Institut National Polytechnique de Toulouse (INP Toulouse)

Discipline ou spécialité :

Génie des Procédés et de l'Environnement

Présentée et soutenue par :

M. TRUNG DUNG NGUYEN

le mercredi 14 janvier 2015

Titre :

CONCEPTUAL DESIGN, SIMULATION AND EXPERIMENTAL
VALIDATION OF DIVIDED WALL COLUMN: APPLICATION FOR NON-
REACTIVE AND REACTIVE MIXTURE

Ecole doctorale :

Mécanique, Energétique, Génie civil, Procédés (MEGeP)

Unité de recherche :

Laboratoire de Génie Chimique (L.G.C.)

Directeur(s) de Thèse :

M. MICHEL MEYER

MME XUAN MI MEYER

Rapporteurs :

M. JEAN-MICHEL RENEAUME, UNIVERSITE DE PAU ET DES PAYS DE L ADOUR

M. LIONEL ESTEL, INSA ROUEN

Membre(s) du jury :

M. VINCENT GERBAUD, INP TOULOUSE, Président

M. DAVID ROUZINEAU, INP TOULOUSE, Membre

M. MATHIAS BREHELIN, SOLVAY LYON, Membre

Mme XUAN MI MEYER, INP TOULOUSE, Membre

M. MICHEL MEYER, INP TOULOUSE, Membre

M. OLIVIER BAUDOIN, PROSIM SA, Membre

“I dedicated to the enduring memory of my father and to my beloved mother.

*I dedicate to my loving family, my wife NHU Thi Thu Hang, my daughter NGUYEN Ha An,
and my son NGUYEN Duc Trung who have supported me throughout the process”.*

Acknowledgements

I would like to express my sincere gratitude to my supervisor Prof. Michel MEYER for his guidance during the course of this research. I am grateful for his encouragement and giving me an opportunity to use all the facilities available in the department for my research work.

I wish to express my sincere appreciation to Dr. David ROUZINEAU for his suggestions and practical experience during my research.

I am thankful to all the staff members of the department, laboratory, and secretaries for providing a friendly and stimulating environment.

I am very grateful to the Vietnam ministry of education for the financial support during the course of this Ph.D. study.

I would like to express my thanks to all my friends.

I would also like to express my gratitude to my mother for her enormous love, support and sacrifice.

Last but not least, I special thank to my wife and children for their love, understanding during my study.

ABSTRACT

Divided wall column and reactive distillation have many advantages. If a divided wall column and a reactive distillation are integrated, they lead to a higher integrated process is a reactive divided wall column. However reactive divided wall column has still a new research area. First of all, the thesis proposed a procedure for design of divided wall column, which based on the FUGK model. Both technological and hydrodynamic aspects in the divided wall column are considered in the procedure. Design parameters are then provided to the rigorous simulation and optimization in the ProSim^{plus} software. In order to test this procedure, both ideal and non-ideal ternary mixtures are chosen to be separated in a divided wall column. The results show that the procedure can determine parameters quickly in the case studies and can give a good initialization for rigorous simulation. Secondly, a pilot plant has been design, built and operated in our laboratory (LGC, Toulouse, France, 2013). The pilot plant will provide necessary experimental evidence to validate the previous procedure. Ternary mixture and four-component mixture of alcohols have been used in our pilot plant in steady state conditions. The results show that the composition of products, composition and temperature profile along the column are in very good agreement with simulation results. Finally, a conceptual design method for reactive divided wall column is presented. The pre-design method of R. They et al., (2005) and a modified shortcut method for reactive divided wall column that is based on the classical shortcut adapted to a non-reactive divided wall column by C. Triantafyllou and R. Smith (1992) are applied. To verify, simulation and experiment are considered. The methodology has been illustrated for the synthesis of Methyl Acetate from Methanol and Acetic Acid.

Key words: Design, Simulation, Experiment, Divided wall column, Reactive divided wall column

RESUME

Les colonnes à cloison et la distillation réactive présentent de nombreux avantages. Si ces deux concepts sont couplés, cela conduit à un procédé intensifié appelé : colonne à cloison réactive. Ce nouveau procédé intensifié constitue le principal objet d'étude de cette thèse. Dans une première partie, une procédure de design d'une colonne à cloison basée sur le modèle FUGK a été proposée. Dans cette procédure les aspects technologiques et hydrodynamiques sont abordés. Ces paramètres de design obtenus sont ensuite utilisés pour réaliser une simulation rigoureuse et une optimisation de cette colonne en utilisant le logiciel ProSim. Afin de tester cette procédure, des mélanges idéaux et non idéaux ont été utilisés. Il a été montré que cette procédure de design aboutit rapidement aux paramètres de pré design qui permettent d'initialiser de manière satisfaisante la simulation rigoureuse. Dans un second temps, un pilote d'une hauteur de 4m a été conçu, monté et testé au laboratoire. Des résultats expérimentaux ont été obtenus qui valident la procédure sur des mélanges non réactifs en termes de profils de composition et de température ainsi que sur les compositions et les débits de sortie du procédé. Enfin, dans une dernière partie, cette procédure a été adaptée à des mélanges réactifs en combinant les approches de R. They et al (2005) et celle de Triantafyllou et al (1992). Ces ultimes développements ont été testés sur la production d'acétate de méthyl par estérification du méthanol par l'acide acétique à la fois d'un de vue expérimental et théorique.

Mots-Clés: colonne à paroi, économe d'énergie, intensification, conception et simulation

TABLE OF CONTENTS

ABSTRACT

CHAPTER 1

INTRODUCTION 1

1.1 PROCESS INTENSIFICATION 2

1.2 MOTIVATION AND AIM OF THE WORK 4

1.3 OUTLINE OF THE THESIS 5

1.4 PUBLICATION LIST 5

CHAPTER 2

LITERATURE REVIEW 6

2.1 DIVIDED WALL COLUMN FUNDAMENTALS 7

2.1.1 Concept of divided wall columns 10

2.1.2 Advantages and disadvantages of divided wall columns 11

2.1.3 Divided wall column configurations 13

2.1.4 Divided wall column design parameters 14

2.1.5 Control of divided wall columns 15

2.1.6 Simulation of divided wall columns 19

2.1.7 Divided wall column applications 20

2.2 CONCEPTUAL DESIGN OF A DIVIDED WALL COLUMN: REVIEW 23

2.3 CONCEPTUAL DESIGN OF A REACTIVE DIVIDED WALL COLUMN: 28

REVIEW

2.4 CONCLUSION OF CHAPTER 2 34

CHAPTER 3

DESIGN METHODOLOGY OF DIVIDED WALL COLUMN 35

3.1 A PROCEDURE FOR DESIGN OF DIVIDED WALL COLUMNS 36

3.1.1 Assumptions and model design 36

3.1.2 Material balance for divided wall columns 39

3.1.3	Minimum vapor flowrate of divided wall columns	40
3.1.4	Technological and hydrodynamic aspects	44
3.2	SIMULATION WITH PROSIM ^{PLUS} SOFTWARE	49
3.2.1	The model used for simulation	49
3.2.2	Initial parameters for simulation	50
3.3	CASE STUDIES	52
3.3.1	Separation of a ternary mixture	52
3.3.2	Separation of a mixture with more than three components	55
3.3.3	Conclusion	57
3.4	SENSIBILITY ANALYSIS OF DIVIDED WALL COLUMN	58
3.4.1	Effect of the vertical position and height of the wall	58
3.4.2	Effect of the number of stages	59
3.4.3	Effect of the feed composition and ESI of the mixture on the design of divided wall columns	60
3.4.4	Energy usage comparison between traditional columns and divided wall columns	62
3.5	CONCLUSION	67
 CHAPTER 4		
PILOT PLANT AND EXPERIMENTAL VERIFICATION: APPLICATION FOR NON-REACTIVE MIXTURE		
4.1	INTRODUCTION	68
4.2	PILOT PLANT	69
4.2.1	Setup	73
4.2.2	Measurement and startup of the pilot plant	75
4.2.3	HETP experiment	76
4.2.4	Component systems	77

4.3 EXPERIMENTAL RESULTS	77
4.3.1 Separation of ternary mixture: methanol/1-propanol/1-butanol	77
4.3.2 Separation of four - component mixture: methanol/iso propanol/1-propanol/1-butanol	82
4.4 COMPARISON BETWEEN EXPERIMENTAL DATA AND SIMULATED RESULTS	85
4.4.1 Ternary mixture	87
4.4.2 Four-component mixture	92
4.5 CONCLUSION OF CHAPTER 4	94
CHAPTER 5	
DESIGN OF REACTIVE DIVIDED WALL COLUMN	95
5.1 INTRODUCTION	96
5.2 PROCEDURE FOR DESIGN OF REACTIVE DIVIDED WALL COLUMNS	97
5.2.1 Model and assumptions for a reactive divided wall column	97
5.2.2 Classification of feed composition region by predesign method	100
5.2.3 Modified shortcut design method for reactive divided wall column	101
5.2.4 Simulation	104
5.3 CASE STUDY FOR METHYL ACETATE SYNTHESIS	105
5.4.1 Introduction	105
5.4.2 Kinetic and equilibrium equations and thermodynamic model	106
5.4.3 Design Procedure	106
5.4.4 Conclusion	115
5.5 EXPERIMENTAL VERIFICATION FOR A REACTIVE MIXTURE IN A DIVIDED WALL COLUMN	116
5.5.1 Introduction	116
5.5.2 Experiment results	117

5.6 CONCLUSION OF THE CHAPTER 5	120
CHAPTER 6	
GENERAL CONCLUTIONS AND FUTURE WORK	121
6.1 THE MAIN CONTRIBUTIONS OF THE THESIS	122
6.2 PERSPECTIVES	124
APPENDIX	126
Appendix 1	127
Appendix 2	128
Appendix 3	130
Appendix 4	131
Appendix 5	143
Appendix 6	144
Appendix 7	145
Appendix 8	149
NOMENCLATURE	150
REFERENCES	153

LIST OF FIGURES

FIGURE 2.1 Conventional arrangements for separating three component mixtures

FIGURE 2.2 Fully thermally coupled distillation column (Petlyuk column)

FIGURE 2.3 Heat integrate distillation column (HIDiC)

FIGURE 2.4 Divided wall column

FIGURE 2.5 Separation for ternary mixture in the divided wall column

FIGURE 2.6 Energy is lost separating the middle component B in the conventional arrangement

FIGURE 2.7 Basic types of divided wall column: (a) Divided wall column middle, (b) Divided wall column lower, (c) Divided wall column upper

FIGURE 2.8 Different position of dividing wall

FIGURE 2.9 Different sharp of dividing wall

FIGURE 2.10 Divided wall column for separation of four-component mixture
(a) Kaibel column and (b) column with multiple partition walls

FIGURE 2.11 DWC design parameters

FIGURE 2.12 Controller in the Petlyuk column (E.A.Wolff and Skogestad (1995))

FIGURE 2.13 PI controller for a divided wall column (Till Adrian et al., (2004))

FIGURE 2.14 Control structures of divided wall column (Buck et al., (2011))

FIGURE 2.15 Schematic and photograph of the two vapor split valves (Dwivedi D et al., (2012))

FIGURE 2.16 Pump around model of divided wall column

FIGURE 2.17 Two columns sequence model (prefractionator or side column)

FIGURE 2.18 Four columns sequence model

FIGURE 2.19 Decomposition into simple column sequences (grey area: reactive zone) (Mueller, I et al. (2007))

FIGURE 3.1 (a) Divided wall Column; (b) Thermally coupled distillation

FIGURE 3.2 Simplified model design of divided wall column

FIGURE 3.3 The detailed structure and operating variables of divided wall column

FIGURE 3.4 Types and positions of dividing wall in the DWC system

FIGURE 3.5 A procedure for design of divided wall column

FIGURE 3.6 The model for simulation DWC system by ProSim^{plus} software

FIGURE 3.7 Initial parameters need for simulation by ProSim^{plus}

FIGURE 3.8 Design parameters for the divided wall column

FIGURE 3.9 Design parameters for the divided wall column

FIGURE 3.10 Specify variables for four-composition mixture in divided wall column

FIGURE 3.11 Design parameters for the divided wall column

FIGURE 3.12 Temperature and composition profiles in the divided wall column

FIGURE 3.15 Effect of the height and vertical position of the wall on the heat duty of reboiler

FIGURE 3.16 Effect of number of stages on heat duty of reboiler

FIGURE 3.17 Heat duty depend on the feed composition and ESI index of the mixture

FIGURE 3.18 1000TAC depend on the feed composition and ESI index of the mixture

FIGURE 3.19 Energy duty comparison of the mixture M1 (ESI = 1)

FIGURE 3.20 Energy duty comparison of the mixture M2 (ESI > 1)

FIGURE 3.21 Energy duty comparison of the mixture M3 (ESI < 1)

FIGURE 3.32 Comparison energy of use and boundary of distillation

FIGURE 4.1 Flow-sheet of the pilot plant

FIGURE 4.2 Liquid splitter

FIGURE 4.3 Structure parameters of pilot plant

FIGURE 4.4 Experimental temperature profiles for case 1, case 2, case 3, and case 4

FIGURE 4.5 Composition profiles of experimental runs

FIGURE 4.6 Experimental temperature and composition profiles for case 5 and case 6

FIGURE 4.7 Step-to-step to adjust variables for simulation process

FIGURE 4.8 Temperature and composition profile of experimental data and simulation results for case studies

FIGURE 4.9 Difference temperature between the prefractionator and the main column depended on the feed composition

FIGURE 4.10 Vapor split (R_V) depends on the liquid split (R_L)

FIGURE 4.11 Temperature and composition profile compare between the experimental data and simulation of case 5 and case 6

FIGURE 5.1 Processes integration of reactive distillation and divided wall column

FIGURE 5.2 Restriction of the model for reactive divided wall column

LIST OF TABLES

TABLE 1.1 Process intensification technologies in the petrochemical industry (Harmsen, 2010)

TABLE 2.1 Industrial applications of DWCs for ternary systems (Yildirim et al., 2011)

TABLE 2.2 Industrial applications of divided wall column for multicomponent mixtures

TABLE 2.3 Summary of several shortcut methods for design divided wall column

TABLE 2.4 Works published for reactive divided wall column

TABLE 3.1 Twelve unknown variables for ternary mixture separation

TABLE 3.2 Relationship between feed quality and internal flowrates

TABLE 3.3 Relative errors between specify product purity and simulation of key component

TABLE 3.4 Relative errors between specify product purity and simulation of key component

TABLE 3.5 Relative errors between specify product purity and simulation of key component

TABLE 3.6 Three ternary mixtures

TABLE 3.7 Three different feed compositions

TABLE 3.8 Energy consumption and TAC of the divided wall column

TABLE 3.9 Four different feed compositions

TABLE 3.10 Energy duties of the arrangements

TABLE 3.11 Comparing the results with guess of the Kiss et al., (2012)

TABLE 4.1 Overview of various DWC or RDWC pilot plants

TABLE 4.2 Operating parameters and results for experimental steady-state runs

TABLE 4.3 Operating parameters and results for experimental steady-state runs

TABLE 4.4 Least square error and relative error of key component

TABLE 4.5 Detail comparisons between experimental data and simulated result of case 1

TABLE 4.6 Least square error and relative error of key component

TABLE 5.1 Ranking of azeotropes temperature and pure component normal boiling point temperature

TABLE 5.2 Classification of feed composition for direct separation

TABLE 5.3 Relative errors between simulation and specification of key component (Case 1)

TABLE 5.4 Corrected the composition of the distillate product

TABLE 5.5 Relative errors between simulation and specification of key component (case 2)

TABLE 5.6 Mass balance of total and each component

TABLE 5.7 Experimental results at steady-state run compare with simulation result

Chapter 1
INTRODUCTION

1.1 PROCESS INTENSIFICATION

Nowadays, because of environmental problems and the energy crisis, both industrial and academic research efforts aim to develop process design methodologies for reducing the energy usage, waste and impact of chemical processes on the environment. If only considering process-related energy for the manufacture of products from feed stocks, the total global energy consumption of the chemical and petrochemical industry is estimated at 15 E_jyr⁻¹ and the world total GHG emissions attributed to chemical and petrochemical processes amounts to 1.24 GtCO₂-eq annually (IEA, 2013).

Process integration is a method to process design and operation that emphasizes the unity of the process. From an Expert Meeting in Berlin, October 1993, the IEA (International Energy Agency) definition of process integration is:

“Systematic and general methods for designing integrated production systems, ranging from individual processes to total sites, with special emphasis on the efficient use of energy and reducing environmental effects”.

One of the most significant examples of process integration is process intensification. It is a process in which multiple phenomena such as reaction, separation and heat transfer are integrated in one single equipment. This process is attracting more and more attention. The first definition of process intensification is offered by Cross and Ramshaw (1986):

“Process intensification is a term used to describe the strategy of reducing the size of chemical plant needed to achieve a given production objective”.

In 2000, Andrzej I. Stankiewicz and Jacob A. Moulijn proposed a more particular definition:

“Any chemical engineering development that leads to a substantially smaller, cleaner and more energy efficient technology is process intensification”.

The objectives in this definition are smaller, cleaner, and more energy efficient technology. According to David Reay, Colin Ramshaw and Adam Harvey (2013), they added a new objective, “safer”, to the definition:

“Any chemical engineering development that leads to a substantially smaller, cleaner, and safer and more energy efficient technology is process intensification”.

The main advantages of process intensification are:

- Cheaper processes;
- Smaller equipment and plant;
- Safer processes;
- Reduced energy consumption;
- Shorter time to the market;
- Less waste or by product;
- Better company image.

Process intensification includes **(1) process – intensifying equipment** such as novel reactors, and intensive mixing, heat transfer and mass transfer devices and **(2) process – intensifying methods** such as new or hybrid separations and multifunctional reactors.

Nowadays, process intensification technology has potential to development the chemical industry and is one of the most significant trends in chemical engineering. Both divided wall columns and reactive distillation are excellent examples of process intensification methods. They are both improvements of traditional distillation units but at the same time they correspond to two different ways of integration: Divided wall columns are a combination of two separations while reactive distillation is combined reaction and separation in a single unit (Mueller and Kenig, 2007). In the petrol-chemical industry, process intensification technology has been applied more than 150 times with reactive distillation and more than 100 times with divided wall columns (Harmsen, 2010) as shown in Table 1.1.

TABLE 1.1 Process intensification technologies in the petrochemical industry (Harmsen, 2010)

Technologies	Capital cost reduction	Energy reduction	Commercial implementation
Reactive distillation	20 – 80%	20 – 80%	> 150
Divided wall column	10 – 30%	10 – 30%	> 100

1.2 MOTIVATION AND AIM OF THE WORK

The concept of divided wall columns has been known for a long time as having a large potential for savings in both energy and investment costs proven by process applications and academic studies. The concept of reactive distillation has also been applied with many advantages such as overcoming of chemical equilibrium limitations, achievement of higher selectivity and use of reaction heat in separation process, (Kai Sundmacher and Achim Kienle, 2002).

The integration of divided wall columns and reactive distillation leads to a better integrated process is a reactive divided wall column. It is noted that reactive divided wall columns is still a new research area (Guido Daniel, 2006). Therefore:

“The motivation of this study will focus on the conceptual design, simulation, and experiment for reactive divided wall column”.

In order to achieve this objective, in the study, we focus on:

- For the divided wall column, a large number of publications have been written on this equipment, Z. Olujić et al (2009), I. Dejanović et al (2010), and Omer Yildirim et al (2011). However, a comprehensive review covering all aspects of optimal design, analysis, simulation, and experimental data of divided wall column is still missing. Moreover, we need to develop a simulation model for divided wall columns carried out in ProSim^{plus} software. Therefore, firstly, an approach to optimal design, simulation model in ProSim^{plus} software, and experimental runs with non-reactive mixtures are considered.
- For reactive distillation, a methodology to design the reactive distillation column developed by They et al (2007) will be applied.
- Based on the shortcut method to design divided wall columns and the method of design for reactive distillation developed by They et al (2007), a proposed method to design reactive divided wall column is proposed. After that, experimental runs for reactive mixtures are verified.

1.3 OUTLINE OF THE THESIS

The thesis is divided into 6 chapters: Chapter 1 gives the introduction, motivation and aim of this work, and outline of the thesis. Chapter 2 is a literature review concerning publications on divided wall columns and reactive divided wall columns. Chapter 3 focuses on the development of a procedure for optimal design of divided wall columns. Then, the shortcut results will be introduced into ProSim^{plus} to carry out simulations. The analysis of divided wall column performance is also considered. Chapter 4 shows the pilot plant for the divided wall column in our laboratory in which the structure of pilot plant and experimental results are presented. Non-reactive mixtures were tested in the pilot plant. The focus of Chapter 5 is the design of a reactive divided wall column. Then, an experimental run for reactive mixtures was carried out in reactive divided wall column.

1.4 PUBLICATION LIST

NGUYEN Trung-Dung, David ROUZINEAU, Michel MEYER, and Xuan MEYER. (2013). A new procedure for design of divided wall column, *ECCE9/ECAB2*, April 21-25, The Hague, The Netherlands.

NGUYEN Trung-Dung, David ROUZINEAU, Michel MEYER, and Xuan MEYER. (2013). A new Procedure for optimal design of divided wall column, *SFGP 2013*, 8 – 10 Octobre, Lyon, France.

NGUYEN Trung-Dung, David ROUZINEAU, Michel MEYER, and Xuan MEYER. (2014). Is divided wall column always better than traditional distillation column?, *GPE – 4th International Congress on Green Process Engineering*, 7 – 10 April, Sevilla, Spain.

NGUYEN Trung-Dung, David ROUZINEAU, Michel MEYER, and Xuan MEYER. (2014). Conceptual design, simulation, and experiment for a reactive divided wall column, *10th International conference on Distillation and Absorption*, 14 – 17 September, Friedrichshafen, Germany.

Chapter 2

LITERATURE REVIEW

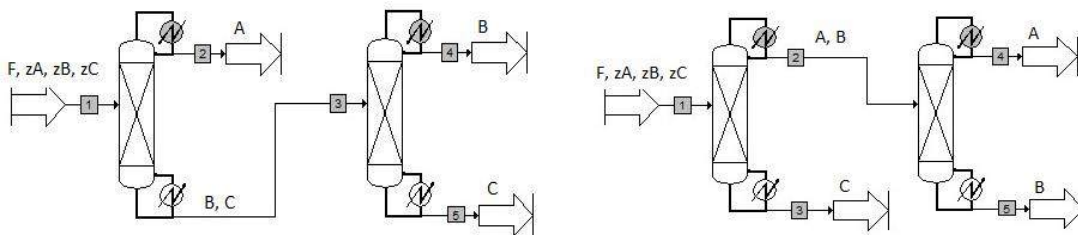
2.1 DIVIDED WALL COLUMN FUNDAMENTALS

The chemical and petrochemical sectors are the largest industrial energy users, accounting for roughly 10% of total worldwide energy demand and 7% of global GHG emissions. In the chemical process industry, approximately 40% of total energy is used by distillation processes (Dejanovic, 2011). In the distillation technique, heat is used as a separating agent. Heat is supplied to the bottom reboiler to evaporate a liquid mixture at high temperature and is lost at low temperature when liquefying in the condenser at the top of the distillation column. Therefore it is highly inefficient in the use of energy.

With the beginning of the oil crises of the 1970s and 1980s, the energy costs became the major factor in column costs and created an urgency to find ways to reduce the energy requirements of distillation. Therefore, a primary target in new distillation process designs is how to reduce the energy demand of distillation systems. Various methods can be used to make the distillation process more energy efficient and more sustainable such as thermally coupled distillation columns (Petlyuk column), heat integrated distillation columns (HIDic), and divided wall columns (DWC).

To separate a multicomponent mixture, one often uses a sequence of distillation columns. We consider separation of a ternary mixture A, B, and C, for instance, Figure 2.1 shows the typical arrangements (direct, indirect and sloppy sequence) that use at least two columns, two reboilers and two condensers to produce three pure products.

The three components of the mixture are A, B and C, in which A is the light boiling component, B is the middle boiling component and C is the heavy boiling component. In the direct configuration, figure 2.1 (a), the component A will be separated in the first column and B and C will be separated in the second column. In the indirect configuration, figure 2.1(b), the component C will be separated in the first column with A and B being separated in the second column. In the sloppy sequence, figure 2.1 (c), the component B is a distributed component. That means, in the first column, A and C will be separated and B is distributed. The second column separates the A and B components. The third column separates the B and C components.



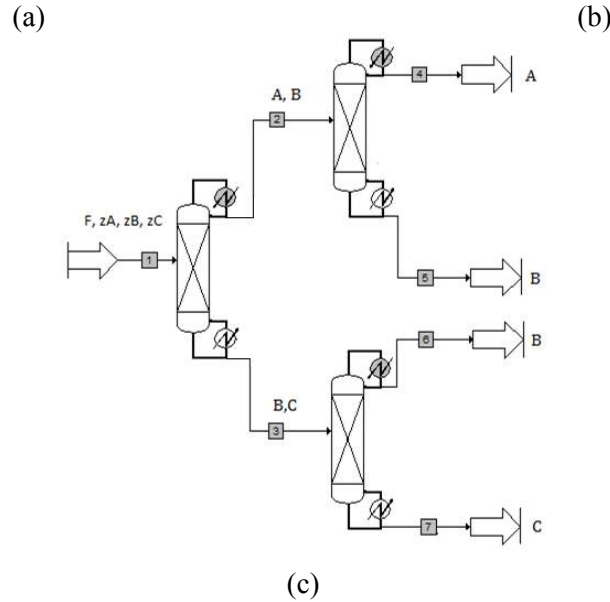


FIGURE 2.1 Conventional arrangements for separating three component mixtures
 ((a) Direct, (b) indirect and (c) sloppy sequences)

A thermally coupled distillation column was first patented by Brugma, 1942. For ternary mixture separations, there are three configurations: side rectifier, side stripper, and fully thermally coupled distillation. The fully thermally coupled distillation column is known as a Petlyuk column as shown in the figure 2.2. It consists of a prefractionator connected with a distillation column (main column). It requires only one reboiler and one condenser. However, it is difficult to operate and control.

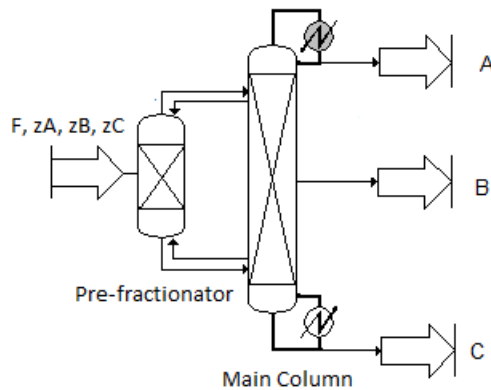


FIGURE 2.2 Fully thermally coupled distillation column (Petlyuk column)

The basic idea of the heat integration approach, where hot streams are heat exchanged with cold streams, was first introduced about 70 years ago. There are various heat integrated distillation processes that have been proposed. One of the important applications is heat

integrated distillation columns (HIDiC) in which a compressor is installed between the stripping section and the rectifying section. The stripping section of the column is operated at a relatively low pressure while the rectifying section of the column is operated at a relatively high pressure. The pressure difference implies a corresponding difference in operating temperature. Therefore, the heat can be transferred directly from the rectifying section to the stripping section.

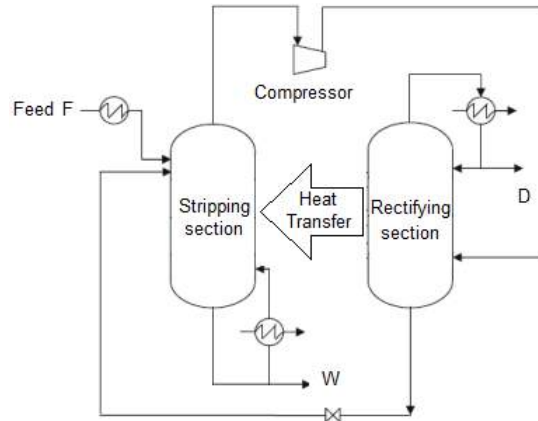


FIGURE 2.3 Heat integrate distillation column (HIDiC)

The HIDiC as shown in the figure 2.3 gives a substantial energy savings of around 30 – 50% in the separation of various mixtures when compared with a conventional column (Amiya K. Jana, 2010; B. Suphanit, 2010).

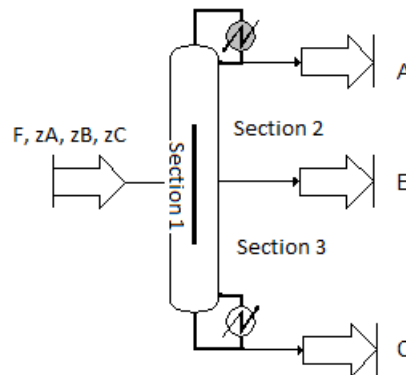


FIGURE 2.4 Divided wall column

In the figure 2.4, the divided wall column (DWC) was first presented in the Wright's patent in 1949. It can save both energy consumption and capital cost compared to conventional distillations. The energy consumption reduces about 20% to 30% compare to other

distillation configurations (C. Triantafyllou and R. Smith, 1992; Michael A. Schultz et al., 2002). It can also be used for the separation of multicomponent mixtures. Therefore, because of these reasons, nowadays, industrial and academic research gives more and more attention to divided wall columns.

2.1.1 Concept of divided wall columns

Divided wall columns integrate two (or more) different separation units into one single device with one (or more) vertical partitions in the central section. Dividing wall splits a single column into two parts: a pre-fractionator section and a main column. It uses only one reboiler and one condenser.

Figure 2.5 shows a divided wall column for separation of a ternary mixture. Considering separation of a ternary mixture A, B, and C, in which the component B is the distributed component. The feed is introduced into the prefractionator while distillate, side, and bottom products are removed from the main column. Component B is distributed between the top and bottom of the prefractionator section. The top of the prefractionator section contains mainly component A, a part of component B and a little component C. The bottom of the prefractionator section contains mainly component C, a part of component B and a little of component A. The upper part of the main column separates components A and B and the lower part of the main column separates components B and C.

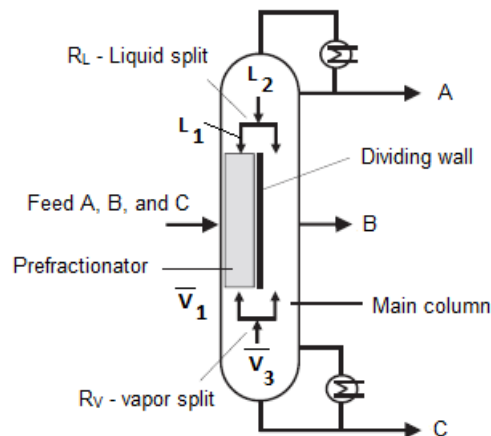


FIGURE 2.5 Separation for ternary mixture in the divided wall column

The liquid stream (L_2) from the condenser and vapor stream (\bar{V}_3) from the reboiler are split on the two sides of the dividing wall. The liquid split R_L is the ratio between the liquid stream

L_1 and liquid stream L_2 while the vapor split R_V is ratio between the vapor stream \bar{V}_1 and the vapor stream \bar{V}_3 .

2.1.2 Advantages and disadvantages of divided wall columns

Divided wall columns can save both energy demand and capital cost. In fact, depending on the type of applications, desired purities of products, and relative volatilities of component, energy and capital costs are often reduced by 20 to 50% compared to traditional configurations (Olga A. Flores, 2003; B. Kaibel, 2006; Massimiliano Errico, 2009; Barbel Kolbe, 2004; Agrawal, 1999). The DWC offers the following advantages:

(1) Lower capital investment

For separation of the ternary mixture shown in figure 2.1, the traditional sequences require at least two columns with two re-boilers and two condensers. However, the divided wall column needs only one column, one re-boiler and one condenser. Therefore, it leads to savings in investment cost.

(2) Reduced energy requirements

The conventional arrangement for separating a ternary mixture uses a direct sequence with two columns to obtain three pure products as shown in figure 2.6.

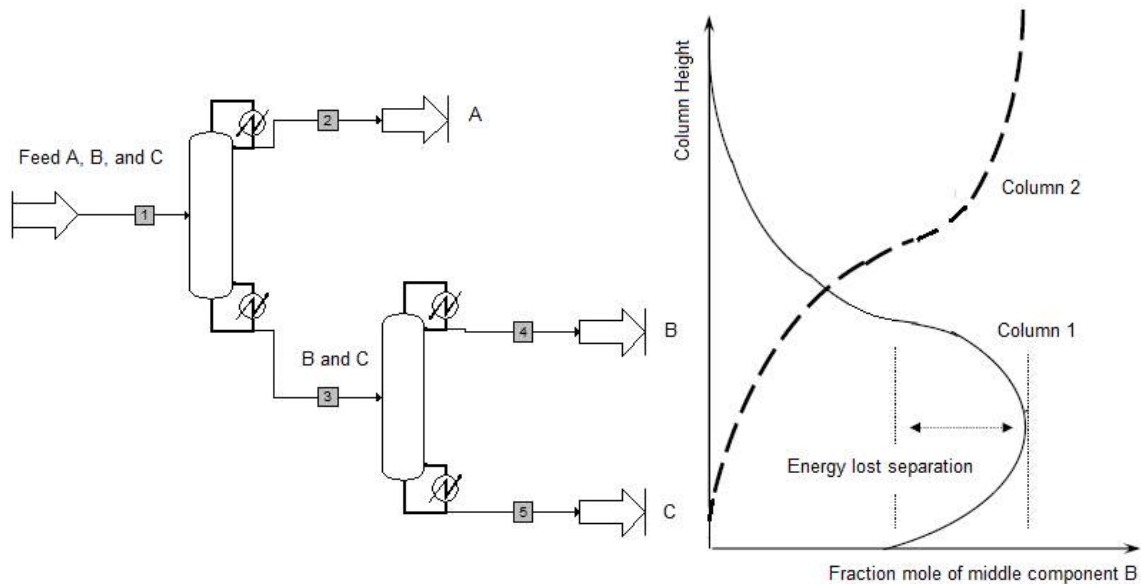


FIGURE 2.6 Energy is lost separating the middle component B in the conventional arrangement

In that case the composition of component B reaches a maximum in the middle of the first column and then decrease again but because it is remixed and diluted with the less volatile component C at the bottom of the first column. Similarly, with the first column in the indirect sequence, the composition of the middle component B reaches a maximum near the top of the first column and then decreases because of remixing and diluting with the more volatile component A at the top of the first column. Some energy is used to separate the component B to the maximum purity, but this energy is lost and for this reason the remixing effect leads to a thermal inefficiency.

Now we consider separating a ternary mixture in divided wall column. In the prefractionator, the component B is distributed between the top and bottom of the column. Therefore, the rectifying section of the prefractionator separates A and B from component C and the stripping section of the prefractionator separates B and C from component A. In this way, the remixing effects can be avoided.

(3) High purity for all products

Compared with a simple side-draw column, a higher purity of middle product can be achieved in the divided wall column. Therefore, when a high purity middle component is desired, a divided wall column should be considered.

(4) Less construction volume

For multicomponent mixture separations, a divided wall column has only one reboiler and one condenser to obtain pure products. Therefore, the system needs less construction volume than traditional sequences. Moreover it does not need pipes connecting the two columns.

Although a divided wall column may offer the potential for a savings in both capital and energy costs, the dividing wall columns have some main drawbacks. They are:

(1) Higher columns owing to the increased number of theoretical stages.

A divided wall column will be taller and have a larger diameter than either of the two conventional columns.

(2) Increased pressure drop due to the higher number of theoretical stages.

A divided wall column operates with one reboiler and one condenser. Therefore, the condenser operates at the lowest temperature while the reboiler operates at the highest temperature. However, compared to the direct or indirect sequences with two columns, the reboiler of first column and the condenser of second column operate at middle range temperatures.

(3) Only one operating pressure is available.

A divided wall column operates at only one operating pressure. In comparison, traditional sequences may operate with different operating pressures in the two columns.

2.1.3 Divided wall column configurations

For ternary mixture separation, divided wall columns can be classified into one of three types, based on the position of the dividing wall: middle divided wall column (DWC_M), lower divided wall column (DWC_L), and upper divided wall column (DWC_U) as shown in Fig. 2.7

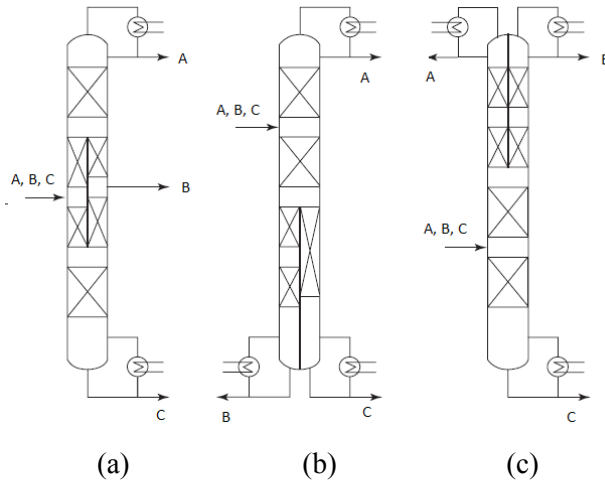


FIGURE 2.7 Basic types of divided wall column: (a) Divided wall column middle, (b) Divided wall column lower, (c) Divided wall column upper

Moreover, the dividing wall can use centered, off-centered or diagonal dividing walls, as shown in Figure 2.8 and Figure 2.9.

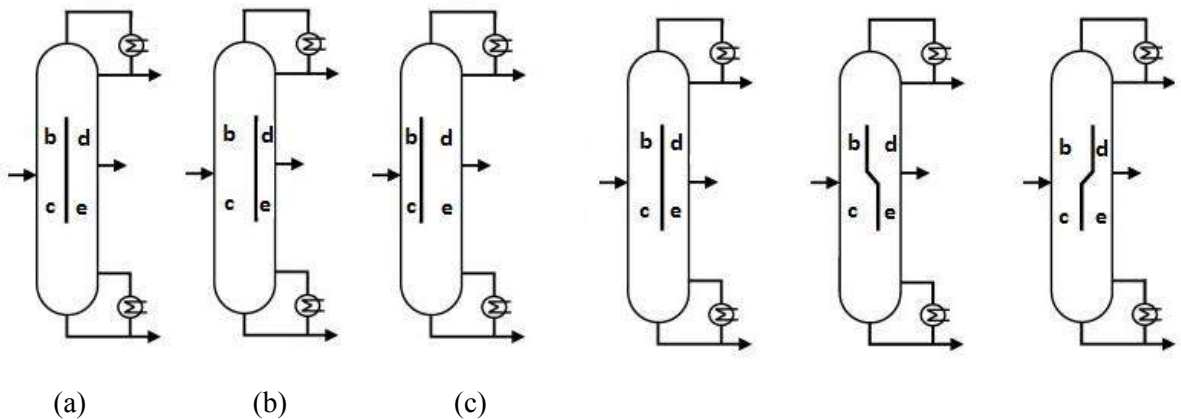


FIGURE 2.8 Different position of dividing wall FIGURE 2.9 Different shape of dividing wall

The dividing wall usually is placed in the middle as shown in the figure 2.8 (a), but off center positions of the dividing wall are also applied as the figure 2.8 (b) and (c) when the amount of the medium boiling component is small compared to the top and bottom products (Asprion, 2010).

For vapor feed and/or vapor side-draws a diagonal off center position of the dividing wall can be useful. In this case a more uniform distribution of the F factors, a measure of the maximum allowable vapor velocity for column, can be obtained in the partitioned sections of the column (Asprion, 2010).

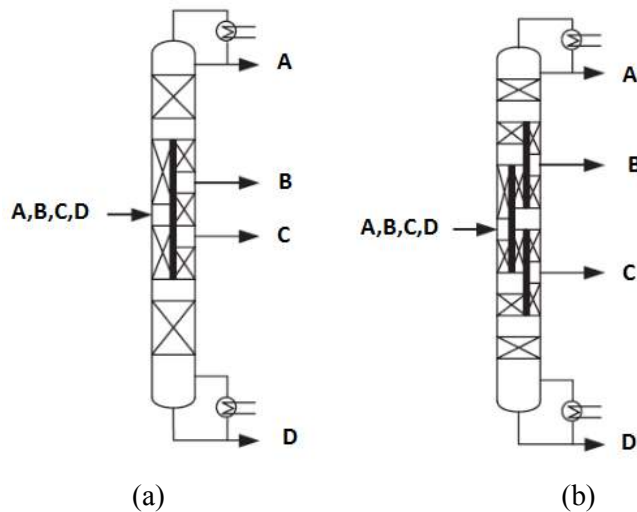


FIGURE 2.10 Divided wall column for separation of four-component mixture
 (a) Kaibel column and (b) column with multiple partition walls

Dividing wall columns could be used for the separation of mixture that has more than three components. The number of configurations of the DWC systems has increased corresponding to an increased number of components. To separate a four component mixture, dividing wall columns could be applied as shown in Figure 2.10.

2.1.4 Divided wall column design parameters

The divided wall column has more design variables than a conventional distillation column. Figure 2.11 shows that there are ten design parameters, namely: reboiler duty (Q_b), reflux ratio (R), number of theoretical stages ($N_1 \div N_6$), liquid split (R_L), and vapor split (R_V).

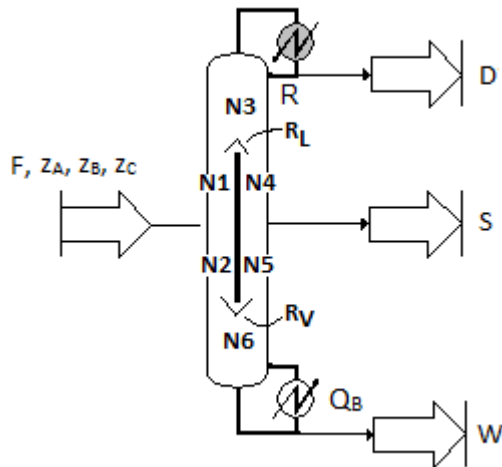


FIGURE 2.11 DWC design parameters

Design Parameters

N1 - N6 - Number of stages of each section

R_L – Liquid split

R_V – Vapor split

R – Reflux ratio

Q_B – Energy consumption

Specification

F – Feed flow rate

z_A, z_B, z_C – Feed composition

D – Top product

S – Side product

W – Bottom product

The liquid and vapor splits are defined as the ratio of the streams going to the prefractionator to the amount coming to the joint. At the top of the dividing wall, the flow of liquid is split (R_L). At the bottom of the dividing wall, the flow of vapor is split (R_V).

Thus, compared to a conventional distillation column, the design of divided wall columns is more difficult because of the larger amount of designed variables.

2.1.5 Control of divided wall columns

To separate a ternary mixture, the divided wall column offers significant savings in both energy and capital costs. More than 100 divided wall columns have been built globally by BASF. This section will give some relevant studies in which control and simulation aspects are presented.

In principle, Figure 2.11 shows the theoretically possible manipulated variables. They are the distillate stream (D), the reflux flow rate (R), the side stream (S), the bottom product stream (W), the feed stream (F), heat duty of the reboiler (Q_B), the liquid split (R_L), and the vapor split (R_V).

The simplest control structure is an extension of the control of a regular distillation column with a side stream (E. A. Wolff and Skogestad (1995)). Consider a ternary mixture A, B, and C carried out in the divided wall column. The distillate product purity ($x_{D,A}$) is controlled by manipulating the reflux flow rate (L_2), the side stream purity ($x_{S,B}$) is controlled by manipulating the side stream flow rate (S) and the bottom product purity ($x_{W,C}$) is

controlled by manipulating the vapor boilup(v). In this case R_L and R_V are fixed and the outputs and inputs are:

$$y = \begin{pmatrix} x_{D,A} \\ x_{S,B} \\ x_{W,C} \end{pmatrix} \quad u = \begin{pmatrix} L_2 \\ S \\ v \end{pmatrix}$$

The mixture of ethanol/propanol/butanol is studied. By using linear tools, they concluded that the system is easy to control. However, if the desired purity of the product is higher, the system is difficult to control. To solve this problem, the reflux stream (L_2), side stream (S), and boilup (v), the liquid split (R_L) can be added to the set of manipulated variables to control the purity of the side stream but both linear and nonlinear tools predicted difficult control. M. Serra et al., (1999, 2000, and 2001) studied a hypothetical system with constant relative volatilities. Different controllability indices were used to select the pairing in a three-point control structure. The results show that the control structure of E. A.Wolff and Skogestad (1995) is the best structure.

Halvorsen and Skogestad (1997, 1999) proposed two important tasks that should be achieved by the prefractionator: Keep the heaviest component from going out to the top of the prefractionator and keep the lightest component going out to the bottom of the prefractionator. Therefore, in the control structure, the liquid split (R_L) is used to control the level of the heavy impurity in the top of the prefractionator as shown in Figure 2.12.

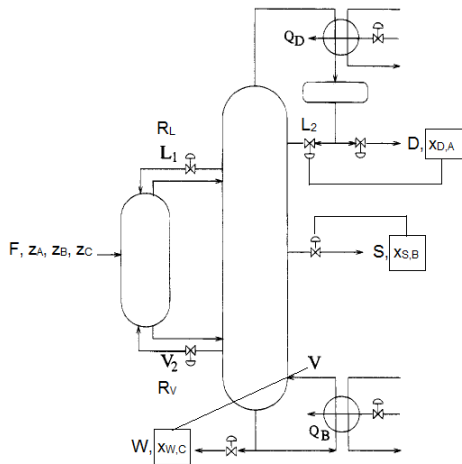


FIGURE 2.12 Controller in the Petlyuk column (E.A.Wolff and Skogestad (1995))

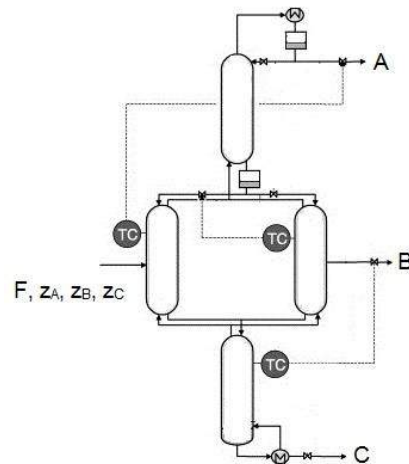


FIGURE 2.13 PI controller for a divided wall column (Till Adrian et al., (2004))

Till Adrian et al. (2004) reported experimental results of a butanol (15 wt. %), pentanol (70 wt. %), hexanol (15 wt. %) system in which temperature control was used instead of

concentration control. The column used for the study was built at the Ludwigshafen site of BASF Aktiengesellschaft. The total height of the divided wall column was 11.5 m with a column diameter of 40 mm for the two parallel middle part of the column, and 55 mm for the upper part and lower part of the column. The positions of the controlled temperatures included the top of the prefractionator to control the heavy boiling component C from passing the top of the prefractionator, a stage above the side product to correct separation of component A and B and the lower part of the column to control the light boiling component A passing the lower part of the column as shown in Figure 2.13. A predictive control model was used to control the three temperatures. In this case, the maximum deviations of the controlled temperatures lie in the range of 2°C – 3°C. Moreover, the time to reach steady state is 2h at maximum for the pilot plant.

Wang and Wong (2007) also used temperature control instead of composition control in the divided wall column. A ternary mixture including ethanol – 1 propanol – 1 butanol is considered. The temperature in the bottom of the prefractionator was controlled by manipulating reboiler heat input. The temperature in the upper part of main column was controlled by manipulating reflux flowrate and the temperature near the base of the column was controlled by manipulating the side stream flowrate. In this article, liquid split is not used as a manipulate variable.

Ling and Luyben (2009) proposed a method to control the impurity of the three products and one composition in the prefractionator. The reflux flowrate, side stream flowrate, vapor boil up, and liquid split were chosen to be manipulated. Dynamic simulations demonstrated improved performance. Ling and Luyben (2010) also used temperature control. In the study, the separation of ternary mixture benzene – toluene – o xylene is considered.

Kiss A.A and R.C. van Diggelen (2010) applied more advanced controllers such as Linear Quadratic Gaussian control, Generic Model control and higher order controllers based on a H_{∞} loop shaping design procedure and the μ synthesis procedure. The controllers were applied to a divided wall column in an industrial case study.

Buck et al. (2011) developed and test of a control system on a pilot plant. For the separation of the alcohols n-hexanol, n-octanol and n – decanol. It has a diameter of 68 mm and height of 11 m. In this study, the temperatures are also used as controlled variables instead of compositions to assure product purities because temperature measurement requires less effort and shorter time than online measurement of product purities. Three temperatures are controlled. One located at the top of the main column, one in the feed section, and one at the bottom of main column. The manipulated variables that are used to control these

temperatures are the distillate stream, the side stream, and the heat duty in the reboiler. In order to evaluate, compare and test the whole control system, the simulation and actual experiments are carried out in the pilot plant. The authors claimed that it is valuable to include the liquid split ratio above the dividing wall in the control system.

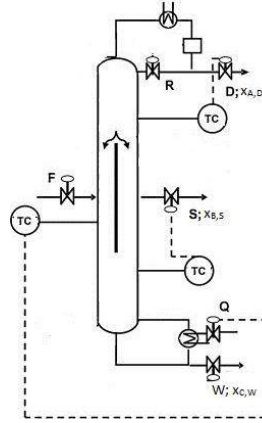


FIGURE 2.14 Control structures of divided wall column (Buck et al., (2011))

Deeptanshu Dwivedi et al. (2012) demonstrated experimentally that the vapor split can be used in practice for continuous operation as shown in Figure 2.15. The height of the column is 8 m and the inner diameter for the two parallel middle section is 50 mm while upper and lower parts are 70 mm diameter. To control the four-product Kaibel column, the four-point temperature control scheme is used. The temperature in the prefractionator can be controlled by using the vapor split while the liquid split is constant. In the main column, three temperatures are controlled by reflux ratio rate, upper side product stream, and lower side product stream. In this case, the liquid split is not used to control the system because it is available for optimizing an objective such as to reduce energy for a required purity specification. Experimental results show that the vapor split can be manipulated in feedback mode to achieve more energy efficient operation of the divided wall column.

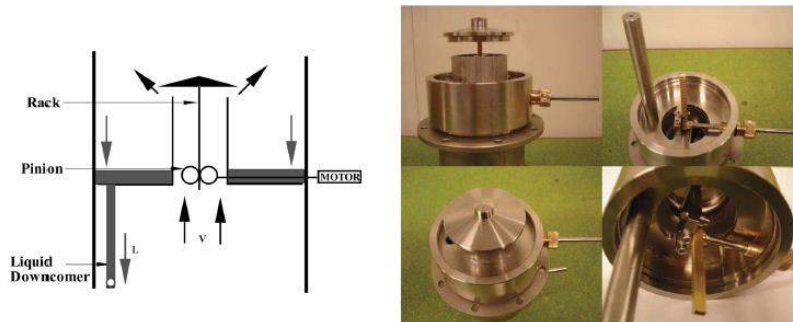


FIGURE 2.15 Schematic and photograph of the two vapor split valves (Dwivedi D et al., (2012))

2.1.6 Simulation of divided wall columns

Although the first application of a divided wall column was built in 1985 in Germany by BASF and have received more and more interest amongst academic and industrial researchers, it still cannot be established as a standard model in the commercial software packages such as Aspen^{plus}, Chemcad or ProSim^{plus}. Therefore, to arrange the divided wall column, there are four ways to simulate the system (Dejanovic et al., 2010). Firstly, for separation of a ternary mixture, divided wall columns can be represented as a single column in which various sections of divided wall column are situated in a vertical arrangement. Vapor and liquid flow within the model is regulated using liquid pumps around streams and vapor bypasses to imitate divided wall column. It is called the pump-around model as shown in Figure 2.16.

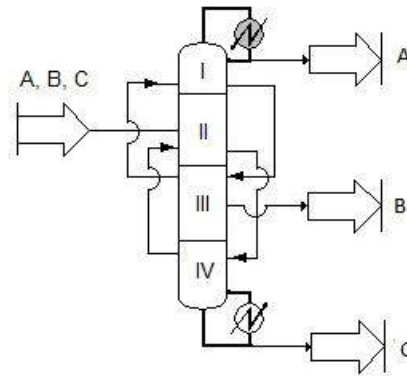


FIGURE 2.16 Pump around model of divided wall column

Secondly, in Figure 2.17, divided wall columns can be represented with a two-column sequence, known as the prefractionator (or side column) and the main column, which are thermodynamically equivalent to a divided wall column.

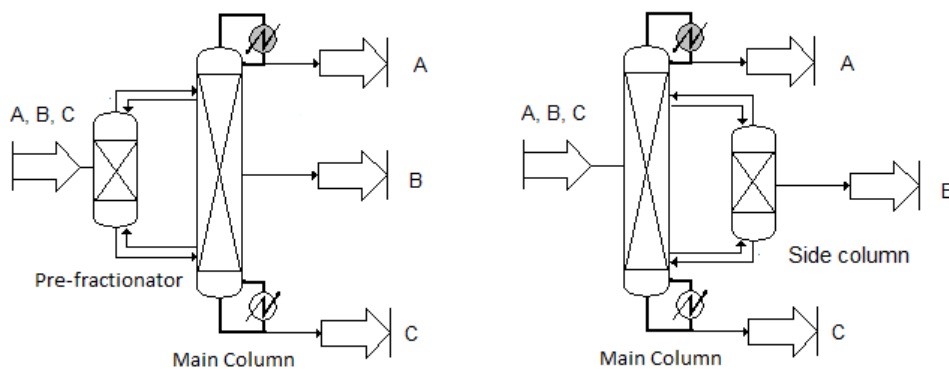


FIGURE 2.17 Two columns sequence model (prefractionator or side column)

This method is easier to set-up and offers a bit more flexibility than the pump around model. Therefore it is usually the preferred choice for design and optimization.

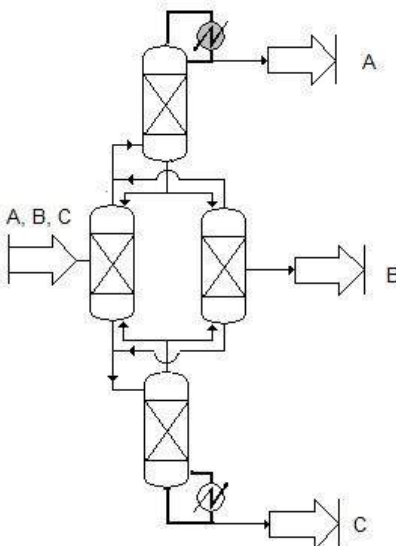


FIGURE 2.18 Four columns sequence model

Thirdly, divided wall columns can be modelled with a four column sequence as shown in Figure 2.18. It reflects the actual situation best and is considered as the most suitable configuration for dynamic simulation. However, it is the most difficult to initialize because it requires initialization of the interconnecting streams.

2.1.7 Divided wall column applications

In 1985, the first application of a DWC was installed by BASF in Ludwigshafen, Germany. In 2010, there are now more than 125 divided wall columns in operation globally, of which 116 are divided wall columns for separation of three-component mixtures, 2 are divided wall columns for separation of mixtures with more than three components. Most of them are installed by BASF (around 70 packed DWC). The number of divided wall columns is expected to reach about 350 DWC in 2015 if the rate of growth remains constant (Yildirim et al., 2011). Structured or random packing or trays are used in the divided wall column. Operating pressures in the system range between 2 mbar and 10 bars. The diameters of dividing wall column are between 0.6 m and 4 m at BASF. The largest column that is constructed by Linde AG for Sasol in Johannesburg, South Africa has a height of 107 m and diameter of more than 5 m (Yildirim et al., 2011; Parkinson, 2005). One typical application for the divided wall column is the reduction of the benzene content in motor gasoline to less

Chapter 2: Literature review

than 1 per cent on a volume basis. The divided wall column can also be applied to the separation of C4 isomers with a feed of mixed C5s and C4s. It can save energy usage by 26.5% compared to conventional systems.

Slade. B et al., (2005) reported the successful revamp of a conventional tray distillation column for xylene separation (3.8/4.3 m diameter). The column takes a xylene side stream from reformat to feed an aromatics plant to make higher value products. The existing distillation column was a traditional column with 51 trays. The feed location was tray 38 and side product was taken at tray 20. The revamp column configuration was a divided wall column with 51 trays. The dividing wall ran from tray 14 up to tray 39. The feed was at tray 27 in the feed section and the xylene product was taken at tray 28 in the side section. Test runs were carried out on the divided wall column during June and July 2005.

Table 2.1 shows the industrially available divided wall column applications for ternary mixtures (Yildirim et al., 2011).

TABLE 2.1 Industrial applications of DWCs for ternary systems (Yildirim et al., 2011)

Company	Mixture	Provider	Description	References
BASF SE, various sites	Mostly undisclosed	Most columns built by Montz GmbH	More than 70 DWCs Diameter 0.6 – 4m Operating pressure 2 mbar to 10 bar	Amminudin and Smith (2001); Olujic et al., (2009); Kaibel, B et al., (2004)
Sasol, Johannesburg, South Africa	Separation of hydrocarbons from a Fischer-Tropsch synthesis unit	Linde AG in 1999	Height 107 m Diameter 5 m Tray column	Michael A. Schultz et al., (2002); Parkinson (2005)
Veba Oel Ag, Munchsmunster, Germany	Separation of benzene from pyrolysis of gasoline	Uhde in 1999	170000 mt yr ⁻¹ feed capacity	Michael A. Schultz et al., (2002); Yildirim, Kiss and Kenig (2011)
Saudi Chevron Petrochemical, Al Jubail Saudi Arabia	Undisclosed	Uhde in 2000	140000 mt yr ⁻¹ feed capacity	Yildirim, Kiss, and Kenig (2011)
highLonza, Visp, Switzerland	Multipurpose, for various ternary mixtures	Undisclosed	Height 10 m Diameter 0.5 m Sulzer Mellapak™ 350Y Hastelloy C-22	Grutzner et al., (2012)
ExxonMobil, Rotterdam, The Netherlands	Benzene – Toluene – Xylene fractionation	ExxonMobil; was planned for 2008	No data available	Parkinson (2007)
Undisclosed	Undisclosed	Sumitomo Heavy	Six DWCs	Premkumar and

Chapter 2: Literature review

		Industries and Kyowa Yuka	No data available	Rangaiah (2009)
Undisclosed	Separation of C ₇₊ aromatics from C ₇₊ olefin/paraffin	UOP	Five DWCs Trap tray	Michael A. Schultz et al., (2002, 2006)
Undisclosed	Undisclosed reactive system consisting of two reactive components and an inert component	UOP	Split shell column with two walls	Michael A. Schultz et al., (2006)
Undisclosed	Undisclosed	Sulzer Chemtech Ltd	20 DWCs No data available	Parkinson (2007)
Undisclosed	Undisclosed	Koch Glitsch	10 DWCs No data available	Premkumar and Rangaiah (2009)

For the separation of mixtures with more than three components, Table 2.2 shows two applications of divided wall columns.

TABLE 2.2 Industrial applications of divided wall columns for multicomponent mixtures

Company	System	Constructor	Features	Reference
BASF SE	Recovery of four component mixture of fine chemical intermediates	BASF SE/Montz GmbH since 2002	Single wall Height 34 m Diameter 3.6 m Column works under high vacuum	Dejanovic et al (2011a), Olujic et al. (2009)
Undisclosed customer in the Far East	Integration of a product separator and an HPNA stripper	Designed by UOP	Five product streams	Schultz et al. (2006), Parkinson (2007)

2.2 CONCEPTUAL DESIGN OF DIVIDED WALL COLUMN: REVIEW

The divided wall column system has many known advantages, but the lack of knowledge for design, operating, and control may cause limited growth of divided wall column in the process industry. Almost all papers that have been published were restricted to ternary mixtures with three products, sharp separations, saturated liquid feed, constant flowrate and constant relative volatility. In the section, a review of the methods for design of divided wall columns and reactive divided wall column will be presented.

The design of divided wall columns or fully thermally coupled distillations is more complex than traditional distillation because it has more degrees of freedom. A number of papers have

been published on the subject which focus on the calculation of the minimum vapor requirement and determined the number of stages in the various column sections.

C. Triantafyllou and Smith (1992) published a design oriented shortcut method for three products in a divided wall column based on the Fenske-Underwood-Gilliland-Kirkbridge model (FUGK). In this paper, they presented a method to decompose a divided wall column into a three-traditional-column model. By using the decomposition method, they assume that heat transfer across the column wall can be neglected, hence making the divided wall column equivalent to a fully thermally coupled distillation. The prefractionator is considered like a traditional column if a partial condenser and a partial reboiler are used. The main column can be represented as two traditional columns if we assume a total reboiler for the upper part of the main column and a total condenser for the lower part of the main column. The interconnecting streams are considered as the feed flowrates with superheated vapor and sub-cooled liquid conditions, respectively. The FUGK method can be applied to determine operational and structural parameters for each column. The minimum number of equilibrium stages can be determined by the Fenske equation, the minimum reflux ratio can be determined by using the Underwood equation, the number of stages can be determined by the Gilliland method when choosing operating reflux ratio, and feed location can be determined by the Kirkbride method. The reflux ratio of the prefractionator is adjusted until its number of stages equals the number of the side section. The recoveries in the prefractionator column are optimized for the minimum vapor flowrate or the minimum number of stages.

Amminidin et al., (2001) proposed a semi-rigorous design method based on equilibrium stage composition concept. Certain assumptions are as follows: constant molar overflow, constant relative volatility, and estimation of component distribution at minimum reflux. Their design procedure starts from defining the products composition, and works backward to determine the design parameters required to achieve them. Therefore, firstly, by using the method of Van Dongen and Doherty (1985), a feasible product distribution is estimated for the composition of the top, middle and bottom products, the minimum reflux ratio and the minimum boil-up ratio. Any distillation operation lies between the two limits of total reflux and minimum reflux ratios. At total reflux ratio, the number of stages is minimized and energy consumption is maximized. At the minimum reflux ratio, the number of stages is maximized and energy consumption is minimized. Therefore, a product distribution must be chosen between the two conditions. Secondly, using the equilibrium stage concept the number of stages, flow rates, feed stage and side stream location for the fully thermally coupled distillation are estimated.

An approximate design procedure for fully thermally coupled distillation column is proposed by Kim, Y.H (2002). The Fenske equation is applied to the main column to determine minimum number of stages. However, the author believed that the design of the prefractionator cannot follow the Fenske equation because the end compositions are unknown. Therefore, a stage-to-stage computation is proposed. Then, the number of stages in the system is taken as twice the minimum number of stages. The minimum vapor flowrate was determined by the Underwood equation. The liquid flowrate of the main column is determined by checking the compositions of the products. Clearly, they take twice the minimum number of stages as the number of theoretical trays is considered to be equal to two times the minimum number of stages. It is not always true.

Halvorsen, I.J and Sigurd Skogestad (2003) proposed the V_{\min} diagram method to determine the minimum energy consumption. To use the method, they assume constant molar flowrates, constant relative volatilities, and an infinite number of stages. Firstly, the V_{\min} diagram is drawn based on the Underwood equation. The minimum energy requirement for separation of a feed mixture of n components into n pure products is given by:

$$V_{\min}^{\text{Petlyuk}} = \max \sum_{i=1}^j \frac{\alpha_i z_i F}{\alpha_i - \theta_j}; j \in \{1, n-1\}$$

Here: θ_j are the $n-1$ common Underwood roots found from:

$$1 - q = \sum_{i=1}^n \frac{\alpha_i z_i}{\alpha_i - \theta}$$

Underwood roots obey $\alpha_1 > \theta_1 > \alpha_2 > \theta_2 > \dots > \theta_{n-1} > \alpha_n$

Where: q is liquid fraction in the feed (F)

z is the feed composition

Secondly, they choose the actual flowrate around 10% and the minimum number of stages was calculated based on the Underwood equation.

Calzon-McConville, C. J et al., (2006) presented an energy efficient design procedure for optimization of the thermally coupled distillation sequences with initial designs based on the design of conventional distillation sequences. In the first step, it is assumed that each column performs with specified recoveries of components of 98 % (light and heavy key components) and by using the shortcut method (FUG model), the number of stages of conventional distillation schemes are obtained. In the second step, the stage arrangements in the integrated configurations are obtained; finally, an optimization procedure is used to minimize energy consumption. The energy-efficient design procedure for thermally coupled distillation

sequences is applied not only for the separation of ternary and quaternary mixtures but also to the separation of five or more component mixtures.

Sotudeh, N and Bahram Hashemi Shahraki (2007, 2008) proposed a shortcut method for the design of a divided wall column based only on the Underwood equation because authors believe that using the Fenske equation for calculating the minimum number of stages is not adequate for designing divided wall columns. The theoretical number of stages can be calculated by using the basic Underwood equation. In this method, the number of stages in the prefractionator is set to be the same as in the side section. Clearly, we cannot know that the number of stages of prefractionator is correct or not. Moreover, the paper does not carry out simulations to confirm the method.

Ramirez-Corona, N et al., (2010) presented an optimization procedure for the Petlyuk distillation system. The procedure used the FUG model to determine the structural design of the divided wall column as well as the mass and energy balances, the thermodynamic relationships, and cost equations. The objective function was set as the minimization of the total annual cost. In the procedure, they estimated the composition of the interconnection streams between the prefractionator and the main column by solving the feed line and the operating line equations.

$$y_i = \left(\frac{q}{q-1} \right) x_i - \frac{x_{i,D}}{q-1}$$

$$y_i = \left(\frac{R}{R+1} \right) x_i + \frac{x_{i,D}}{R+1}$$

Combining these equations, one obtains:

$$x_i = \frac{z_i \cdot (R+1) + x_{i,D} \cdot (q-1)}{R+q}$$

$$y_i = \frac{R \cdot z_i + q \cdot x_{i,D}}{R+q}$$

Chu, K. T et al., (2011) presented a new shortcut method based on the efficient net flow model to determine the composition of the key components. They then applied the shortcut method of Fenske, Underwood, Gilliland and Kirkbride to determine the number of stages of each section. Liquid split R_L and vapor split R_V are dependent variables due to the constant molar flow assumption. The values of R_L and R_V are chosen to obtain the same number trays in the prefractionator and side section.

Table 2.3 shows the summary of several shortcut methods for design of divided wall columns.

TABLE 2.3 Summary of several shortcut methods for design divided wall column

References	Model	Method	Hypothesis	Mixture analysis
Triantafyllou and Smith (1992)	Three – column sequence model	FUGK method Minimum cost of system	Constant relative volatilities Constant molar flows	i-butane/1-butene/n-butane/trans-2-butene/cis-2-butene
Amminidin et al. (2001)	Three column sequence model	Semi-rigorous design method based on the equilibrium stage composition concept	Constant molar overflow. Constant relative volatilities. Estimate product distribution at minimum reflux.	Ethylene/Propene/n-Propane/i-butane/1-butane/n-butane/i-Pentane/n-Pentane/n-Hexane
Young Han Kim et al. (2002)	Two – column sequence model (pre-fractionator and main column)	Fenske equation for the main column and a stage-to-stage computation for the pre-fractionator. Take twice the minimum number of stages as the theoretical trays	Ideal equilibrium is assumed between the vapor and liquid of interlinking streams and the shortcut design equations of multi component distillation columns.	Methanol/Ethanol/water Cyclohexane/n-heptane/toluene s-butanol/i-butanol/n-butanol
Ivar J. Halvorsen and Sigurd Skogestad (2003, 2011)	Two – column sequence model (pre-fractionator and main column)	V_{min} diagram method. Underwood's equation.	Constant molar flow Infinite number of stages Constant relative volatilities	
Noori Sotudeh and Bahram Hashemi Shahraki (2007, 2008)	Three – column sequence model	Underwood's equation. Number of stages in the pre-fractionator is set to be the same as in the side section. The compositions of interconnection streams are design variables.	Constant relative volatilities	Benzene/Toluene/Xylene i-butane/1-butene/n-butane/trans-2-butene/cis-2-butene
Nelly Ramirez Corona et al. (2010)	Three – column sequence model	FUGK method They calculate the composition of interconnection streams. Minimization of the total annual cost.	Constant relative volatilities Constant molar flowrate The interconnecting streams are saturated.	n-pentane/n-hexane/n-heptane n-butane/i-pentane/n-pentane i-pentane/n-pentane/n-hexane
Kai Ti Chu et al. (2011)	Six different sections model.	Applied the components net flow model. FUGK method	Constant relative volatilities Constant molar flowrate The column is symmetric	Ethanol/n-Propanol/n-Butanol Benzene/Toluene/EthylBenzene
Christopher Jorge Calzon-McConville et al. (2006)	Superstructure model	Based on the design of conventional distillation sequences, the stages are rearranged to the integrated configurations. Minimize energy consumption		n-butane/ isopentane/ n-pentane/ n-hexane/n-heptane

Based on the above analysis, we can conclude that a lot of papers focused on the design, simulation and control for divided wall column. However, these methods still have drawbacks. The method of C. Triantafyllou et al., (1992) applied the FUGK model that can quickly and easily determine operational and structural parameters of divided wall columns. However the application of the Fenske equation for the estimation of the minimum number of stages of a divided wall column is not correct since the composition of the liquid stream returning from the main column is not equal to the composition of the vapor entering the main column at the connection points. Kim (2002) applied a stage-to-stage computation method instead of the Fenske equation for the prefractionator. However the actual number of stages in the system takes twice the minimum number of stages. Sotudeh (2007) used only the Underwood equation to determine the number of stages in the main column and they set the number of stages of the prefractionator to be the same number of stages as in the side section. Ramirez-Corona et al., (2010) also applied the FUGK method and estimated the composition of interconnecting streams.

Moreover, all the previous methods have not considered the position and configuration of dividing wall in the column and a great part of them are restricted to ternary mixtures with a feed quality (q) equal to 1.

2.3 CONCEPTUAL DESIGN OF REACTIVE DIVIDED WALL COLUMN: REVIEW

A reactive divided wall column represents a combination of a reactor and a separation unit in one divided wall column or a combination of reactive distillation and divided wall column technology. Kaibel and Miller (2005) proposed the reactive dividing wall column as one of the new possible application areas for dividing wall columns. The design of reactive dividing wall columns is considered as a combination of a design of a reactive distillation column and a design of a non-reactive dividing wall column. The design, simulation, and control of reactive divided wall columns is still a new research area.

Mueller, I et al. (2007) decomposed the reactive divided wall column step-by-step into single non-reactive and reactive columns as shown in Figure 2.19. Step 1: if the heat transfer across the dividing wall is neglected, the divided wall column is thermodynamically equivalent to the Petlyuk column. Step 2: If one partial re-boiler and one partial condenser is added into the prefractionator, the four liquid and vapor streams between the columns can be replaced by two streams. Step 3: The three traditional distillation columns are equivalent to the prefractionator configuration if one total

reboiler is added to column 2 and one total condenser to column 3. In this configuration, the reaction and separation processes occur in column 1 (reactive column). In Column 2 and column 3 (non-reactive columns) only separation occurs.

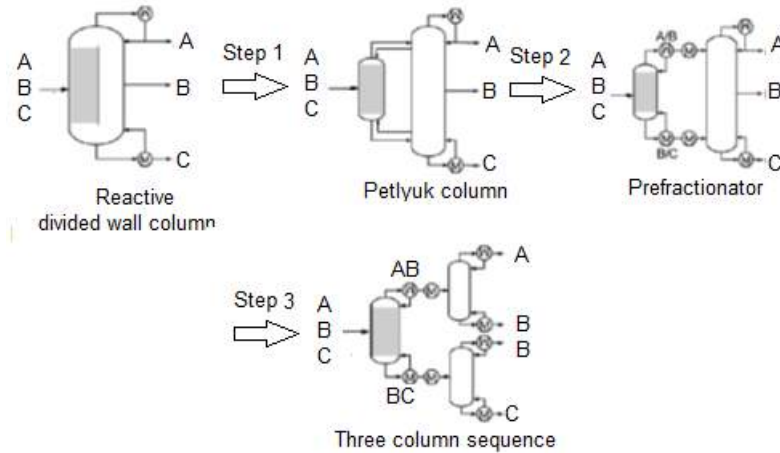


FIGURE 2.19 Decomposition into simple column sequences (grey area: reactive zone) (Mueller, I et al. (2007))

For the non-reactive columns, the shortcut methods suggested by Underwood, Fenske, and Gilliland are applied. The Fenske's equation gives the minimum number of equilibrium stages at total reflux. The minimum reflux ratio is calculated by Underwood's equation. The Gilliland correlation provides the actual number of theoretical stages. Then, the feed position is determined by the Kirkbride equation. For the reactive columns, they applied the rate-based approach. The actual rates of multicomponent mass and heat transport between liquid and vapor phases can be directly accounted for. In the paper, they suggested that the reactive divided wall column should be used for (1) Reactive systems with more than two products which should each be obtained as a pure fraction; (2) Reactive systems with an inert component and with a desired separation of both products and inert component. (3) Reactive systems with an excess of a reagent, which should be separated before being recycled. Mueller et al. (2007) also presented another method to design the reactive dividing wall column in which the rate-based stage model is applied for both non-reactive and reactive sections.

Guido Daniel et al. (2006) proposed a procedure to obtain feasible designs for a reactive dividing wall column. In the paper, the reactive divided wall column is represented by using a prefractionator and a main column. It is assumed that reaction only occurs in the prefractionator and the main column is used to separate the reaction products. The methodology is based on the

boundary value method (BVM) where chemical equilibrium is assumed on every reactive stage of the reactive column. The cost function is used to rank the feasible designs.

Kiss, A.A et al., (2007, 2010, and 2012) investigated a base case design alternative, namely a two column configuration that uses a reactive distillation column, followed by a conventional distillation column. The conceptual design of the reactive distillation column was performed using graphical stage composition lines and boundary value method. Then, they combine reaction and separation into one reactive divided wall column. The key factor that allows such an integration of two columns into one unit is the similar pressure and temperature conditions.

Miranda-Galindo, E. Y et al., (2011) presented a method to design a multi-objective optimization approach for the design of reactive distillation sequences with thermal coupling. A direct thermally coupled distillation sequence, an indirect thermally coupled distillation sequence, and the Petlyuk sequence are analyzed. By using Aspen Plus software, the energy consumption, configurations, size of the reactive section and other valuable information are objectives to minimize.

Cheng K et al., (2013) studied the process biphenyl carbonate, a precursor in the production of polycarbonate, which is traditionally synthesized by the trans-esterification reaction of dimethyl carbonate and phenol. In this work, phenyl acetate was used instead of phenol to react with dimethyl carbonate. In the design, the objective was to minimize the TAC by adjusting the design parameters, such as the number of trays in each zone, the feed location in the distillation column, and so on. TAC is defined as:

$$\text{TAC} = \text{operation cost} + \frac{\text{capital cost}}{\text{payback years}}$$

The simulation of the reactive distillation process was carried out using ASPEN PLUS with the RADFRAC module.

Bumbac G et al., (2007) investigated Tert-Amyl Ethyl Ether (TAEE) synthesis from isoamylene and ethanol with 15 % excess of ethanol in the feed stream. The synthesis is studied in a reactive divided wall column. Feasibility of the separation scheme was established with ASPEN DISTIL and simulated with ASPEN HYSYS. In 2009, Bumbac et al presented the results of the simulation for Ethyl-tert-butyl-ether (ETBE) synthesis in which the excess of ethanol is recycled, also based on Aspen Hysys software, Bumbac G et al., (2009) However, in the papers, the author only mentioned the simulation results but has not shown the design method.

By using the process simulator AspenONE Aspen Plus, the esterification of the mixture of fatty organic acids and methanol to biodiesel has been studied by Cossio Vargas, E et al., (2011). The three complex reactive divided wall columns have been applied in the simulator (complex reactive distillation column, reactive thermally coupled distillation with a side rectifier and reactive Petlyuk

column). Firstly, the initial structure and operation parameters must be chosen for three configurations. Then, they optimize structural parameters to minimize energy duty.

A complete thermodynamic analysis of a reactive dividing wall distillation column was showed by Barroso-Munoz (2009). The results indicate that the reactive dividing wall column presented both higher thermodynamic efficiencies and lower energy losses than those obtained in the classical configurations of a reactor plus a distillation column. The reactive dividing wall distillation column also required lower energy consumption compared to that required by classical processes.

Gomez-Castro, F. I et al., (2010, 2011) proposed a method to design a reactive thermally coupled system. Based on the number of stages of the reactive distillation column, the initial design of a reactive Petlyuk column can be obtained through a rearrangement of the stages of the reactive distillation column. Then, the parameters are used to run the simulations. The number of stages in the main column, the number of stages in the prefractionator, and the stages where the reaction occurs are determined. One step in the design of thermally coupled systems consists of finding the optimal position for the interconnection flows in order to reduce the energy requirements of the system. In this work, the production of biodiesel is considered. The simulations were carried out with Aspen One™ to demonstrate the feasibility of such alternatives to produce biodiesel with methanol at high pressure conditions.

Fernado (2012) presented a method that is based on the shortcut method for the design of thermally coupled reactive distillation systems. For the design, the method is based on the Fenske–Underwood–Gilliland (FUG) equations. The FUG model, mass and energy balances, and phase equilibrium equations are used to formulate the model of the intensified systems. Biodiesel production through the esterification of oleic acid with supercritical methanol is studied.

Sun L and Bi X (2014) applied the minimum vapor flow method and V_{\min} diagram to the design of a reactive dividing wall column (RDWC). A shortcut design method for the conventional dividing wall columns based on the Underwood's equations has been extended by introducing a new parameter that eliminates the effects of the reaction to allow conceptual design of the RDWC. The syntheses of methyl ter-butyl ether (MTBE), ethyl ter-butyl ether (ETBE), and dimethyl ether (DME) are considered. The results show that the minimum vapor flow method and the V_{\min} diagram can be applied to the conceptual design of a RDWC in different reaction systems. The computational procedure to plot the V_{\min} diagram is as follows: Firstly, the extent of reaction ξ and the reactant conversion are calculated. The equilibrium conversion is assumed in each stage in this work. Secondly, the roots of the feed equation are calculated. Finally, the V_{\min} diagram is plotted. The computational procedure for RDWC is similar to the conventional column. Table 2.4 summarizes several design methods for reactive divided wall columns.

TABLE 2.4 Works published for reactive divided wall column

Reference	Hypothesis/Assumption	Design/Simulation	Reaction
Erick Yair et al. (2011)	Two feed streams. Each interconnection stream can be located in a different stage in the main column.	The minimization of four objectives: number of stage in each section, size of the reactive section, heat duty. Aspen ONE Aspen Plus	Alcohol + fatty acid ↔ ester + water
Kai Cheng et al. (2013)	Assumption is not denoted in the paper.	First design reactive distillation and conventional distillation. The objective was to minimize the TAC by adjusting the design parameters. Then, parameters given for reactive thermally coupled distillation. Aspen plus with the Radfrac module.	Dimethyl carbonate + 2Phenyl acetate ↔ Diphenyl carbonate + 2Methyl acetate
Bumbac (2007)	Two – column sequence model. Reactive zone hosted by the pre-fractionator.	Simulated by Aspen Distil™ and Aspen Hysys™	Isoamylene + Ethanol ↔ Tert Amyl Ethyl Ether Iso-Butene + Ethanol ↔ ETBE
Cho Youngmin et al. (2008)	Two reactions occur in one column. Ideal gas is assumed. Heat transfer across the dividing wall was ignored.	AspenONE Aspen Plus	Fatty organic acids + Methanol ↔ Ester + Water
Fabrico Omar Barroso – Munoz et al. (2009)	Assumption is not denoted in the paper.	The design was obtained by using the RADFRAC module of Aspen Plus. An initial tray structure based on conventional distillation sequence column. Aspen plus ONE™	Ethanol + Acetic Acid ↔ Ethyl Acetate + Water Methanol + Isobutylene ↔ Methyl tert Butyl Ether Ethanol + Ethylene Oxide ↔ Ethoxyethanol
Fernado (2010, 2011)	The pressure of the prefractionator is assumed as equal to the pressure of the top of the main column.	First, an initial design is required to run. Then, the number of stages in the main column, in the pre-fractionator and reaction zone have to be determined by rearrangement of stages of the divided wall column. Simulated by Aspen One™	Fatty acid + Methanol ↔ Biodiesel + Water
Guido (2006)	Two column sequence model with two feed streams and one side draw. Pre-fractionator is considered as reactive section. Main column is used to	The boundary value method for non-reactive columns for the main column and for reactive columns by Dragomir (2004). Simulated by Aspen Plus™	Methyl Acetate + Water ↔ Methanol + Acid Acetate

	separate the reaction products.		
Mueller I, C. Pech, D. Bhatia, E. Y. Kenig (2007)	Three column sequence model	Rate based method used to design the reactive divided wall columns. Simulated by Aspen Custom Modeler (ACM) and Aspen Properties™	Dimethyl carbonate + Methanol ↔ diethyl carbonate + methanol
Anton A. Kiss et al. (2007, 2009, 2012)	Operation pressure in the reactive section and in the separation column is the same.	Stage to stage method for design of a reactive distillation and a conventional distillation. Then, combines into one reactive divided wall column. AspenTech Aspen Plus	AkzoNobel Chemical plants 2Methanol ↔ Dimethyl ether + Water
Anton A. Kiss et al. (2013)	Operation pressure in the reactive section and in the separation column is the same.	The SQP optimization method and the effective sensitivity analysis tool from Aspen Plus were employed in the R-DWC optimization procedure. AspenTech Aspen Plus and Aspen dynamics	Fatty acid + Methanol ↔ Biodiesel + Water
Lanyi Sun and Xinxin Bi (2014)	Assumption is not denoted in the paper.	The minimum vapor flow method and V_{min} diagram are applied to the design of a reactive dividing wall column. Aspen Plus	Isobutene + Methanol ↔ methyl tert butyl ether (MTBE) Isobutene + Ethanol ↔ ethyl tert butyl ether 2Methanol ↔ Dimethyl ether + Water

Although papers focusing on the design, simulation, and control of reactive divided wall columns are increasing, it is still a comparatively new research area and has been challenged. Except for the methods of Muller et al., (2007), Kiss et al., (2007, 2009, 2012, 2013), and Guido (2006), other papers have not justified a method to design reactive divided wall columns based on simulation (BumBac (2007)) or optimization methods using simulation tools (Cheng K et al., 2013, Miranda-Galindo et al., 2011).

2.4 CONCLUSION OF THE CHAPTER 2

The chapter reviews several papers addressing divided wall column and reactive divided wall column. The divided wall column fundamentals are presented with important advantages. The

design, simulation, control, and application of divided wall columns also are indicated. For conceptual design of divided wall columns, several shortcut methods are described in the chapter in which all most all are based on the Fenske-Underwood-Gilliland-Kirkbride equations. They are limited to ternary mixtures and unit feed quality ($q = 1$).

The review also shows that process simulators still do not have a standard model for a divided wall column in commercial software packages. It is important to note that simulation processes in the papers published have not yet used ProSim^{plus} to simulate a divided wall column or reactive divided wall column.

A review of reactive divided wall columns is carried out. It is shown that the simulation, design and modelling of reactive divided wall columns is still a comparatively new research area and has been challenged because an agreed method has not yet been accepted by many authors.

Therefore, based on the above analysis, the motivation of this thesis has been the integration between reactive distillation and a divided wall column to produce a reactive divided wall column. Firstly, a shortcut method is developed to design divided wall columns concerning the position and configuration of the dividing wall and enabling the application to both ternary mixtures and multicomponent mixtures with different feed qualities in chapter 3. Secondly, a method will be modified for application to reactive divided wall columns in chapter 5.

Chapter 3
DESIGN METHODOLOGY OF DIVIDED WALL
COLUMN

3.1 A PROCEDURE FOR DESIGN OF DIVIDED WALL COLUMNS

Following the conclusions in chapter 2, this chapter aims to present, by application of standard shortcut method (FUGK model) and using the component net flow model, a procedure for designing divided wall columns.

The approach allows rapid determination of the minimum vapor flow rate, minimum reflux ratio, and number of stages for each section by choosing an operating reflux ratio, liquid and vapor split values, and the possible position and configuration of the dividing wall. Moreover, the compositions of interconnecting streams between the prefractionator and the main column are also estimated and set as the initial conditions for simulation in Prosim^{Plus} software.

3.1.1 Assumptions and model design

To use the standard shortcut method, the component net flow model, and simplified model of a divided wall column, we assume that:

- (1) The relative volatility of components is constant;
- (2) The vapor and liquid flows in each section of the divided wall column are constant;
- (3) The pressure of the system is constant;
- (4) The heat transfer across the dividing wall is neglected;
- (5) The heat losses from the column walls are negligible;
- (6) Vapor-liquid equilibrium is achieved on each stage;
- (7) The heavy non-key component is assumed to go completely to the bottom of section II and the light non-key component is assumed to go completely to the top of section III;

Henry Z. Kister. (1992) defined that key components are the two components in the feed mixture whose separation is specified. They are called light key component (more volatile) and heavy key component (less volatile). Other components are called non-key components. Any components lighter than the light key are called light non-key components, while those heavier than the heavy key are called heavy non-keys components. The components that lie between the light key and the heavy key are called distributed key components.

Chapter 3: Design methodology of divided wall column

The procedure can be applied not only for ternary mixtures but also for multicomponent mixtures. To simplify, we consider separation of a ternary mixture A, B, and C, in which A is the lightest component and C is the heaviest component. The feed flowrate is $F(\text{kmol/h})$, feed composition z_A , z_B , and z_C , and recoveries or purities of component in divided wall column are known.

The volatilities of each component (K -value) are constant (assumption 1) and rank in order $K_A > K_B > K_C$. The relative volatility is a measure of the ease of separation. For multicomponent separation, the relative volatility is defined as the K -value ratio of the more-volatile to the less-volatile component. Therefore, relative volatility is always greater or equal to unity. The relative volatility of component i and j is defined as:

$$\alpha_{i,j} = \frac{K_i}{K_j}$$

Therefore:

$$\alpha_A = \frac{K_A}{K_C}$$

$$\alpha_B = \frac{K_B}{K_C}$$

$$\alpha_C = \frac{K_C}{K_C} = 1$$

The feed composition is listed in order of their relative volatility:

$$\alpha_A > \alpha_B > \alpha_C = 1$$

The minimum number of stages at total reflux may be estimated by using the Fenske equation. It is applied with the assumption that all stages reach equilibrium (assumption 6) and requires a constant relative volatility α throughout the column (assumption 1). To determine the minimum reflux ratio, the equations developed by Underwood are based on the assumption (2): constant molar flowrate. Then, the knowledge of minimum stages and minimum reflux ratio in a column can be related to the actual number of stages and the actual reflux required by the Gilliland correlation. Finally, the feed stage can be estimated by using the Kirkbride equation.

Based on the assumption (4), the divided wall column in figure 3.1(a) is equivalent to the fully thermally coupled distillation in figure 3.1 (b). Therefore, the prefractionator will be used instead of section 1. The main column will be used instead of section 2 and 3. The interconnecting streams are added on and connected between the prefractionator and the main column.

Chapter 3: Design methodology of divided wall column

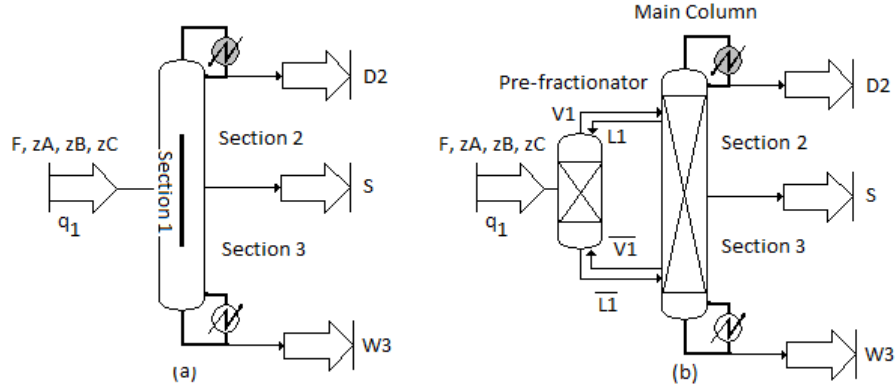


FIGURE 3.1 (a) Divided wall Column; (b) Thermally coupled distillation

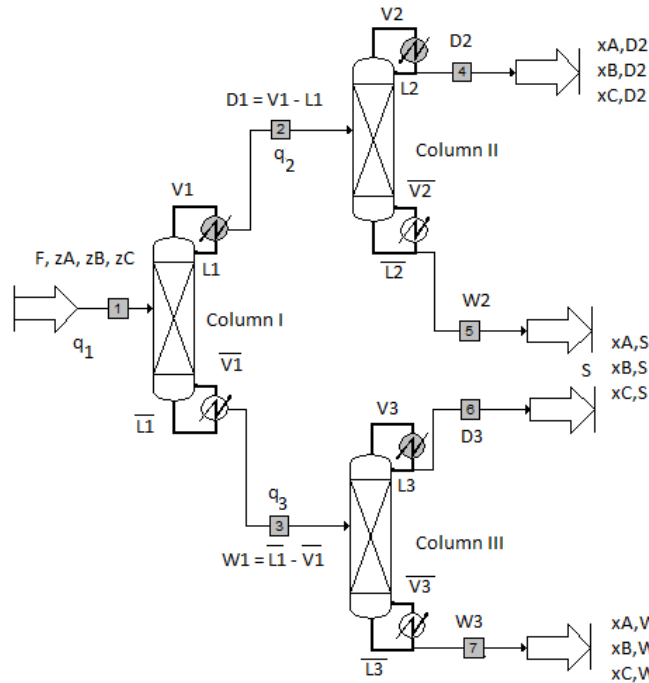


FIGURE 3.2 Simplified model design of divided wall column

Based on the figure of thermally coupled distillation 3.1 (b), the main column can be represented as two traditional columns shown in figure 3.2 if we assume a total reboiler for column II and a total condenser for column III. The pre-fractionator is also considered as a traditional column if we assume a partial condenser and a partial reboiler while the interconnecting streams are considered as the feed flow-rates for column II and III with superheated vapor and sub-cooled liquid conditions, respectively.

Based on the figure 3.2, components A and C are key components and the component B is the distributed component in column I. Therefore, the top of column I is mainly component

Chapter 3: Design methodology of divided wall column

A, a part of component B and a little of component C. The bottom of the column I is mainly component C, a part of component B and a little of component A. Column II separates components A and B. Therefore, A and B are key components and component C is heavy non key component. Based on the assumption (7), all of component C leaves from the bottom of column II. Column III separates components B and C. Therefore, B and C are key components and component A is a light non key component. Based on the assumption (7), all of component A leaves from the top of column III.

3.1.2 Material balance for divided wall columns

Based on the Figure 3.2, material balance equations for each component are as follows:

For the component A:

$$F \cdot z_A = D_2 \cdot x_{A,D_2} + S \cdot x_{A,S} + W_3 \cdot x_{A,W_3}$$

For the component B:

$$F \cdot z_B = D_2 \cdot x_{B,D_2} + S \cdot x_{B,S} + W_3 \cdot x_{B,W_3}$$

For the component C:

$$F \cdot z_C = D_2 \cdot x_{C,D_2} + S \cdot x_{C,S} + W_3 \cdot x_{C,W_3}$$

And we have:

$$x_{A,D_2} + x_{B,D_2} + x_{C,D_2} = 1$$

$$x_{A,S} + x_{B,S} + x_{C,S} = 1$$

$$x_{A,W_3} + x_{B,W_3} + x_{C,W_3} = 1$$

We know the feed flow rate (F) and feed composition (z_A, z_B, z_C). From the above equations, there are twelve unknown variables as listed in Table 3.1, while there are six equations.

TABLE 3.1 Twelve unknown variables for ternary mixture separation

Distillate product	Distillate product stream: D_2 (kmolh^{-1}) Distillate compositions: $x_{A,D_2}; x_{B,D_2}; x_{C,D_2}$;
Side product	Side product stream: S (kmolh^{-1}) Side product composition: $x_{A,S}; x_{B,S}; x_{C,S}$
Bottom product	Bottom product stream: W_3 (kmolh^{-1}) Bottom product composition: $x_{A,W_3}; x_{B,W_3}; x_{C,W_3}$;

Chapter 3: Design methodology of divided wall column

Therefore, in order to solve the equations, six of the unknown variables must be specified. The key component A is collected in the distillate product while component C is zero based on assumption 7, therefore their composition in the distillate product should be specified. In the same way, the composition of component C and A in the bottom product also should be specified. In the side product, the component B is the key component therefore it should be specified along with $x_{A,S}$ or $x_{C,S}$ or $\frac{x_{A,S}}{x_{C,S}}$.

Sotudeh N (2007) suggested that the specified parameters should be:

$$x_{A,D_2}, x_{C,D_2}, x_{A,W_3}, x_{C,W_3}, x_{B,S}, \frac{x_{A,S}}{x_{C,S}}$$

Based on the assumption (7), we have: $x_{C,D_2} = 0$ and $x_{A,W_3} = 0$.

3.1.3 Minimum vapor flow rate of divided wall columns

3.1.3.1 Minimum vapor flow rate of column I

In column I, the recovery of component i in the top and bottom product is defined as:

$$\tau_{i,T} = \frac{x_{i,D_1} \cdot D_1}{F \cdot z_i}$$

$$\tau_{i,B} = \frac{x_{i,W_1} \cdot W_1}{F \cdot z_i}$$

Recovery of component A:

We have recovery of component A in the top product of the column I:

$$\tau_{A,T} = \frac{x_{A,D_1} \cdot D_1}{z_A \cdot F}$$

Firstly, the assumption of a sharp split of component A (lightest component) in the top of the column I is not suitable for a realistic design because it requires an infinite number of stages.

Thus, recovery of component A in the top has to be less than 1.

$$\tau_{A,T} < 1 \quad (1)$$

We also have:

$$\tau_{A,T} = 1 - \tau_{A,B} = 1 - \frac{x_{A,W_1} \cdot W_1}{z_A \cdot F} \quad (2)$$

Where:

$\tau_{A,B}$ is the recovery ratio of component A in the bottom of the column I.

Secondly, also based on the assumption (7), and because the assumption of a sharp split of component A in the top of the column II is not suitable, we have:

$$x_{A,W_1} \cdot W_1 < x_{A,S} \cdot S \quad (3).$$

Chapter 3: Design methodology of divided wall column

From (1), (2), and (3), the recovery ratio of component A in column I should be chosen between:

$$1 > \tau_{A,T} > 1 - \frac{x_{A,S} \cdot S}{z_A \cdot F}$$

Recovery of component C:

In the same way, the recovery ratio of component C in the top of the column I is also analyzed. We have:

$$\tau_{C,T} = \frac{x_{C,D_1} \cdot D_1}{z_C \cdot F}$$

Firstly, because the assumption of a sharp split of component C (heaviest component) in the top of the column I is not suitable, recovery of component C in the top product has to more than 0.

$$\tau_{C,T} > 0 \quad (4)$$

Moreover, based on the assumption (7), and because the assumption of a sharp split of component C (heaviest component) in the top of the column III is not suitable:

$$x_{C,D_1} \cdot D_1 < x_{C,S} \cdot S \quad (5)$$

From (4) and (5), we must choose the recovery of component C in the top of column I between:

$$0 < \tau_{C,T} < \frac{x_{C,S} \cdot S}{z_C \cdot F}$$

Recovery of component B:

The recovery ratio of component B is calculated by Stichlmair's equation (Stichlmair, 1988). It is called the preferred split β_p . The equation of Stichlmair (1988) is established in the Appendix [1]:

$$\tau_{B,T} = \beta_p = - \frac{\left(\frac{\alpha_A \cdot z_A \cdot F}{\alpha_A - \theta_1} \right) - \left(\frac{\alpha_A \cdot z_A \cdot F}{\alpha_A - \theta_2} \right)}{\left(\frac{\alpha_B \cdot z_B \cdot F}{\alpha_B - \theta_1} \right) - \left(\frac{\alpha_B \cdot z_B \cdot F}{\alpha_B - \theta_2} \right)}$$

Where:

θ_1, θ_2 - are two roots of Underwood's equation at the minimum reflux condition. They must be within the following ranges: $\alpha_A > \theta_1 > \alpha_B > \theta_2 > \alpha_C$

$$(1 - q_1) = \sum_{i=A}^C \frac{\alpha_i \cdot z_i}{\alpha_i - \theta}$$

Where: $q_1 = \frac{\bar{L}_1 - L_1}{F}$ - the quality q_1 is the liquid fraction of the feed of the first column.

And the minimum vapor flowrate in the prefractionator:

Chapter 3: Design methodology of divided wall column

$$V_{1,\min} = \sum_{i=A}^C \frac{\alpha_i \cdot x_{i,D_1} \cdot D_1}{\alpha_i - \theta}$$

And we choose:

$$V_{1,\min} = \max\{V_{1,\min}(\theta_1); V_{1,\min}(\theta_2)\}$$

3.1.3.2 Minimum vapor flow rate of column II

The stream from the top of column I to the feed of column II is a saturated vapor flow rate (V_1) and a saturated liquid flow rate returning (L_1) to column I. These interconnecting flows can be modified by an equivalent feed stream with a superheated vapor condition.

The quality of the feed for the column II is:

$$q_2 = \frac{\bar{L}_2 - L_2}{D_1} = -\frac{V_{1,\min} - D_1}{D_1}$$

At the minimum reflux condition, the Underwood's equation can be written as:

$$(1 - q_2) = \sum_{i=A}^C \frac{\alpha_i \cdot x_{i,D_1}}{\alpha_i - \theta'}$$

Where:

θ'_1, θ'_2 are two roots of Underwood's equation at the minimum reflux condition. They must be within the following ranges: $\alpha_A > \theta'_1 > \alpha_B > \theta'_2 > \alpha_C$

And the minimum vapor flowrate in the column II is:

$$V_{2,\min} = \sum_{i=A}^C \frac{\alpha_i \cdot x_{i,D_2} \cdot D_2}{\alpha_i - \theta'}$$

And we choose:

$$V_{2,\min} = \max\{V_{2,\min}(\theta'_1); V_{2,\min}(\theta'_2)\}$$

3.1.3.3 Minimum vapor flow rate of column III

The stream from the bottom of the column I used as the feed of column III represents actually two streams : a saturated liquid flow rate (\bar{L}_1) and a saturated vapor flow rate (\bar{V}_1) returning in the column I. These interconnecting flows can be modified by an equivalent feed stream with a sub-cooled liquid condition. The quality of the feed for the column III is:

$$q_3 = \frac{\bar{L}_3 - L_3}{W_1} = \frac{V_{1,\min} - D_1 + q_1 \cdot F}{W_1}$$

At the minimum reflux condition, the Underwood's equation can be written:

Chapter 3: Design methodology of divided wall column

$$(1 - q_3) = \sum_{i=A}^C \frac{\alpha_i \cdot X_{i,W_1}}{\alpha_i - \theta''}$$

Where:

θ_1'' , θ_2'' are two roots of Underwood's equation at the minimum reflux condition. They must be within the following ranges: $\alpha_A > \theta_1'' > \alpha_B > \theta_2'' > \alpha_C$

And the minimum vapor flowrate in the column III is:

$$\bar{V}_{3,\min} = - \sum_{i=A}^C \frac{\alpha_i \cdot X_{i,W_3} \cdot W_3}{\alpha_i - \theta''}$$

And we choose:

$$\bar{V}_{3,\min} = \max\{\bar{V}_{3,\min}(\theta''_1); \bar{V}_{3,\min}(\theta''_2)\}$$

3.1.3.4 Minimum vapor flow rate of DWC system

The minimum vapor flowrate from the top of DWC system should be chosen by Halvorsen et al., (2003).

$$V_{\min,DWCs} = \max\{V_{2,\min}, \bar{V}_{3,\min} + (1 - q_1) \cdot F\}$$

3.1.3.5 Number of stages for each section of the DWC system

The minimum reflux ratio of the DWC system can be calculated as:

$$R_{\min} = \frac{V_{\min,DWCs}}{D_2} - 1$$

The operating reflux ratio of the DWC system can be chosen between:

$$1.2R_{\min} < R < 1.5R_{\min}$$

The liquid and vapor splits between the prefractionator and the main column can be defined as:

$$R_L = \frac{L_1}{L_2}$$

$$R_V = \frac{\bar{V}_1}{\bar{V}_3}$$

Starting from the structure as shown the Figure 3.2, an evaluation of the NTS for each section and the reflux ratio for each column are computed based on the shortcut method using the Fenske, Underwood, Gilliland and Kirkbride equations by Kister (1992). The minimum number of stages can be determined by the Fenske equation for column i:

$$N_{i,\min} = \frac{\ln(S)}{\ln(\alpha_{av})}$$

Chapter 3: Design methodology of divided wall column

Where S was given by the equation:

$$S = \left(\frac{x_{LK}}{x_{HK}} \right)_{D_i} \cdot \left(\frac{x_{HK}}{x_{LK}} \right)_{W_i}, i = 1, 2, 3$$

Then, we calculate the number of stages by using the Gilliland equations:

$$Y = 0,75 \cdot (1 - X^{0,5668})$$

Where X and Y was given by equation:

$$X = \frac{R - R_{\min}}{R + 1}$$

$$Y = \frac{N - N_{\min}}{N + 1}$$

Feed location in each column can calculate by the Kirkbridge equation:

$$\left(\frac{N_R}{N_S} \right)_i = \left\{ \left(\frac{z_{HK}}{z_{LK}} \right)_i \cdot \left(\frac{x_{LK,W_i}}{x_{HK,D_i}} \right)^2 \frac{W_i}{D_i} \right\}$$

3.1.3.6 Estimating the composition of interconnecting streams

To simulate the system in ProSim^{plus} software, the composition of interconnecting streams must be estimated. They can be approximated by solving the feed line and the operating line of columns II and III. Ramirez Corona, N et al., (2010) suggested that:

The composition of upper interconnecting stream is:

$$x_{i,L1} = \frac{x_{i,D1} \cdot (R_2 + 1) + x_{i,D2} \cdot (q_2 - 1)}{R_2 + q_2}$$

$$y_{i,V1} = \frac{R_2 \cdot x_{i,D1} + q_2 \cdot x_{i,D2}}{R_2 + q_2}$$

The composition of lower interconnecting stream is:

$$x_{i,\bar{L}1} = \frac{x_{i,W1} \cdot (R_3 + 1) + x_{i,S} \cdot (q_3 - 1)}{R_3 + q_3}$$

$$y_{i,\bar{V}1} = \frac{R_3 \cdot x_{i,W1} + q_3 \cdot x_{i,S}}{R_3 + q_3}$$

3.1.4 Technological and hydrodynamic aspects

3.1.4.1 Technological aspect

Divided wall columns can be equipped with trays as well as with random or structured packing. For the tray column or packing column, the number of stages or HETP (Height Equivalent to Theoretical Plate) of the dividing wall can be different or equal on the two sides of the wall. However, if it differs, in the case using the same packing for either side of

Chapter 3: Design methodology of divided wall column

the wall, extending the wall to include more stages or HETP may help improve one side but it will also increase the cost of the other side. In the case of using different packing, it is difficult to determine very precisely the HETP for each side of column and moreover it is not necessarily always best to equalize the number of stages on the two sides of the wall. Clearly, investment costs can be reduced if the number of stages on the two sides of the wall are the same. Therefore, concerning the aspect of technology, it is easier if the number of stages or HETP in the prefractionator and the side section are the same.

The value of the liquid splits must be found to get this condition because the liquid split affects the internal reflux ratios in each section of the column as shown as figure 3.3. If the liquid split increases there is a larger internal liquid stream in the prefractionator. This leads to fewer stages in the prefractionator and more stages in the side section. If liquid split decreases, the internal liquid stream in the prefractionator is less, leading to more stages in the prefractionator and fewer stages in the side section. Therefore, we can find the liquid split value in order to obtain the condition 1:

$$N_1 + N_2 = N_4 + N_5$$

Firstly, we chose a value of liquid split (R_L), if it is not in agreement with condition 1 we adjust the liquid split until the number of stages are equal.

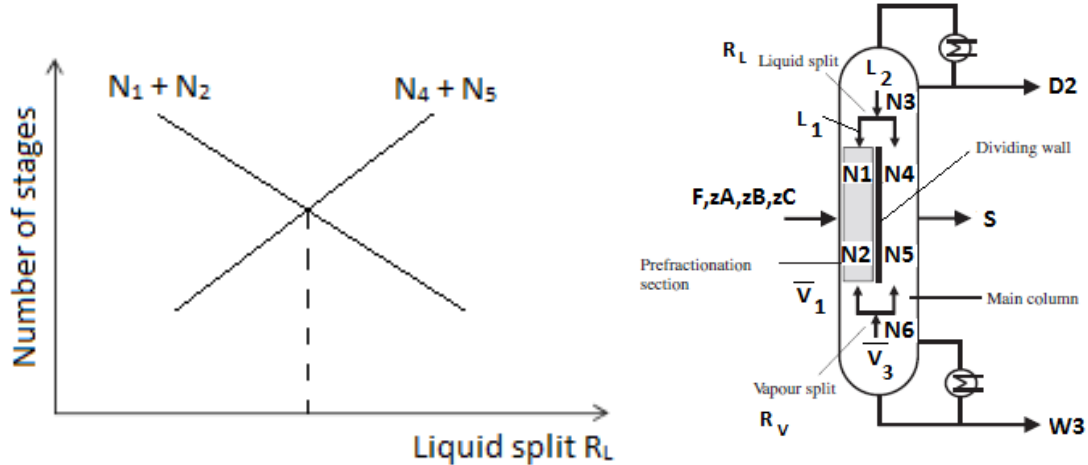


FIGURE 3.3 The detailed structure and operating variables of a divided wall column

3.1.4.2 Hydrodynamic aspect

The quality of a stream (q) is the liquid fraction of the stream. That means that qF is the quantity of liquid contained in the feed and $(1 - q)F$ is the quantity of the vapor in the feed stream. The quality of the feed affects to the operation of the divided wall column. Table 3.2

Chapter 3: Design methodology of divided wall column

shows the relationship between feed quality and internal flows in which L (V) and \bar{L} (\bar{V}) are the liquid (vapor) flowrates in the rectifying and stripping sections, respectively.

TABLE 3.2 Relationship between feed quality and internal flowrates

Feed condition	q	Equations	Relationship between	
			L and \bar{L}	V and \bar{V}
Sub-cooled liquid	> 1	$q = 1 + \frac{C_{pL}(T_{BP} - T_f)}{H_V}$	$\bar{L} > L$	$\bar{V} > V$
Saturated liquid	1	$q = 1$	$\bar{L} > L$	$\bar{V} = V$
Vapor – liquid mixture	$0 < q < 1$	q = molar liquid fraction of feed	$\bar{L} > L$	$\bar{V} < V$
Saturated vapor	0	$q = 0$	$\bar{L} = L$	$\bar{V} < V$
Superheated vapor	< 0	$q = \frac{-C_{pV}(T_f - T_{DP})}{H_V}$	$\bar{L} < L$	$\bar{V} < V$

Concerning the hydrodynamic aspects of the distillation process, the patent of Kaibel et al., (2006) defined gas loading factor, or F-factor, as a measure of the maximum allowable vapor velocity for the column, in the divided wall column.

The F-factor is:

“The product of the gas velocity u_G of dimensions ms^{-1} , multiplied by the square root of gas density ρ_G of dimensions kgm^{-3} ”.

Therefore, F – factor can determine:

$$F = u_G \sqrt{\rho_G}$$

The figure 3.4 shows that the dividing wall divides the column into four sections (b) , (c), (d) and (e).

Figure 3.4 (a) shows the dividing wall is constructed with a central or off-center dividing wall, thus the cross-sectional area of the feed section (b and c) equals or differs to the cross-sectional area of the side section (d and e). Figure 3.4(b) and 3.4(c) describes a divided wall column having an off-center dividing wall in which the cross-sectional area A_b of the section b is smaller or larger than the cross-sectional area A_d of the section d and the cross-sectional area A_c of the section c is larger or smaller than the cross-sectional area A_e of the section e.

Kaibel et al., (2006) claimed that the divided wall column performs best if the F-factor remained the same in all sections of the DWC system.

$$F_i = (u_G \cdot \sqrt{\rho_G})_i ; (i = \text{section b, c, d, e})$$

That means, condition 2 is given as:

$$F_b = F_d = F_c = F_e = \text{constant}$$

Chapter 3: Design methodology of divided wall column

The feed quality (q) and the side stream quality (q_s) affect to the liquid and vapor flowrate in each section b, c, d, e in the divided wall column. The feed quality is a specification while the side stream quality is a variable to get condition 2. Figure 3.5 provides the procedure for optimal design and operation of the divided wall column.

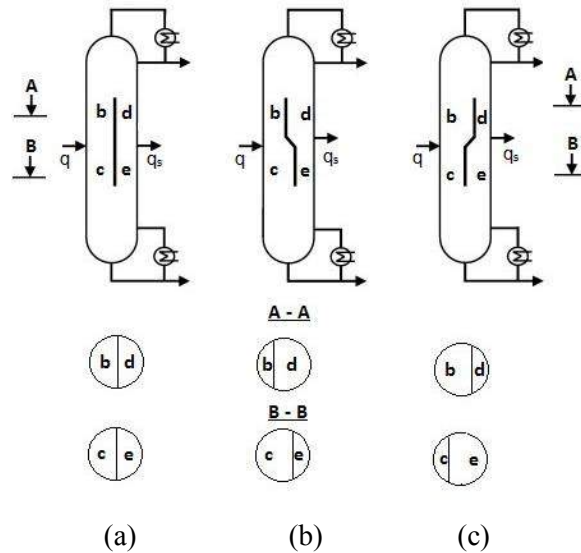


FIGURE 3.4 Types and positions of dividing wall in the DWC system

It is noted that if the feed quality is a saturated liquid ($q = 1$) the internal vapor flowrates in each section of the divided wall column are constant as shown in table 3.2. That means that side quality is also always a saturated liquid. Therefore, the dividing wall should be constructed with a centrally or off-center arranged dividing wall as in figure 3.4 (a). If feed quality is lower than 1 the internal vapor flowrate in the stripping section is less than in the rectifying section. Therefore the off-center dividing wall should be used as in figure 3.4 (c). If feed quality is higher than 1, the dividing wall as shown in figure 3.4 (b) should be used.

Chapter 3: Design methodology of divided wall column

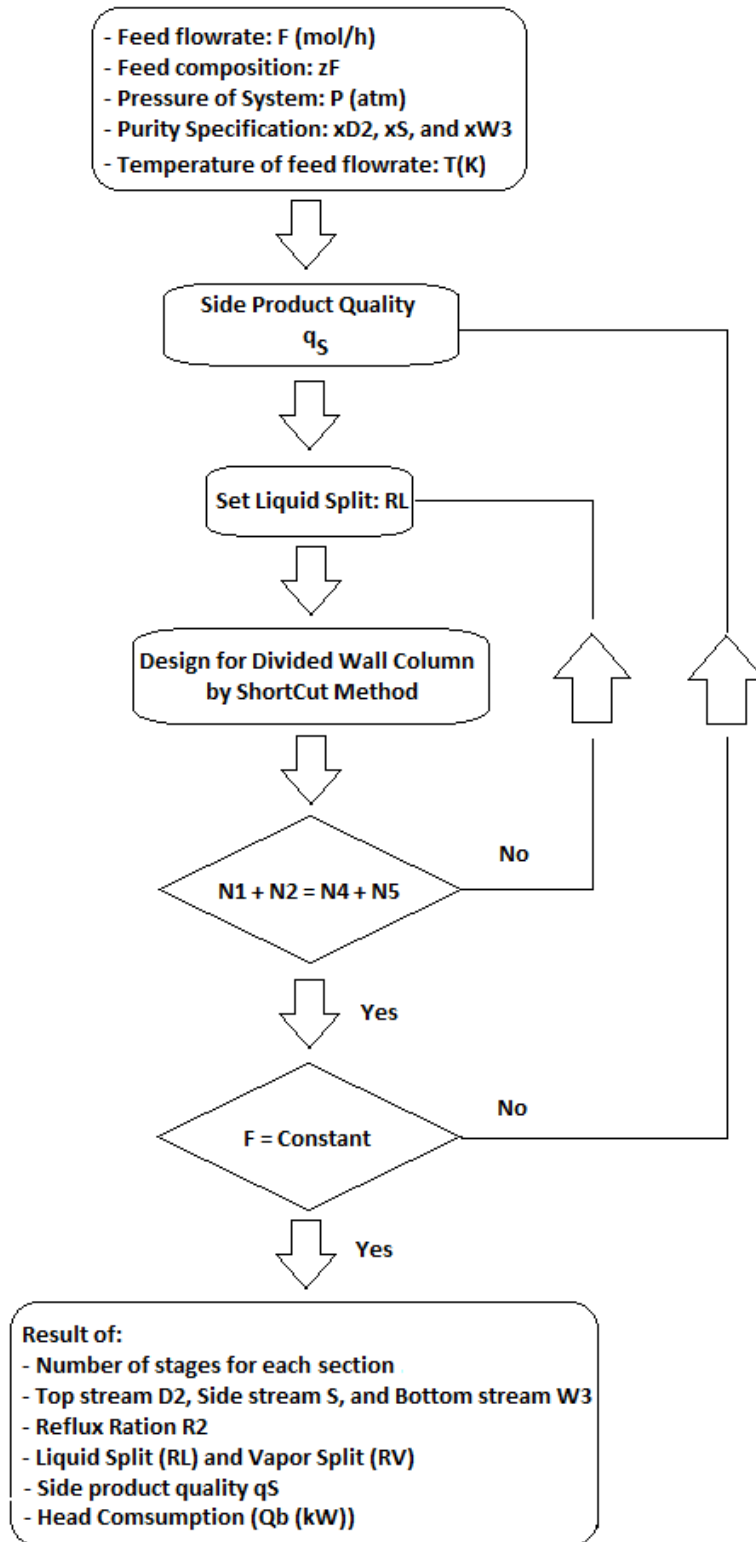


FIGURE 3.5 A procedure for design of divided wall columns

3.2 SIMULATION WITH PROSIM^{PLUS} SOFTWARE

3.2.1 The model used for simulation

There is no standard model for the simulation of a divided wall column in commercial software. As showed in Chapter 2, there are four possible models for simulation: –pump around sequence, two - column sequence with prefractionator, two - column sequence with postfractionator, and four – column sequences. For the pump around sequence, Becker, H et al., (2001) reported that the model can lead to convergence problems because in two points of the column entire vapor and liquid are drawn off, and none remains to “flow” to the next tray. The four-column sequence model reflects the actual situation best, but it is most difficult to initialize, because initial values of more interconnecting streams are required. It is also the slowest model to converge. It is considered for use with dynamic simulations (H. Ling and W.L. Luyben, 2009).

Based on these reasons, the two – column sequence with prefractionator will be used to simulate the system in ProSim^{plus}. As show in Figure 3.6, the first column is considered as the prefractionator and the second column as the main column. The interconnecting streams 2, 3, 4, and 5 connect the two columns. The top, side and bottom product are the stream 6, 7, and 8, respectively and the feed flow rate is stream 1.

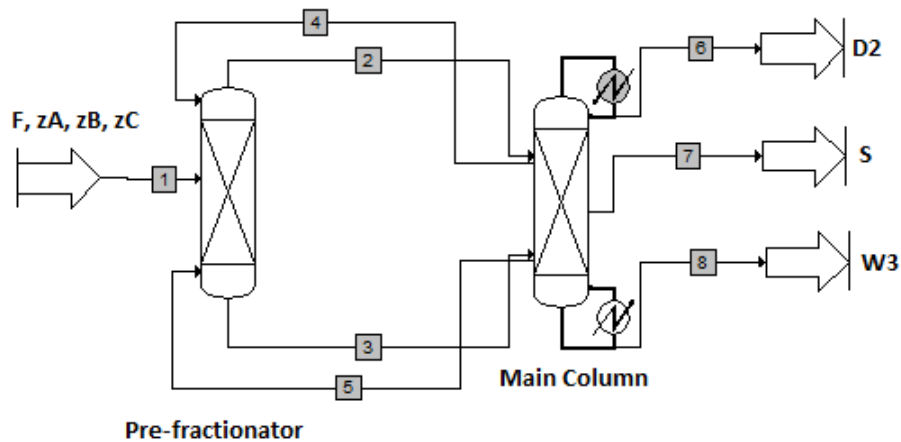


FIGURE 3.6 The model for simulation of the DWC system by ProSim^{plus} software

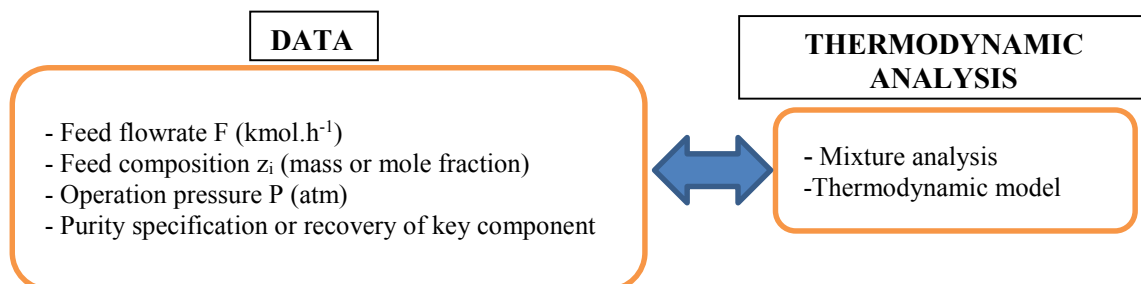
3.2.2 Initial parameters for simulation

Chapter 3: Design methodology of divided wall column

The structural and operational parameters are determined by shortcut method, they are used as initial parameters for the simulation in ProSim^{plus} as shown in figure 3.7.

- Firstly, Simulis thermodynamic is used to calculate relative volatilities of the components.
- Secondly, Excel calculates various parameters of the divided wall column in an Excel worksheet such as number of stages, product flowrate streams, recovery of components, internal liquid and vapor in the prefractionator and main column, etc.
- Finally, data from the shortcut results were inputted into the ProSim^{plus} software.

Besides the above necessary information, it is noted that the composition, temperature, and flowrates of interconnecting streams [2], [3], [4], and [5] must be set in the model. Streams [2] and [3] are set as the initial data and streams [4] and [5] are fixed based on the liquid and vapor splits. If they are not specification, the simulation runs cannot work. Not only because the stream [1] is the feed stream but also because streams [4] and [5] are the feed streams for the prefractionator. Therefore, they must be specified for the initial run of the simulation.



SHORTCUT RESULTS

DATA FOR SIMULATION

FIGURE 3.7 Initial parameters need for simulation by ProSim^{plus}

3.3 CASE STUDIES

3.3.1 Separation of ternary mixture

3.3.1.1 Ideal ternary mixture

The separation of a ternary mixture, Benzene, Toluene, and o-Xylene, is carried out in a divided wall column. The mixture has been studied in several articles (Kolbe, B et al., 2004; Sotudeh et al., 2007; H. Ling and W.L. Luyben., 2009; A.A. Kiss et al., 2011). The feed flowrate is $100\text{kmol}\cdot\text{h}^{-1}$ and contains 33.33 % mole fraction Benzene, 33.34% mole fraction Toluene, and 33.33% mole fraction o-Xylene. The feed quality (q_1) is equal to 1. The operating pressure is 1 atm. The specifications for the product purities for distillate and bottom products are 98 % mole fraction and the side product is 95 % mole fraction.

Firstly, the shortcut design procedure determines the structural and operational parameters of the divided wall column. Then, steady-state simulations were carried out in ProSim^{plus} software. Figure 3.8 provides the results of design parameters for the divided wall column, while table 3.2 shows the relative error between the specified product purities and simulation results of the key components. Notice that in order to simulate in ProSim^{plus}, the information required to initialize a simulation is given from the figure 3.7.

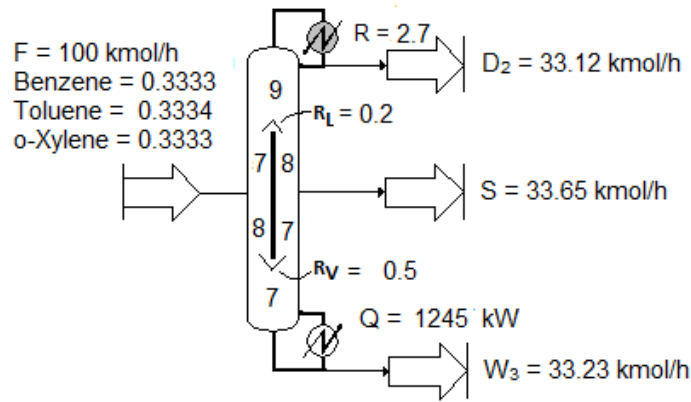


FIGURE 3.8 Design parameters for the divided wall column

Based on the volatilities of the components, benzene is the lightest component and is collected as distillate product, toluene is the distributed component collected in the side stream, and o-Xylene is the heaviest component collected as the bottom product.

In figure 3.8, the structure of the divided wall column consisted of 31-stages, with 15-stages in the pre-fractionator located between stages 9 and 24, the feed location is at stage 16, the

Chapter 3: Design methodology of divided wall column

side stream at stage 17, a liquid and vapor split of 0.2 and 0.5, respectively, the reflux ratio of 2.7 and a reboiler duty of 1245 kW.

TABLE 3.3 Relative errors between specify product purity and simulation of key component

Key component	Specification of products	Simulation	Relative error (%)
Benzene	$x_{B,D2} = 0.98$	$x_{B,D2} = 0.990$	1.02
Toluene	$x_{T,S} = 0.95$	$x_{T,S} = 0.946$	-0.42
o-Xylene	$x_{X,W} = 0.98$	$x_{X,W} = 0.966$	-1.42

The table 3.3 compares the specification of key product purities with simulated results. The results show that the purity of Toluene in the side product and purity of o-Xylene in the bottom product do not reach the specification in the simulated results whereas the purity of benzene at top product is reach (99% mole).

In order to achieve the specified purities of Toluene and o-Xylene, the reflux ratio (R_2), side stream (S) and liquid split (R_L) need to be adjust slightly. The reflux ratio is adjusted to achieve purity of benzene in the distillate product, the side stream is adjusted to achieve purity of toluene in the side stream, and liquid split is adjusted to achieve purity of o-Xylene in the bottom product. The results show that the reflux ratio increases from 2.7 to 3.2 (roughly an 18.5 % increase), liquid split increases from 0.2 to 0.24 (roughly a 20 % increase). The side product remains the same. Thus, the energy duty increases from 1245 kW to 1267 kW (roughly a 1.7 % increase) due to the increased reflux ratio.

3.3.1.2 Non-ideal ternary mixture

Our procedure is also applied for a non-ideal mixture composed of methanol of 33.33 % mole fraction, water of 33.34% mole fraction, and n,n dimethyl formamide of 33.33 % mole fraction, the feed flowrate is $100\text{kmol}\cdot\text{h}^{-1}$, the feed quality is equal to 1, the operating pressure is 1 atm and the specified product purity of the key components is greater than or equal to 95 % mole fraction. The NRTL model was selected to calculate the volatilities of the components for the simulation. The thermodynamic parameters are presented in Appendix [2A].

Chapter 3: Design methodology of divided wall column

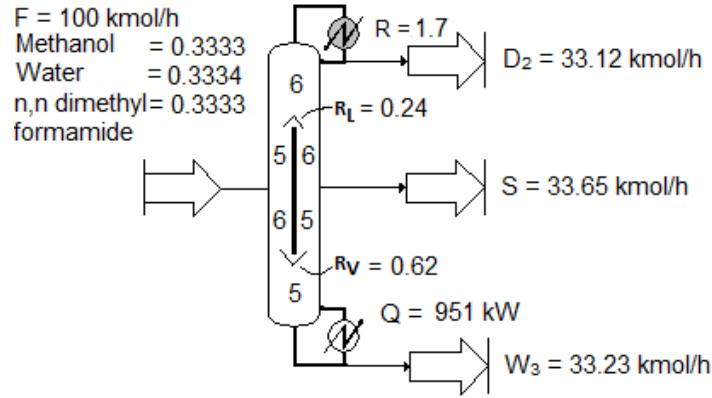


FIGURE 3.9 Design parameters for the divided wall column

Figure 3.9 shows the resulting design parameters for the divided wall column with 22 stages. The prefractionator has 11 stages and is located between stages 6 and 17. The feed stage is on stage 11 and the side stream on stage 12. The liquid and vapor split are 0.24 and 0.62, respectively, the reflux ratio is 1.7 and the reboiler energy consumption is 951 kW.

TABLE 3.4 Relative errors between specified product purity and simulation results for key components

Key component	Specification of products	Simulation	Relative error (%)
Methanol	$X_{M,D2} = 0.98$	$X_{M,D2} = 0.984$	0.41
Water	$X_{W,S} = 0.95$	$X_{W,S} = 0.930$	-2.11
n,n dimethyl formamide	$X_{DF,W3} = 0.98$	$X_{DF,W3} = 0.956$	-2.45

The table 3.4 presents the results comparing the specified product purities and the simulated results.

The results for non-ideal mixtures are similar to the results of ideal mixtures in that the purity of water and n.n dimethyl formamide in the side and bottom product do not reach the specified level in the simulation results. Thus the reflux ratio is increased from 1.7 to 1.78 (roughly a 4.7 % increase), the liquid split is decreased from 0.24 to 0.1 (roughly a -58 % decrease). Therefore, the energy duty increases from 951 kW to 1000 kW (roughly a 5% increase).

Based on tables 3.2 and 3.3, the maximum relative error of the non-ideal mixture is higher than the maximum relative error of the ideal mixture. The maximum relative error of the non-ideal mixture is -2.45% while that of the ideal mixture is -1.42%. The energy duty increases

Chapter 3: Design methodology of divided wall column

for the non-ideal mixture by +5 % while that of the ideal mixture increases by +1.7%. Clearly, the procedure used for the ideal mixture gives better results than for the non-ideal mixture. The constant relative volatilities assumption is well adapted for ideal mixtures and is not relevant for non-ideal mixtures.

3.3.2 Separation of a mixture with more than three-components

When three-component mixture A, B, and C are separated in the divided wall column, the lightest component A is collected in the distillate product, the middle component B is collected in the side stream, and the heaviest component C is collected in the bottom product. Therefore, three pure components can be obtained in three product streams. However, if the separation of a mixture has more than three components in the divided wall column, it is difficult to obtain each pure component. This section develops the procedure for multicomponent mixtures. The separation of a four-component mixture will be considered.

The separation of a four-component mixture composed of methanol (A) 40% mole fraction, isopropanol (B) 30% mole fraction, 1-propanol (C) 20% mole fraction, and 1-butanol (D) 10% mole fraction is considered. Feed flowrate is 100kmol/h, feed quality is 1, and operating pressure is 1 atm. The desired side product is isopropanol. Therefore, the distillate product contains methanol and a little isopropanol, and the bottom product contains a little isopropanol, 1-propanol, and 1-butanol.

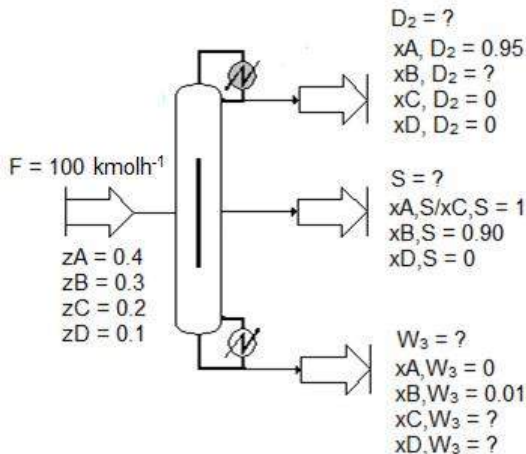


FIGURE 3.10 Specified variables for four-component mixture in divided wall column

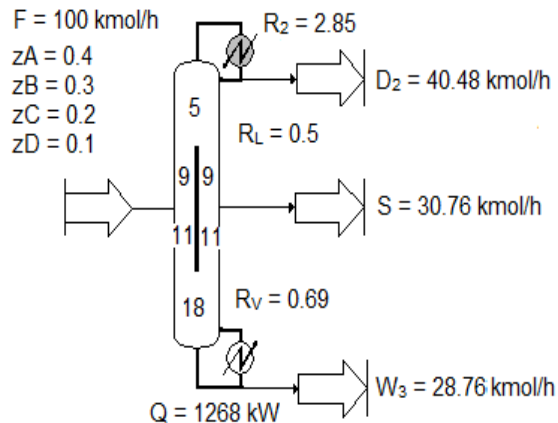


FIGURE 3.11 Design parameters for the divided wall column

Chapter 3: Design methodology of divided wall column

In the case of the four-component mixture, from the balance equations, there are seven equations with fifteen unknown variables. Therefore, to solve the balance equations, 8 variables have to be specified:

$x_{A,D2}$; $x_{C,D2}$; $x_{D,D2}$; $x_{B,S}$; $\frac{x_{A,S}}{x_{C,S}}$; $x_{D,S}$; $x_{A,W3}$; $x_{B,W3}$ as shown in the figure 3.10.

In the top product, $x_{A,D2}$ should be specified because it is a key component while $x_{C,D2}$ and $x_{D,D2}$ are set to zero because we have made the assumption that heavier components are not present in the top product. In the side product, $x_{B,S}$ is the key component so it is specified. The composition of component A and C also should be known. Therefore $x_{A,S}$ or $x_{C,S}$ or $\frac{x_{A,S}}{x_{C,S}}$ should be specified. Finally, in the bottom product, the lightest component A ($x_{A,W3}$) is fixed as zero and the composition B ($x_{B,W3}$) is specified.

In this case, the methanol is specified at 95 % mole in the top product, isopropanol is specified at 90 % mole in the side stream and isopropanol is specified at 1 % mole instead of 1-propanol or 1-butanol in the bottom product as shown in Figure 3.10.

Firstly, the shortcut design procedure determines the structural and operational parameters of the divided wall column. Then, the simulation of the divided wall column is carried out in ProSim software. The results of structural and operational parameters from the shortcut method are shown in figure 3.11 and relative errors of key components in the product streams are shown in the table 3.4.

The results show that the divided wall column has 43 stages in which the number of stages in the prefractionator is 20 stages. Feed and side positions are located at stage 14. The liquid and vapor splits are 0.5 and 0.69, respectively. The reflux ratio is 2.85 and the reboiler duty of 1268 kW.

TABLE 3.5 Relative errors between specified product purity and simulation of key components

Key component	Specification of products	Simulation	Relative error (%)
Methanol	0.95	0.918	- 3.36
Isopropanol	0.90	0.860	- 4.44
Isopropanol	0.01	0.0096	- 4.00

The table 3.5 shows that all relative errors are negatives that means that the simulated results do not reach to the specification. All relative errors are less than -5%.

Chapter 3: Design methodology of divided wall column

In order to achieve the specified purities of key components, the reflux ratio is increased from 2.85 to 4.13 (increasing by about 45%). The liquid split is the same as 0.5 but actually the internal liquid stream L_1 [4] increases from 57.68 kmolh^{-1} to 83.59 kmolh^{-1} . The energy duty increases by approximately 70% from 1268 kW to 2151 kW due to the reflux ratio increase.

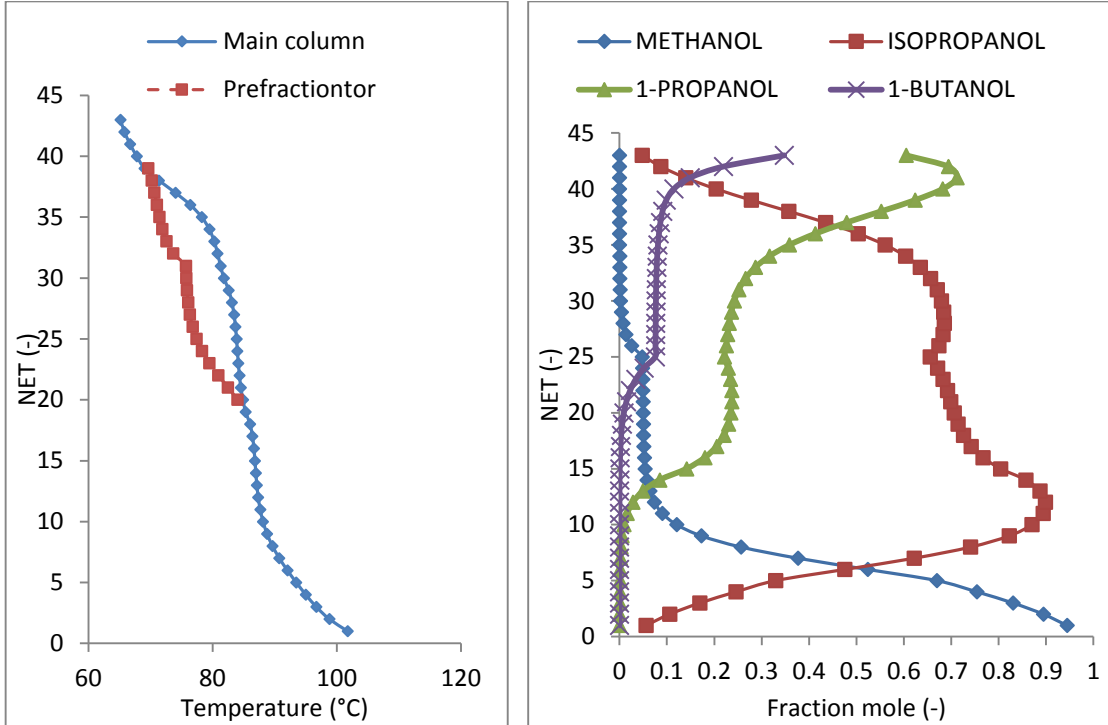


FIGURE 3.12 Temperature and composition profiles in the divided wall column

Figure 3.12 illustrates the temperature and composition profile in the divided wall column. The results show that high purity of methanol is collected in the top column; high purity of isopropanol is collected in the side product; in the bottom, 1-propanol and 1-butanol is collected as a mixture. Therefore, to separate the mixture of 1-propanol and 1-butanol, we need to use more traditional distillation or to use more dividing walls. It is important to note that at the side product, the divided wall column enables us to obtain high isopropanol purity and 1-butanol is not present in the side product thus it is concluded that the divided wall column can still be applied for separation of a four-component mixture.

3.3.3 Conclusion

Even though our case studied requires some slight adjustments to achieve the specified purities of key components, all relative errors in the case studied between specification and

Chapter 3: Design methodology of divided wall column

simulated results are less than 5 %. The relative errors between specification and simulation result in the top product are positive. That means that the purity of the key components reaches the specification. It is noted that the design parameters from the shortcut method can give a good indication of the parameters required to obtain purity of key components for the distillate product. In order to achieve the specified product purities of all key components, reflux ratio and liquid split should be adjusted, thus the required energy duty of the reboiler increases. It is concluded that the method works well not only for ideal or non-ideal ternary mixtures but also with multicomponent mixtures.

3.4 SENSIBILITY ANALYSIS OF DIVIDED WALL COLUMN

In section 3.4, firstly, a design parameter of the divided wall column is determined by our approach. Then, in order to determine the optimal parameters of divided wall columns, the effects of the structural parameters of the divided wall column such as the height of the wall, the vertical position of the wall and number of stages of each section are analyzed. Notice that the purity specifications of key components of product streams have to be obtained in all cases. The ternary mixture consisting of benzene 33.33 % mole fraction, toluene 33.34% mole fraction and o-Xylene 33.33% mole fraction is chosen for investigation, as in section 3.3.1.1.

3.4.1 Effect of the vertical position and height of the wall

The purpose of this section is to investigate how the energy consumption changes when the vertical position and height of the wall change.

Firstly, the vertical position of the wall is moved from the bottom to the top along the column while the height of the wall is constant at 15 stages. The numbers of stages have not changed, and the feed and side stream locations are the same as the shortcut results. The position of the dividing wall is marked as zero in figure 3.11 and is the same position that comes from shortcut results. It is located between stages 9 and 24. In the negative range, the vertical position of the dividing wall is lower than the initial position, and in the positive range, the vertical position of the dividing wall is higher than the initial position.

As in figure 3.15, the heat duty of the divided wall column is lower at the initial position $Q_b = 1245$ kW. The lower or higher the position of the wall, the divided wall column has a higher energy demand. The energy duty of reboiler is 2400 kW when the vertical position of the

Chapter 3: Design methodology of divided wall column

dividing wall is 3 stages lower. It is located between stages 12 and 27. The energy duty of the reboiler is 1850 kW when the vertical position of the dividing wall is 3 stages higher. It is located between stages 6 and 21.

The result shows that the vertical position of the dividing wall from the shortcut results requires less energy when the structure changes.

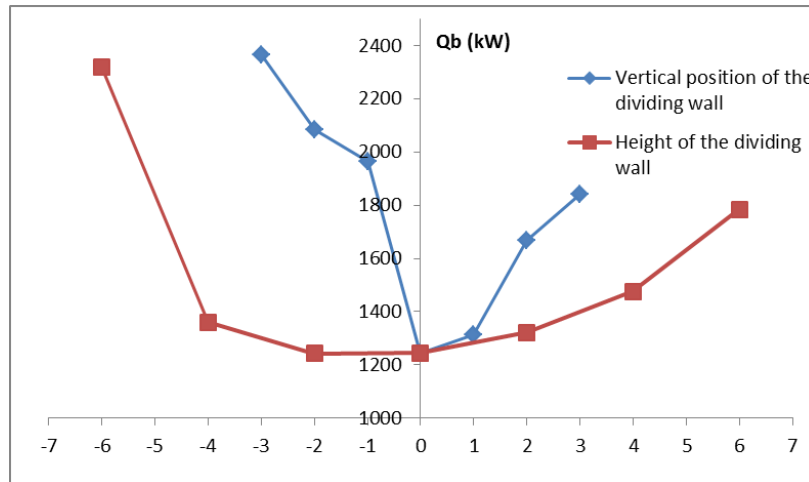


FIGURE 3.15 Effect of the height and vertical position of the wall on the heat duty of reboiler

Secondly, the change of the energy duty of reboiler is also analyzed and compared with the height of the dividing wall. The height of the wall is 15 stages, as per the shortcut result, marked zero in figure 3.15. In the negative range, the number of stages of the dividing wall is decreased while in the positive range, the number of stages of the dividing wall is increased. The feed and side product position remains the same as the initial parameters. The figure 3.15 shows that the energy consumption of the divided wall column is lower if the number of stage decreases from 15 to 13 stages. The energy duty of the reboiler is around 1245 kW. The energy duty of the reboiler increased to 2300 kW when the height of the dividing wall decreases to 9 stages. The energy duty of reboiler also increased to 1800kW when the height of the dividing wall increases to 21 stages.

Clearly, our procedure for design of divided wall columns gives structural parameters corresponding to minimum energy demand of the column.

3.4.2 Effect of the number of stages

Chapter 3: Design methodology of divided wall column

In the section, the change of the energy duty of the reboiler is studied when the number of stages of one section has changed while other sections are fixed the same as initial parameters.

The figure 3.16 shows that the heat duty of the reboiler changes with the number of stages of each section. The initial parameters from the shortcut results are marked zero as shown in the figure 3.15 including $N_1 - 8$ stages, $N_2 - 9$ stages, $N_3 - 9$ stages, $N_4 - 8$ stages, $N_5 - 7$ stages, and $N_6 - 7$ stages. In the negative range, the number of stages decreases and in the positive range, the number of stages increases.

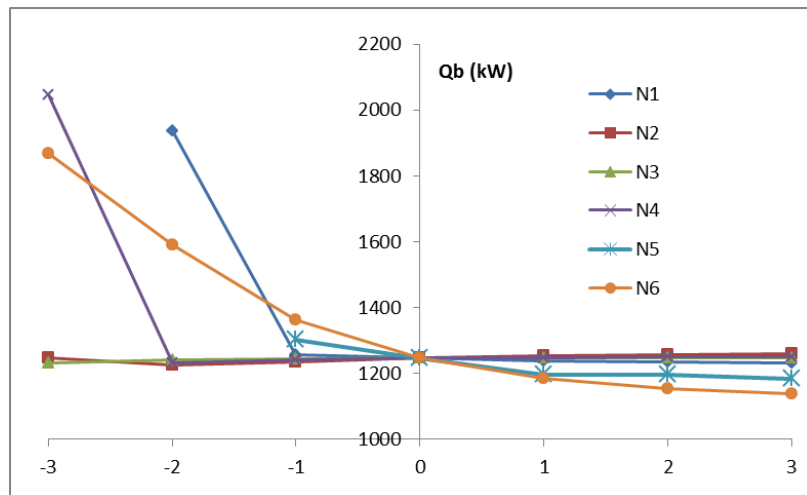


FIGURE 3.16 Effect of number of stages on heat duty of reboiler

The figure 3.16 shows that the heat duty of the reboiler increases when the number of stages of each section decreases. Theoretically, the numbers of stages decreases, in order to retain the specified product purity, the reflux ratio has to increase. Therefore the energy duty of the reboiler will increase.

In figure 3.16, the numbers of stages in the section 1, 4, and 6 has a significant effect on the heat duty of the reboiler while the number of stages in sections 2 and 3 are not affected significantly.

The number of stages in sections 1 and 5 cannot decrease more as the purity specification cannot be reached, regardless of the energy supplied to the column.

The number of stages in each section increases, the energy duty of reboiler slightly decreases as shown in figure 3.16. Clearly, it is important to notice that the number of stages increases that means the capital cost of the system will increase.

3.4.3 Effect of the feed composition and ESI of the mixture on the design of divided wall columns

Three ternary mixtures are considered, each with different values of the ease of separation index (ESI) defined by Tedder and Rudd (1978) and different feed compositions as shown in the table 3.6.

The value ESI equal (or less than, or more than) to 1 that means the split A/B is as difficult as (or more than, or less than) the split B/C.

$$ESI = \frac{K_A K_C}{K_B^2}$$

Where K_A, K_B, K_C are volatilities of component A, B, and C.

Three different feed compositions and purities of the products are assumed in the Table 3.7. The feed flowrate is 100kmolh^{-1} . The operating pressure for each mixture is chosen to ensure the use of cooling water in the condensers.

TABLE 3.6 Three ternary mixtures

Mixture	Components A,B,C	ESI	Pressure (at)
M1	n-pentane/n-hexane/n-heptane	1.04	2
M2	n-butane/i-pentane/n-pentane	1.86	4.7
M3	i-pentane/n-pentane/n-hexane	0.47	2

TABLE 3.7 Three different feed compositions

Feed	Feed Composition (% mole fraction)	Specification of the products A/B/C (mole fraction)
FEED 1	40/20/40	0.99/0.95/0.99
FEED 2	30/40/30	
FEED 3	15/70/15	

Some articles studied the effect of the quantity of middle component (B) and ESI of the mixture to the performance of a divided wall column (K. Muralikrishna et al, 2002; Chu KT et al, 2011). They claimed that these parameters significantly affect the energy consumption and the total annual cost (TAC) of the system. In terms of economic analysis, in this work, to estimates the minimum TAC, the cost function is given by K. Muralikrishna et al., (2002) was used

$$1000TAC = 0.23 * N_{total}(1 + R_2) + 1.98 * (1 + R_2) + 9.35 * (1 + R_2)$$

Table 3.8, figure 3.17 and 3.18 show the heat duty and 1000TAC depend on the feed composition and ESI index. The results show that the energy consumption and the TAC

Chapter 3: Design methodology of divided wall column

increase when the middle component B increases in the feed. The results also show that the energy consumption and the TAC of the system are the lowest when ESI of the mixture is equal to 1. When ESI is smaller or greater than one, the divided wall column needs more energy and the TAC increases. **TABLE 3.8** Energy consumption and TAC of the divided wall column

		Q_b (kW)	1000TAC	Difference between M1 vs M2 and M3 (%)	
FEED 1	M 1	900.162	59.95	-	-
	M 2	1965.47	250.8	19.8	66.7
	M 3	2372.52	306.01	35.0	342.8
FEED 2	M 1	1079.264	99.98	-	-
	M 2	2407.41	432.03	22.4	72.2
	M 3	2616.75	416.14	40.8	355.6
FEED 3	M 1	1215.335	265.5	-	-
	M 2	2767.94	1142.739	10.3	35.9
	M 3	2709.79	921	14.2	200

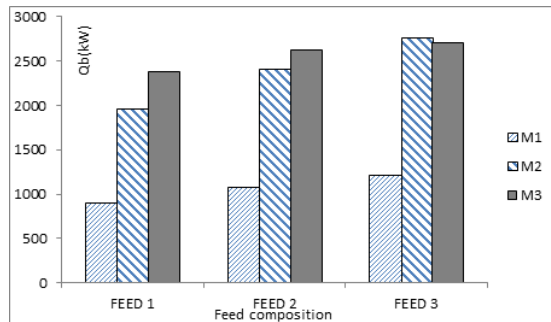


FIGURE 3.17 Heat duty depend on the feed composition and ESI index of the mixture

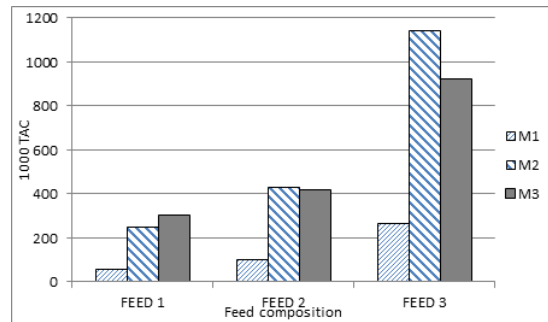


FIGURE 3.18 1000TAC depend on the feed composition and ESI index of the mixture

3.4.4 Energy consumption comparison between traditional columns and divided wall columns

To compare the energy usage of the traditional distillation column and divided wall column, three ternary mixtures are considered with different values of the ease of separation index (ESI) in table 3.6. In this section, the feed composition is shown in table 3.9.

TABLE 3.9 Four different feed compositions

Feed	Feed Composition (% mole)	Specification of the products A/B/C
FEED 1	80/10/10	0.99/0.95/0.99

Chapter 3: Design methodology of divided wall column

FEED 2	10/80/10	
FEED 3	10/10/80	
FEED 4	30/40/30	

The structural parameters and energy duty of conventional arrangements is calculated with the traditional shortcut method that is available in the ProSim^{plus} software, whereas the structural parameters and energy duty of the DWC system is calculated from our procedure. The energy duty comparisons are shown in Table 3.10, Figure 19, 20, and 21.

Clearly, the energy duty of the reboiler is influenced by the feed composition. It increases with the amount of component B. Increasing the amount of component B in the feed composition also increases both the energy duty of the divided wall column and traditional distillation columns. The results in Table 3.10 shows that when component B increases by 10 % mole, 40 % mole, and 80 % mole, the energy duty increases by 779 kW, 1023 kW, and 1104 kW in the mixture M1, respectively. The trend is the same for mixture 2 and 3. The type of mixture also effects the energy duty of the reboiler. The lowest energy duty is observed for the mixture 1 which has an ESI value equal to 1, and it is higher for mixture M2 and M3 which have ESI values higher or lesser than 1.

The results also show that when the amount of component B in the ternary mixture is lower than other components, the traditional distillation column should be chosen. In the case M1-FEED1, M2-FEED1 and M3-FEED1, the direct sequence should be chosen instead of the DWC system because it needs the lowest or at least equal energy duty of the reboiler. In the case M1-FEED3, M2-FEED3, and M3-FEED3, the divided wall column or indirect sequence should be chosen. Although the energy usage of the divided wall column is better than the traditional distillation column the difference is not very large (less than 10%). If the amount of component B in the ternary mixture is larger than other components the energy duty can be reduced by up to 33 % when compared with a traditional distillation. Therefore, in these cases, the divided wall column should be used.

TABLE 3.10 Energy duties of the arrangements

		Heat duty Q_b (kW)			% saving energy relative to DWC	
		DWC	Direct Sequence	Indirect Sequence	Direct sequence	Indirect Sequence
M1	FEED 1	942	628	1314	-50	28
	FEED 2	1104	1442	1418	23	22

Chapter 3: Design methodology of divided wall column

	FEED 3	779	953	848	18	8.0
	FEED 4	1023	1244	1430	18	28
M2	FEED 1	1139	1163	1709	2.0	33
	FEED 2	2674	3314	3221	19	17
	FEED 3	2640	3384	2919	22	10
	FEED 4	2407	2954	3070	19	22
M3	FEED 1	2977	2721	3477	-9	14
	FEED 2	2326	3000	2942	22	21
	FEED 3	988	1325	1046	25	6.0
	FEED 4	2430	2802	2954	13	18

Based on the discussion, the divided wall column can save energy duty compared with the traditional sequence. However, the selection of the best arrangement is based on the feed composition and ESI value of the mixture.

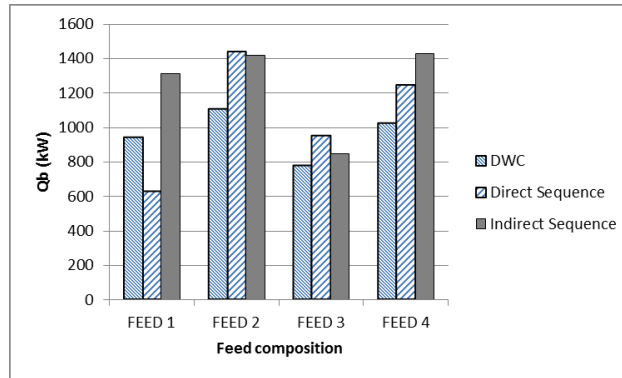


FIGURE 3.19 Energy duty comparison of the mixture M1 (ESI = 1)

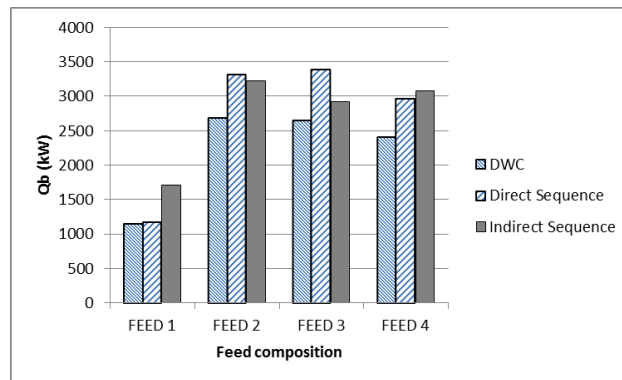


FIGURE 3.20 Energy duty comparison of the mixture M2 (ESI > 1)

Chapter 3: Design methodology of divided wall column

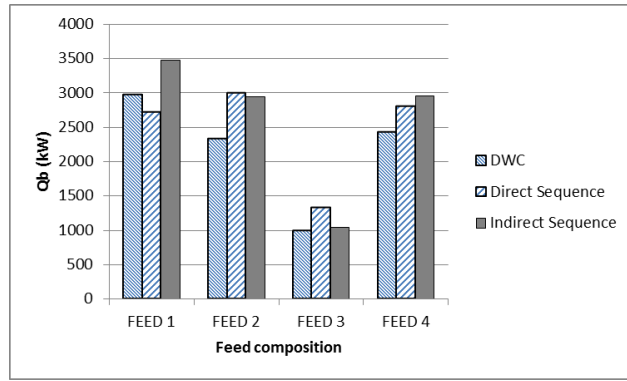


FIGURE 3.21 Energy duty comparison of the mixture M3 (ESI < 1)

A.A Kiss et al., (2012) show a procedure to make the right choice between process heat integration or traditional arrangements based on the difference in boiling points between the top and bottom product (ΔT_b), feed flowrate of each component (F_D – product flowrate at the top of the column, F_S – product flowrate of the side product of the column, and F_W – product flowrate at the bottom of the column), and product purity (x_D , x_S , and x_W).

TABLE 3.11 Comparing the results with the estimations of Kiss et al., (2012)

Mixture		$\Delta T_b \geq 150^\circ\text{C}$	$F_S \geq F_D, F_W$	$x_S \approx x_D, x_W$	Choice of Kiss et al., (2012)	Choice of the study
M1	FEED 1	No	No	Yes	DWC or DC	DC
	FEED 2	No	Yes	Yes	DWC	DWC
	FEED 3	No	No	Yes	DWC or DC	DWC or DC*
	FEED 4	No	Yes	Yes	DWC	DWC
M2	FEED 1	No	No	Yes	DWC or DC	DWC or DC*
	FEED 2	No	Yes	Yes	DWC	DWC
	FEED 3	No	No	Yes	DWC or DC	DWC or DC*
	FEED 4	No	Yes	Yes	DWC	DWC
M3	FEED 1	No	No	Yes	DWC or DC	DC
	FEED 2	No	Yes	Yes	DWC	DWC
	FEED 3	No	No	Yes	DWC or DC	DWC or DC*
	FEED 4	No	Yes	Yes	DWC	DWC

It is noted that the marker (*) means the divided wall column can save energy consumption when compared with a traditional column but it is not huge as shown in Table 3.10. Therefore in these cases we can chose the divided wall column or the conventional distillation column. Based on Table 3.11, the results of the study are agreement with the guess of the Kiss et al., (2012).

Chapter 3: Design methodology of divided wall column

The idea is to build a ternary diagram and find the boundary where the configuration of distillation is most economical. In order to do this, the mixture M3 including i-pentane/n-pentane/n-hexane was chosen. To find out what is the most economical configuration for several compositions of a mixture, the energy consumption is used to compare among a divided wall column, and direct and indirect columns. The lightest component is recovered at the top of the column at 99%, the heaviest component is recovered at the bottom of the column at 99% and the intermediate component is recovered in the middle of the column at 95%.

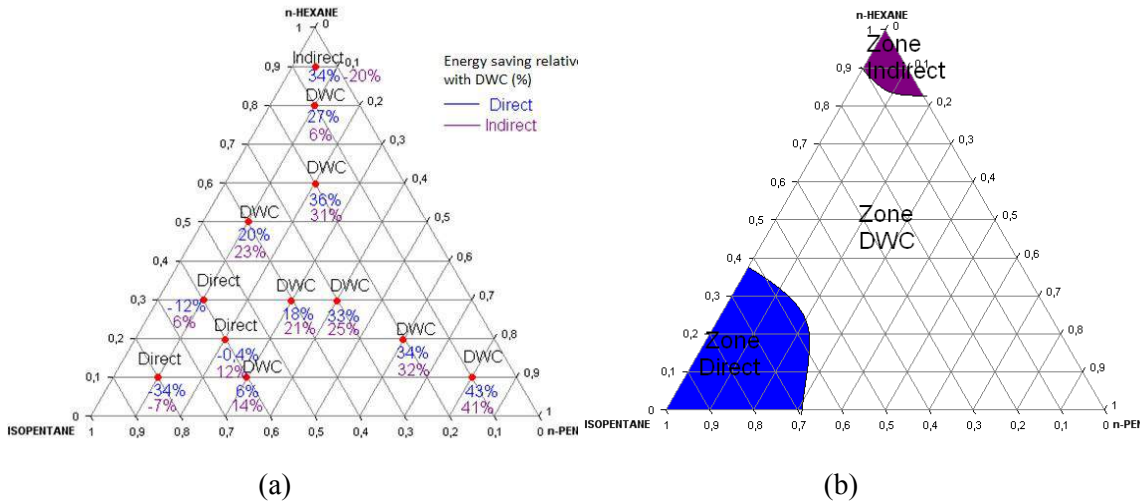


FIGURE 3.32 Comparison energy of use and boundary of distillation

Figure 3.32 (a) shows the energy saving related to the divided wall column while Figure 3.32 (b) shows the distillation zones. In Figure 3.32 (a), the divided wall column can save energy of use up to 43% if the intermediate component is 80% mole fraction. However, if the amount of intermediate component in the feed decreases from 80% to 30%, the energy saving will decrease from 43% to 18%. It is noted that the energy saving depends on the amount of intermediate component in the feed.

Figure 3.32 (b) shows that there are three distillation zones: the direct zone, the indirect zone, and the divided wall column zone, in which, the indirect zone should be used if the amount of the heaviest component is more than 90% mole fraction and the direct zone should be used if the amount of the lightest component is more than 60% mole fraction.

It is concluded that the ternary diagram is useful as an indicator both in showing what is the most economical configuration is and in showing the distillation boundary.

3.5 CONCLUSION OF THE CHAPTER 3

Chapter 3 has proposed a new procedure for optimal design of divided wall columns in which both the structural and operating variables of the system are determined. Our approach has shown that to get the optimal structure the value of the liquid split is adjusted, and to get the optimal performance of the DWC system, the F-factor must remain constant in each section on both sides of the dividing wall by adjusting the value of the side product quality.

Our approach is applied not only for ideal mixture (benzene, toluene, and o-xylene) and non-ideal mixture (methanol, water, and n,n dimethyl formamide) but also for multicomponent mixtures, for instance, four-component mixtures (methanol, isopropanol, 1-propanol, and 1-butanol). The results show that our procedure can give a good initialization for rigorous simulation.

The chapter has also investigated a sensibility analysis of divided wall columns. The energy consumption of the reboiler will be used as performance criteria. The results indicate that the initial structural parameters of the divided wall column determined from our method are a good estimation.

Finally, by applying our procedure, the performance of the traditional arrangements and the divided wall column are compared. The separations of three ternary mixtures with different ESI values and feed compositions are studied. In our study, for most separations, the energy consumption of the DWC system is lower than the traditional arrangements and can save up to 33 %. However, the DWC system is not always the best compared with the conventional arrangements. The selection depends on the feed composition and the ESI value of the mixture.

Chapter 4

PILOT PLANT AND EXPERIMENTAL VERIFICATION: APPLICATION FOR NON-REACTIVE MIXTURE

Chapter 4: Pilot plant and experimental verification

Application for non-reactive mixture

4.1 INTRODUCTION

A lack of knowledge for operation and control of divided wall columns is a significant reason to limit building the system in industry. To understand the process of divided wall columns, laboratory experiments studying divided wall columns need to be carried out. The experimental verification not only demonstrates the functionality and stability of the divided wall column, but also provides the optimum solution and allows feedback for the simulation.

The structures of several pilot plants for non-reactive and reactive mixtures in divided wall columns are listed. Abdul Mutalib et al. (1998a, b) reported the first experimental data for separation of a ternary mixture of methanol, isopropanol, 1-butanol. The feed to the column was equimolar. The specification for each product was 98.5 % mole fraction. Feed flowrate is 75lh^{-1} . The pilot plant uses structured packing material Gempak 4A, and a thin metal plate was placed vertically inside the middle section to form the dividing wall. The ratio of the cross sectional area between the side section and feed section is 1.29. The inner diameter was 0.305m and the total height of column was 10.97m. The operating pressure was 1 atm. The liquid stream from the top section is taken out from the column and stored temporarily in a tank before being split and returned to each side of dividing wall at a ratio of 4.8.

Adrian et al. (2004) reported experiments in a mini plant laboratory at the Ludwigshafen site of BASF Aktiengesellschaft. The mixture includes of butanol 15 % mass, pentanol 70 % mass, and hexanol 15 % mass. Feed flowrate is from 2 to 3kg h^{-1} . The operating pressure is 900 mbar. The divided wall column included four sections: upper and lower sections with inner diameter 55 mm, two parallel sections with inner diameter 40 mm. The total height of the column was 11.5 m.

Strandberg and Skogestad (2006) built a pilot plant of the Kaibel column in the Chemical Engineering Department of NTNU Trondheim. In the study, the four-component mixture included methanol, ethanol, propanol, and butanol. Feed composition is equimolar and feed quality is 0.48. The purity of the top product and bottom product were specified as 0.975 mass fraction and two side products were specified as 0.94 mass fraction. The reboiler is a kettle-type boiler of 3 kW capacity. The internal diameter of all sections is 50 mm. Glass Raschig rings for packing were filled in the column. There are 24 temperature sensors distributed inside the column sections. Dwivedi D et al., 2012 also demonstrated

Chapter 4: Pilot plant and experimental verification

Application for non-reactive mixture

experimentally the startup and steady state operation of a four-product Kaibel column separating methanol, ethanol, propanol, and n-butanol. In the pilot plant, it was possible to adjust the vapor split ratio between the prefractionator and main column by using a valve.

Niggemann et al. (2010) realized the separation of a ternary mixture of n-hexanol, n-octanol, and n-decanol into products with purities of around 99 % mass fraction at Hamburg University of Technology, Germany. The inner diameter of the column was 68 mm and the four column sections each contained a 980 mm bed consisting of Montz B1-500 structured packing. The total height of the divided wall column was approximately 12 m. A welded wall in the middle part of the column divides the column vertically into two parts. The liquid is distributed by a funnel, which is placed above the wall and can move by two electromagnets.

Buck C et al., (2011) reported the systematic development and testing of a decentralized temperature control concept based on simulation and experimental studies. The pilot plant is used for the separation of the fatty alcohols n-hexanol, n-octanol, and n-decanol.

Barroso-Munoz F.O et al., (2010) studied the hydrodynamic behavior of a dividing wall distillation column. The experimental divided wall column had three sections packed with Teflon Raschig rings with a diameter of 20 mm. The diameter and height of the packed bed of the pilot plant are 0.17 and 2 m, respectively.

Sander S et al., (2007) examined the heterogeneously catalyzed hydrolysis of methyl acetate in a reactive dividing wall column. A laboratory scale reactive dividing wall column was installed in a mini plant laboratory at BASF in Ludwigshfen. There are four sections of dividing wall column: prefractionator, side section, upper and lower section. The total packing height of the system is about 6.5 m. The height of the upper and lower sections are 1.5 m and the inner diameter is 55 mm. Both heights of the parallel columns are 3.5 m. The inner diameter of the prefractionator is 50 mm. The inner diameter of the side section is 40 mm. For the non-reactive sections, the structured packing elements are Sulzer CY or Kuhni Rombopak. For the reactive section, Sulzer Katapak-SP 11 is used with Amberlyst 48 as the catalyst. Based on the result of the simulation and the results of the tests at BASF, an industrial scale reactive divided wall column was set up and operated at Sulzer Chemtech in Winterthur. The inner diameter of the column is 220 mm and the total height of the packing

Chapter 4: Pilot plant and experimental verification

Application for non-reactive mixture

section is 14.3 m. The liquid from the top is completely taken out of the column into two defined flows and feed back into the divided sections of the column.

Hernandez S et al., (2009) performed steady state and dynamic simulations of a reactive Petlyuk column through an equivalent reactive divided wall column. In the study, the reaction between ethanol and acetic acid was catalyzed by sulfuric acid to produce ethyl acetate and water. A pilot plant made from stainless steel 316L was constructed. The reactive divided wall column contained three packed sections of Teflon Raschig super-rings. The dividing wall was implemented in the middle section and can move to three positions to manipulate the vapor split. This study focuses on the experimental study of the hydraulics, steady state and closed loop dynamics of the reactive divided wall column.

Delgado R et al., (2012) presented experimental results for the production of ethyl acetate in a reactive dividing wall distillation column. The column has three packed sections with a total height of 2.5 m filled with random packing made of TeflonTM and a dividing wall is located inside the second packed section. The column has six thermocouples in different sections of the column. The liquid from the top of the column can be split to both sides of the dividing wall using a side tank with two valves to manipulate the liquid flows. The vapor flow is not controlled, it depends on the dividing wall position along the column diameter and the pressure drop inside the packed section. Ethanol and acetic acid fed are fed at a rate of 60molh^{-1} to the column.

An overview of the various pilot plants for divided wall columns and reactive divided wall columns is presented. It is noted that most focus is given to the control and hydraulics processes of the column. Furthermore, most authors only separate ternary mixtures apart from Strandberg and Skogestad (2006) who investigated a four-component mixture, carried out in the four-product Kaibel column. Thus, most authors do not consider distribution compositions in the divided wall column if a mixture has more than three components. Furthermore, the pilot plant columns reviewed measure only the composition of products and several temperature points in the pilot plant. Therefore they cannot measure the gradient of composition and temperature along the entire pilot plant column. The composition and temperature profiles are important data for comparison with simulation results. Further pilot plant columns for reactive mixtures are reported in several papers but our knowledge of the reactive divided wall column is still limited. Based on the analysis, our pilot plant column is

Chapter 4: Pilot plant and experimental verification

Application for non-reactive mixture

built for both non-reactive mixtures and reactive mixtures. The composition and temperature along the entire pilot plant column are measured.

TABLE 4.1 Overview of various DWC or RDWC pilot plants

Authors	Structure of pilot plants	Reactive or non-reactive System
Abdul Mutalib et al. (1998)	A thin metal was placed vertically inside the column. Inner diameter 0.305 (m) Total height: 10.97 (m) Operation Pressure: 1 atm Packing: Gempak 4A	Methanol/Isopropanol/1-Butanol
Adrian et al. (2004)	Inner diameter of upper and lower part: 55 mm Inner diameter of the two parallel part: 40 mm Total height: 11.5 m Operation pressure: 900 mbar Feed flowrate: 2 to 3 kg ^h ⁻¹	Butanol/Pentanol/Hexanol
Strandberg and Skogestad (2006); Deepthanshu Dwivedi et al., 2012	Inner diameter of all sections: 50 mm Packing: Glass Raschig rings Reboiler: 3 kW Four products Feed quality: 0.48	Methanol/Ethanol/Propanol/Butanol
Niggemann et al. (2010)	Inner diameter of all sections: 68 mm Total height: 12 m Packing: Montz B1-500 A welded wall inside the column Two electromagnets to control the liquid distribution	n-Hexanol/n-Octanol/n-Decanol
Fabrico et al. (2010)	Inner diameter: 170 mm Total height: 2 m Packing: Teflon Raschig	
Buck et al (2011)		n-Hexanol/n-Octanol/n-Decanol
Sander et al (2007)	Total height: 6.5 m Height and inner diameter of upper and lower part: 1.5 m/ 55 mm Height and inner diameter of the two parallel part: 3.5 m/ 50 mm Non-reactive packing: Sulzer CY or Kugni Rombopack Reactive packing: Sulzer Katapak-SP 11 with Amberlyst 48	Hydrolysis of Methyl Acetate
Salvador Hernandez et al., (2009)	A pilot plant made from stainless steel 316L is constructed. Teflon rasching super-rings	Ethyl acetate production
Raul Delgado Delgado et al.,(2012)	The total height of column is 2.5 m including three sections. Random packing made of Teflo™	Ethyl acetate production

4.2 PILOT PLANT

4.2.1 Setup

Chapter 4: Pilot plant and experimental verification
Application for non-reactive mixture

A pilot plant for the divided wall column was set up in our laboratory (LGC, Toulouse, France, 2013). Figure 4.1 shows the diagram of the pilot plant for separation of a multi-component mixture into three pure products. Appendix [8] shows several figures of our pilot plant.

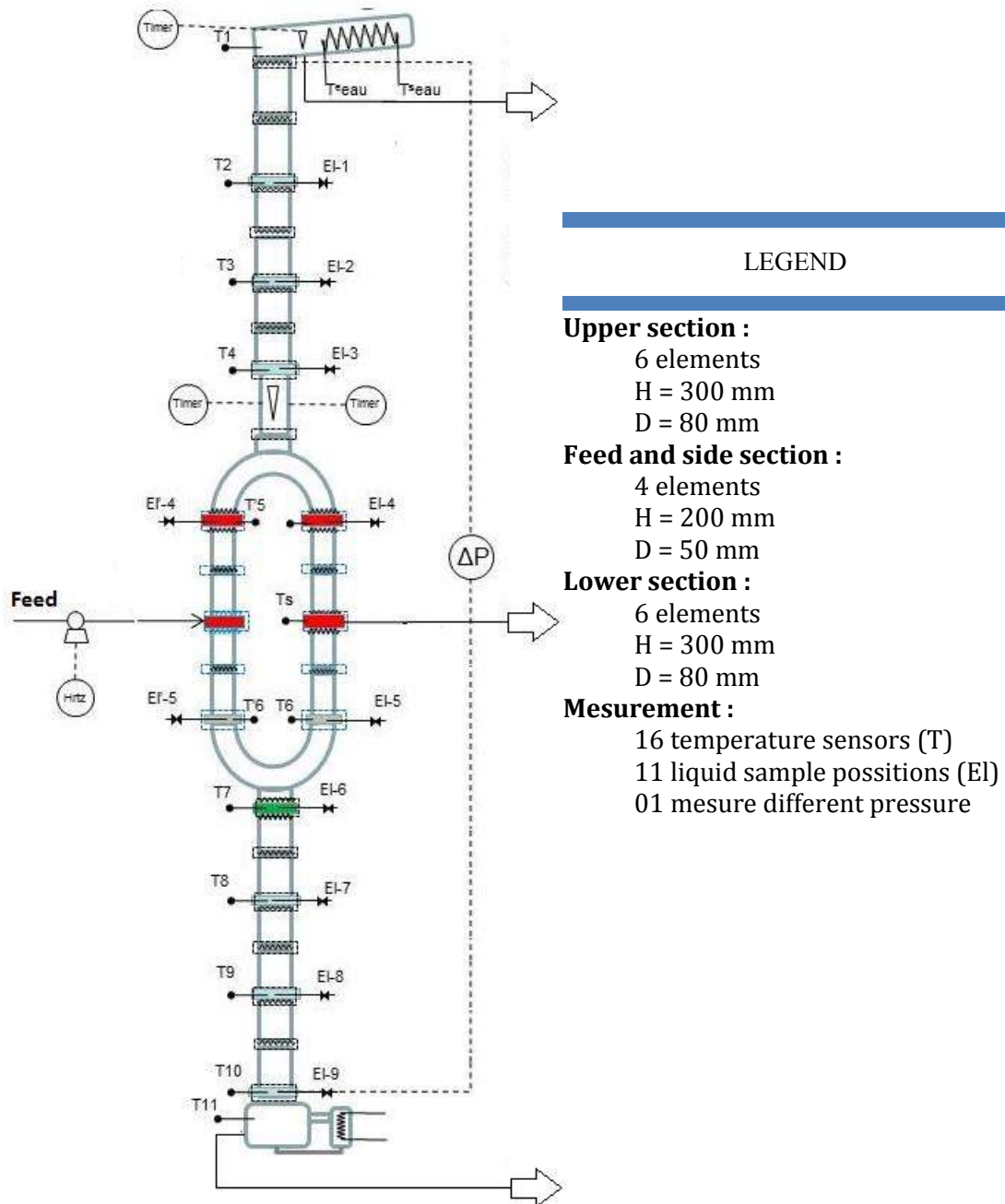


FIGURE 4.1 Flow-sheet of the pilot plant

Total height of the pilot plant is 5.53 m. It is made of glass and operates under atmospheric pressure. The column is divided into three parts. The upper and lower parts of the column

Chapter 4: Pilot plant and experimental verification

Application for non-reactive mixture

have 6 elements each with a height of 0.3 m and an inner diameter of 80 mm. The middle part of the column is divided into the feed section and the side section. Each section has 4 elements with the height of each element being 0.2 m and having an inner diameter of 50 mm. The height of the connecting elements between the upper part and lower part with the middle part are Y-shaped and approximately 280 mm in length. The height of the splitting element is 170 mm. The structured packing used in the pilot plant is Sulzer DX for the separation section and Katapak packing for the reactive section. Our pilot plant has a parallel structure in the middle section. This was chosen due to the small inner diameter. If we put a dividing wall inside, the liquid distribution will be effected. Moreover, the heat transfer across the dividing wall is not considered in the study.

At the top of the column, the condenser is installed and operated with cooling water. The condensate returns to the column due to gravity and a part is taken out as the distillate product through the liquid reflux split valve. The top product is drawn off into a distillate tank. At the bottom of the column, the mixture in the reboiler is heated by a vapor stream. A fraction is taken out as the bottom product. The side product, located at the side section, is cooled by cooling water and is drawn off into the side tank by gravity. The feed stream, from a feed tank through the pump, was heated by a preheater and fed into the feed location in the feed section. The feed flowrate is varied from 5 to 7 kg h⁻¹.

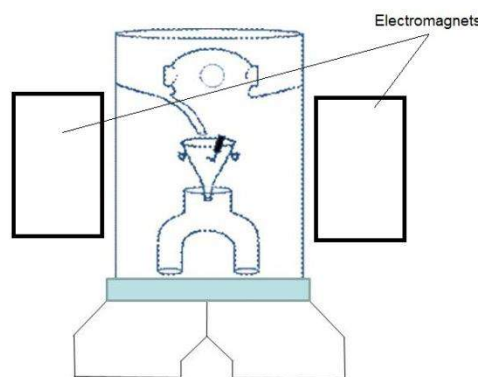


FIGURE 4.2 Liquid splitter

To reduce the heat losses through the wall of the column, a jacket is installed along the entire length of the column. The liquid splitter defines the liquid load between the feed section and the side section. The liquid from the top of the column is drawn off via a funnel which is placed in the splitting element and is moved by two electromagnets to facilitate the liquid distribution to each side of the section. The magnets are fixed on opposing sides of the outer column as shown in Figure 4.2.

Chapter 4: Pilot plant and experimental verification

Application for non-reactive mixture

The vapor is not controlled but is dependant on the inner diameter of the feed and side section and the pressure drop inside the packed section. In our pilot plant, the inner diameters of the feed and side section are the same. Moreover the height of the packing of each section is also the same. Therefore, theoretically, the vapor spilt is around 0.5.

4.2.2 Measurement and startup of the pilot plant

The liquid inlet and outlet streams in the pilot plant are measured by weighing the quantity of liquid collected in the product tanks or lost in the feed tank. The information is noted every 30 min during the steady state experimental runs. The accuracy of a weighing machine is 0.001 g. The pilot plant is equipped with the sixteen temperature sensors (T) along the column, of which, two temperature sensors measure the temperature of cooling water in and out as shown in the flow-sheet in Figure 4.1. All temperatures are automatically recorded. The liquid samples (El) are taken from the feed stream, three products and 11 points along the column. They are analyzed by using gas chromatography as shown in Appendix [7]. Two pressure sensors record the pressure drop between the top and the bottom of the column during pilot plant operation. The heat duty of the system was calculated by measuring the quantity of liquid leaving as condensate from the bottom of the column. The step by step start up procedure of the plant is outlined below:

1. Prepare a mixture with the same composition as the bottom product and fill the reboiler of the pilot plant column.
2. Use the control valve to set the pressure drop across the top and bottom of the column to zero.
3. Open vapor valve to heat the mixture to boiling point. The pilot plant column works under total reflux.
4. Set the required liquid split with the controller timer.
5. Wait until the temperature at the top of the column is stable.
6. Open feed valve and control it to around 6kg h^{-1} . Set the required reflux ratio. Open side product valve and control it to the required value. It is noted that we have to make sure that the side stream leaves as a liquid.
7. Control vapor valve to get the required heat consumption.
8. Wait until the pilot plant column works at steady state condition. Take the samples.

4.2.3 HETP experiment

Chapter 4: Pilot plant and experimental verification
Application for non-reactive mixture

HETP experiments need to be performed to calculate HETP (height equivalent to a theoretical plant) value of the packing used in the pilot plant. The standards for the experimental method of separating a binary mixture at total reflux that are defined by Fractionation Research Inc. (FRI) and Separation Research Program (SPR) will be applied. A standard cyclohexane and n-heptane mixture is carried out in the divided wall column system at atmospheric pressure with different runs. Firstly, the flooding point was determined, then backing off to roughly 20% of the flood flowrate to unload the bed. Secondly, the tests are run at the targeted reboiler duty. The liquid samples were taken only from EI-7, EI-8, and EI-9 with the height of each unit at 0.6 m as shown in Figure 4.1. It is not necessary to analyse more liquid samples as the sample composition has stabilised. The samples are analyzed by a refractometry method in the refractometer to assess the composition of the samples. The number of equilibrium stages is determined by using the Fenske equation. The results show that the average F-factor is equal 2.01 and the number of theoretical stages between EI-7 and EI-8 or EI-8 and EI-9 is 5.21, as shown in Figure 4.1. Thus the average HETP was 0.115.

To ensure that the result is valid, it is compared with data from Sulzer chemtech. Based on the data of Sulzer chemtech with Sulzer DX packing, the F-factor is 2.01 therefore the HETP is approximately 0.07. Hence the number of theoretical stages is 8.57 with the height of unit being 0.6 m. Although the number of stages per unit is lower than result from Sulzer chemtech, it can accepted because of experimental conditions. For example, Sulzer chemtech's experimental test operated at 100 and 950 mbar while our experimental test in our pilot plant operated at 1000 mbar, plus pressure drop.

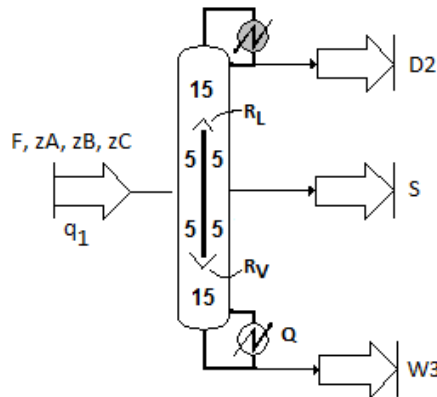


FIGURE 4.3 Structure parameters of pilot plant

We assume that the numbers of stages of upper, lower, feed and side elements of each unit are the same. Hence the experimental results lead to the conclusion that: the numbers of

Chapter 4: Pilot plant and experimental verification

Application for non-reactive mixture

stages of the lower section and of the upper section are 15 stages. The number of stages of the feed section and side section are 10 stages as shown in Figure 4.3. These structural parameters will be set in the simulation tool (ProSim^{plus}).

4.2.4 Component systems

As per the conclusion of chapter 3, the procedure for designing a divided wall column applies not only for ternary mixtures but also for multi-component mixtures. Therefore, to verify the procedure, ternary mixtures and four-component mixtures are investigated in the pilot plant.

In the first case, a ternary mixture of methanol, 1-propanol and 1-butanol are chosen for investigation in our pilot plant. This mixture was chosen because the maximum boiling point of the mixture is 118 °C while the preheater of the pilot plant can heat the mixture up to 150°C. Moreover, the alcohols can be easily bought in the chemical industry. According to their boiling points from lowest to highest, methanol is obtained in the top product, 1-propanol is obtained as the side product, and 1-butanol is obtained as the bottom product. The different feed compositions of the mixture and different liquid splits will be considered.

In the second case, the four-component mixture of the methanol, isopropanol, 1-propanol, and 1-butanol also is carried out in the divided wall column. The distribution of the components to the products will be studied. Firstly, isopropanol is a distributed component. Therefore, methanol is obtained as the top product, isopropanol is obtained as the side product, and 1-propanol and 1-butanol are obtained as the bottom product. Secondly, 1-propanol is a distributed component. Therefore, methanol and isopropanol are obtained as the top product, 1-propanol is obtained as the side product, and 1-butanol is obtained as the bottom product.

4.3 EXPERIMENTAL RESULTS

4.3.1 Separation of ternary mixture: methanol/1-propanol/1-butanol

Table 4.2 displays four steady-state experimental runs of the ternary mixture methanol, 1-propanol, and 1-butanol with different feed compositions, feed flowrates, reflux ratios, liquid splits, and reboiler heat duty. The feed streams can be classified as follows: Case 1 has the same mass fraction of 1-propanol and 1-butanol and a higher mass fraction of methanol; Case 2 has the same mass fraction of methanol and 1-butanol and a higher mass fraction of 1-

Chapter 4: Pilot plant and experimental verification

Application for non-reactive mixture

propanol; Case 3 represents a feed mixture with almost equal mass fraction of all components; Case 4 has the same mass fraction of methanol and 1-propanol and a higher mass fraction of 1-butanol. Cases 1 and 2 have liquid split equal to 0.5, however, cases 3 and 4 have liquid split of 0.4 and 0.6, respectively. Reflux ratios are determined from simulation results and set into the actual experiments. The pressure drop of each experiment was changed from 2.8 to 6.6 mbar while the heat duty changed from 4.3 kW to 5.4 kW.

TABLE 4.2 Operating parameters and results for experimental steady-state runs

Parameters	Case 1	Case 2	Case 3	Case 4	
Feed (kg/h)	5.41	5.77	6.12	5.97	
Methanol (wt. %)	0.4	0.29	0.32	0.3	
1-Propanol (wt. %)	0.3	0.46	0.36	0.24	
1-Butanol (wt. %)	0.3	0.25	0.32	0.46	
Distillate (kg/h)	2.66	2.00	1.95	1.80	
Methanol (wt. %)	0.814	0.85	0.98	0.93	
1-Propanol (wt. %)	0.186	0.15	0.02	0.07	
1-Butanol (wt. %)	0	0	0	0	
Side stream (kg/h)	1.038	2.17	2.12	0.918	
Methanol (wt. %)	0	0	0	0	
1-Propanol (wt. %)	0.995	1	0.998	0.96	
1-Butanol (wt. %)	0.005	0	0.002	0.04	
Bottom stream (kg/h)	1.872	1.7	1.93	3.144	
Methanol (wt. %)	0	0	0	0	
1-Propanol (wt. %)	0.21	0.114	0.06	0.19	
1-Butanol (wt. %)	0.979	0.886	0.94	0.81	
Liquid split (-)	0.5	0.5	0.4	0.6	
Reflux ratio (-)	3	6	4	4	
Heat duty (kW)	5.17	5.1	4.3	5.4	
Heat condenser (kW)	2.67	2.2	2.24	2.5	
Pressure drop (mbar)	2.8	6.6	3.1	2.4	
Relative error (%) of mass balances	Total	-2.92	-1.73	1.96	-1.80
	Methanol	0.47	-1.59	2.40	7.51
	1-Propanol	2.12	-0.11	-3.04	-7.12
	1-Butanol	-12.48	-4.88	7.15	2.81

Feed and product flowrates, and temperatures along the column are noted during the experimental runs. The experimental runs are at steady-state when process variables are constant. In our pilot plant, an experiment is called steady-state if constant column temperatures, constant pressure drop, constant products qualities, and a good agreement of the component and total mass balances are obtained. Table 4.2 shows the results of the component and total mass balances of experimental runs at steady-state conditions. In our study, the component and total mass balance is considered to be in agreement if the relative error between IN and OUT is less than 10%. The relative errors (%) can be calculated:

Chapter 4: Pilot plant and experimental verification Application for non-reactive mixture

$$\text{The relative error (\%)} = \frac{(\text{IN} - \text{OUT})100}{\text{IN}} (\%)$$

The results show that all of them are less than 10% except for the mass balance of 1- butanol in case 1. The relative error is -12.48%. One of the reasons that the flowrate of the bottom product may be higher is due to the fact that the level of the pipe collecting bottom product is lower than level of the liquid in the reboiler. Therefore the bottom product included a liquid and a vapor phase. From the result in table 4.1, it is possible to notice that the experimental runs are validated.

Figure 4.4 illustrates the temperature profiles for the four cases studies. They look very similar for all of case studies. The vertical S-shape of the temperature profiles of the main column indicates two regions: The first is the separation of methanol and 1-propanol in the upper part and the second is the separation of 1-propanol and 1-butanol in the lower section. It is noted that the temperatures of the prefractionator are close to the temperatures found in the main column at the interconnecting points. It is indicated that the composition of each mixture located between the feed and side section are in agreement.

The temperature found in the top of the column in cases 1 and 2 are around 70°C. It is indicated that the quantity of methanol in the top product is low because of the boiling point of methanol being 64.7°C. Table 4.1 shows clearly that the composition of methanol in the top product of cases 1 and 2 are 81.4% mass fraction and 85% mass fraction, respectively. In contrast to this, in cases 3 and 4, temperatures at the top of the column are around 65°C. Therefore, the composition of methanol in the top product obtained higher purity of around 98 % mass fraction and 93% mass fraction for cases 3 and 4. It is concluded that the composition of the key component in the products is related to the column temperature. Hence, in order to obtain the desired product, we can control the temperature of the products instead of controlling the composition.

Chapter 4: Pilot plant and experimental verification
Application for non-reactive mixture

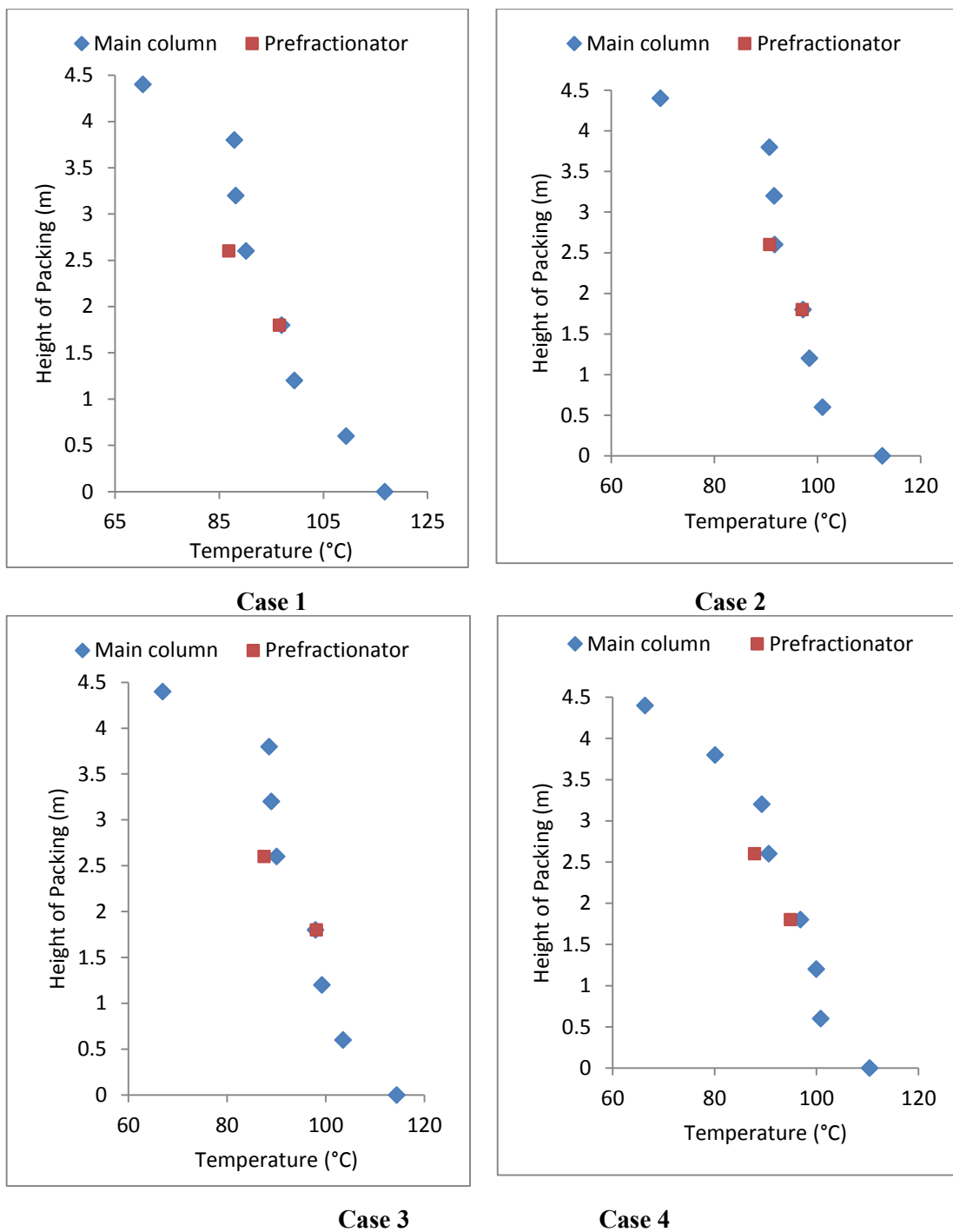


FIGURE 4.4 Experimental temperature profiles for case 1, case 2, case 3, and case 4

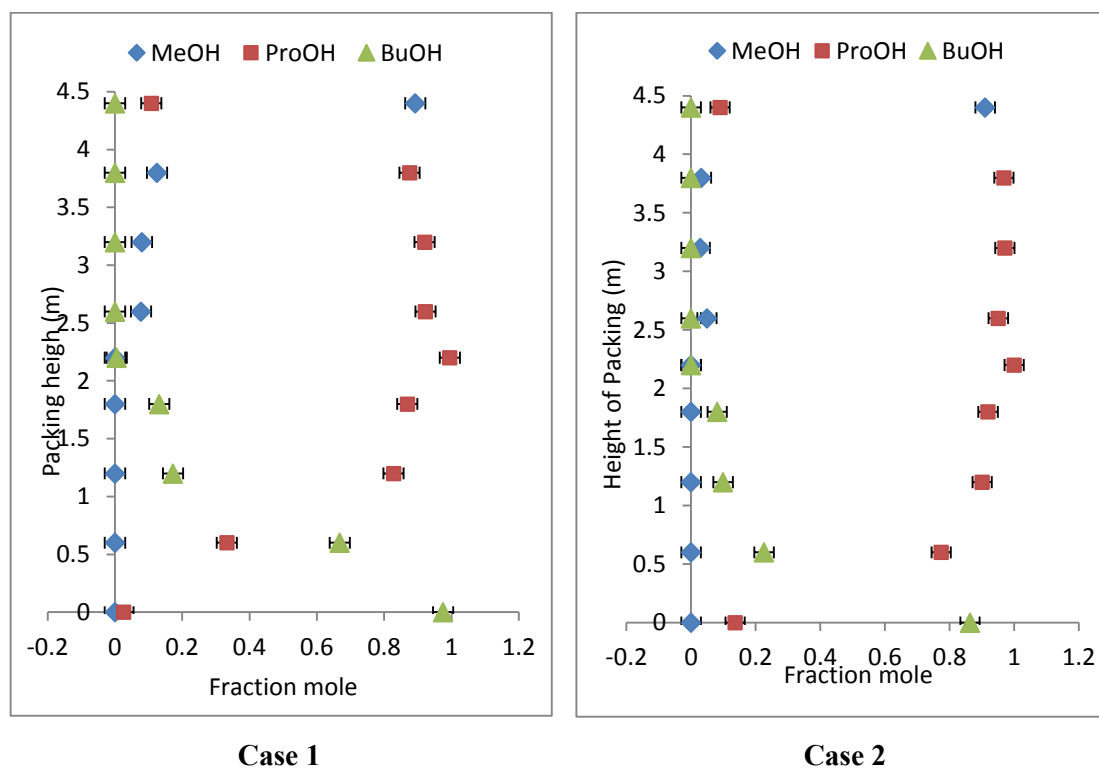
Figure 4.5 shows the composition profiles of experimental runs in the main column not including in the prefractionator. The results show that composition profiles look very similar for all cases studied, in which can indicate two regions: Methanol and 1-propanol are separated in the upper part where 1-butanol is almost zero from a packing

Chapter 4: Pilot plant and experimental verification Application for non-reactive mixture

height of 2.6 m to 4.4 m. The 1-propanol and 1-butanol are separated in the lower part where methanol is = almost zero from 0 to 2.2 m. Clearly the upper part is used to separate methanol and 1-propanol and the lower part is used to separate 1-propanol and 1-butanol. In the middle part, 1-propanol reaches a maximum thus it is collected as the side product.

Figure 4.5 also shows that the content of methanol increases and the content of 1-propanol decreases significantly from 3.8 to 4.4 m and the content of 1-propanol decreases and 1-butanol increases notably at 0 to 0.6 m.

All experimental data have associated uncertainties. Uncertainty is a part of the experimental process and one tries to minimize it. Thus, it is important to express uncertainty clearly when giving experimental results. In order to determine the uncertainty, 14 samples are made, and then they will be analyzed by Chromatography. From there, the uncertainty will be determined. It is noted that if the composition is close to 1, the uncertainty is smaller and if the composition is far from 1, the uncertainty is higher. Thus the mean uncertainty will be used in the study. The detailed calculation are presented in Appendix [3].



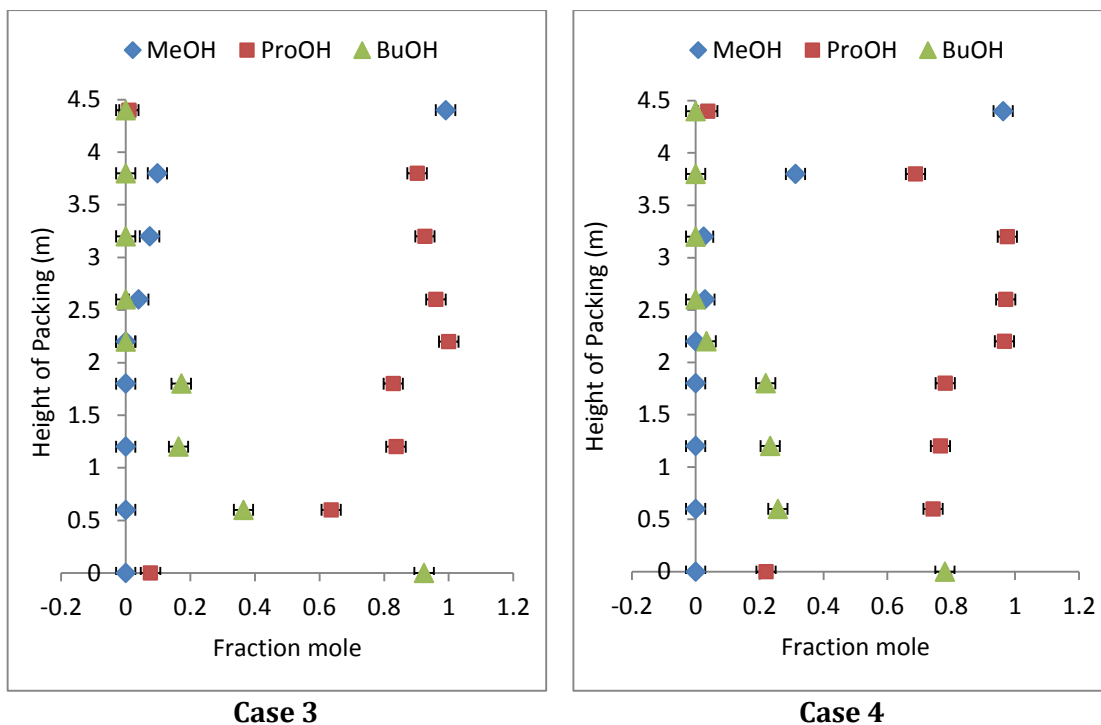


FIGURE 4.5 Composition profiles of experimental runs

4.3.2 Separation of four - component mixture: methanol/iso propanol/1-propanol/1-butanol

The separation of a four-component mixture in a pilot divided wall column is also investigated in table 4.3. Normally, the divided wall column with a single dividing wall can separate a three component mixture into three high purity products. However, the separation of a mixture of four or more components carried out in a divided wall column achieves only two high purity products and one mixed product. Therefore this section investigates the distribution of components in the divided wall column to see if the fourth component is has an effect on the purity of the products.

In table 4.3, the feed stream of the fifth case contains 8 % mass fraction methanol, 16 % mass fraction isopropanol, 45 % mass fraction 1 - propanol, and 31 % mass fraction 1 - butanol. This mixture is prepared because we would like to collect 1-propanol as the side product. Therefore, methanol and isopropanol are collected in the top product and 1-butanol is collected in the bottom product.

In the sixth case, the desired side product is isopropanol. Therefore, the feed stream of the mixture contains 29 % mass fraction methanol, 35 % mass fraction isopropanol, 22 % mass

Chapter 4: Pilot plant and experimental verification

Application for non-reactive mixture

fraction 1-propanol, and 14 % mass fraction 1-butanol. The feed flowrate of the cases studied are around 6 kg/h. The liquid split, and reflux ratio are 0.5 and 6 for cases 5 and 6, respectively. Table 4.2 provides the relative error of the total and component mass balances, while Figure 4.6 shows the experimental temperature and composition profiles of the cases studied. The component and total mass balances are calculated. In case 5, the distillate product included methanol (26% mass fraction), isopropanol (49% mass fraction), 1-propanol (25% mass fraction), and 1-butanol (0% mass fraction). In this case, 1-propanol has a large mass fraction in the distillate because the distillate flowrate is 1.8kg h^{-1} , which is higher than it should be, at 1.3kg h^{-1} . In case 6, the bottom product included only 1-propanol (59% mass fraction) and 1-butanol (41% mass fraction). Concerning the side products of the two cases, it was possible to achieve high purity of key components: 97% mass fraction of 1-propanol for case 5 and isopropanol for case 6. It is indicated that a high purity of key components can be obtained in the side product of the divided wall column. All of the relative errors of mass balance are less than 10%. It is concluded that the experimental runs are validated at steady-state conditions.

TABLE 4.3 Operating parameters and results for experimental steady-state runs

Parameters	Case 5	Case 6	
Feed (kg/h)	5.640	5.892	
Methanol (wt. %)	0.08	0.29	
Isopropanol (wt. %)	0.16	0.35	
1-Propanol (wt. %)	0.45	0.22	
1-Butanol (wt. %)	0.31	0.14	
Distillate (kg/h)	1.800	2.400	
Methanol (wt. %)	0.26	0.719	
Isopropanol (wt. %)	0.49	0.276	
1-Propanol (wt. %)	0.25	0.005	
1-Butanol (wt. %)	0.00	0.000	
Side stream (kg/h)	1.933	1.374	
Methanol (wt. %)	0.00	0.00	
Isopropanol (wt. %)	0.02	0.97	
1-Propanol (wt. %)	0.97	0.03	
1-Butanol (wt. %)	0.01	0.00	
Bottom stream (kg/h)	1.732	2.028	
Methanol (wt. %)	0.00	0.00	
Isopropanol (wt. %)	0.00	0.00	
1-Propanol (wt. %)	0.08	0.59	
1-Butanol (wt. %)	0.92	0.41	
Liquid split (-)	0.5	0.5	
Reflux ratio (-)	6	6	
Heat duty (kW)	4.47	5.47	
Heat condenser (kW)	2.23	2.69	
Pressure drop (mbar)	3.1	7.6	
Relative error of mass balance (%)	Total	+ 3.1	+1.53
	Methanol	- 3.53	-0.99
	Isopropanol	- 2.10	+3.45
	1-propanol	+2.91	+3.89
	1-butanol	+7.78	-1.80

Chapter 4: Pilot plant and experimental verification
Application for non-reactive mixture

In figure 4.6, the vertical S-shape of the temperature profile of the main column is established. For the fifth case, the temperature at the top of the column was found to be approximately 80° C due to the boiling point of the mixture of methanol and isopropanol. The temperature of the bottom product is 114°C due to the boiling point of the mixture containing mainly 1-butanol and a little 1-propanol. However, for the sixth case studied, the temperature at the top of the column was found to be approximately 67°C which is lower than first case because of the boiling point of the mixture containing mainly methanol (64.7°C) and a little isopropanol. The temperature at the bottom of the column is 105°C lower than the first case because of boiling point of the mixture of 1-propanol and 1-butanol.

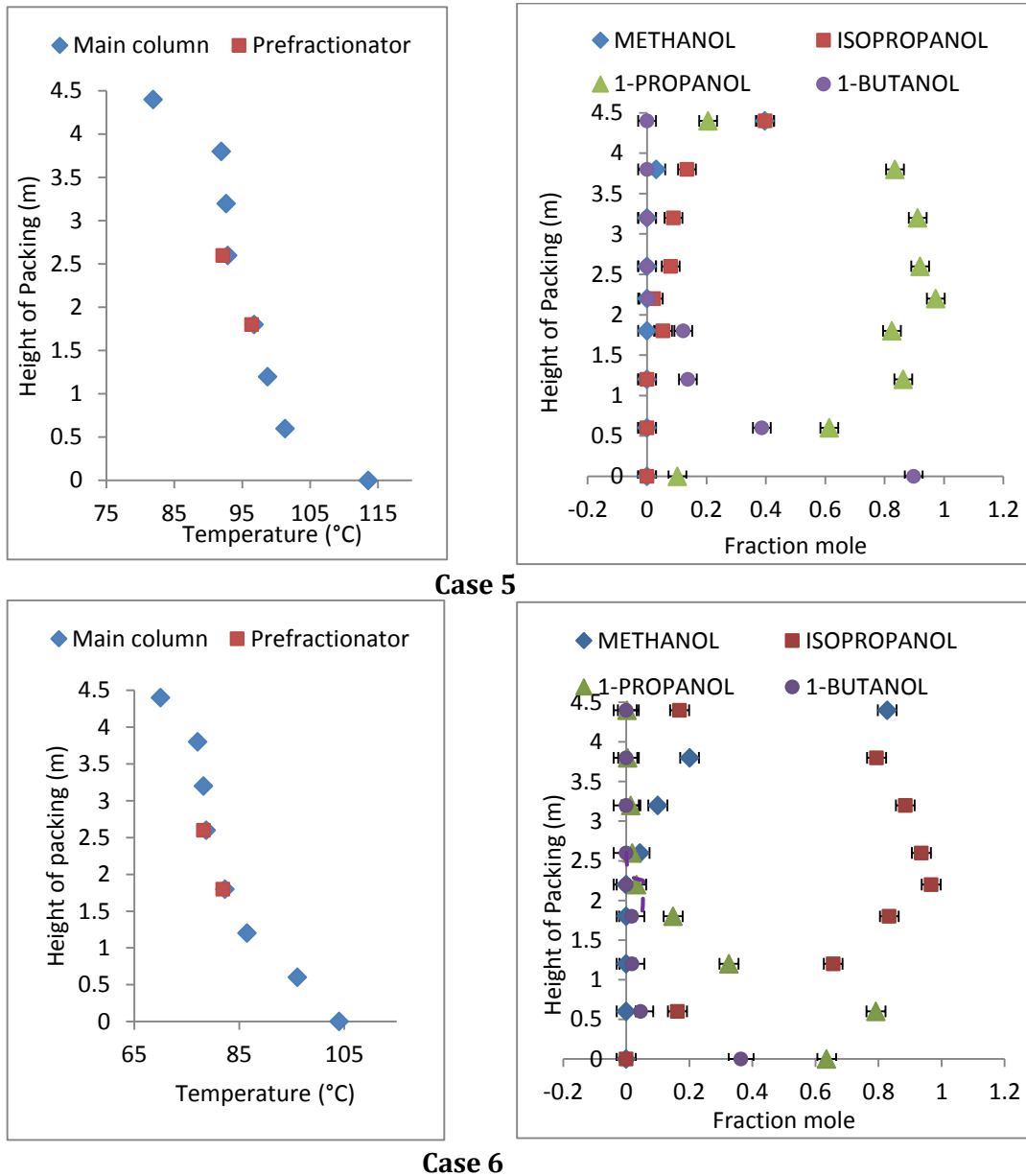


FIGURE 4.6 Experimental temperature and composition profiles for case 5 and case 6

Chapter 4: Pilot plant and experimental verification

Application for non-reactive mixture

The composition profiles of cases 5 and 6 are presented in Figure 4.6. In the case 5, 1-propanol is collected as the side product while methanol and isopropanol are collected as the top product. In the case 6, isopropanol is collected as the side product while 1-propanol and 1-butanol are collected as the bottom product. Clearly, the high purity of the side product can be obtained with a divided wall column even if the mixture has more than three components, as displayed the in case 5 where the content of 1-propanol is 97% fraction mass and the content of isopropanol in case 6 is 97% fraction mass.

4.4 COMPARISON BETWEEN EXPERIMENTAL DATA AND SIMULATED RESULTS

In this section, based on the structure of the pilot plant and operational parameters, a simulation of the process will be carried out in ProSim^{plus} software. The simulated results are used to predict operating parameters in actual experiments such as feed flowrate (F), reflux ratio (R_2), liquid split (R_L), heat consumption (Q_b), and temperature of the top, side, and bottom products. And then, the operational parameters of experimental runs are used for simulations. In order to fit data between simulated and experimental results, several variables need to be adjusted such as feed flowrate, top, side and bottom products, and vapor split. The comparison with experimental and simulation data is necessary to verify and increase the acceptance of the simulated results.

The comparison between experimental and simulated data is performed for different operating conditions as shown in table 4.1 and 4.2. The table 4.1 and 4.2 provided feed and product streams, liquid split, reflux ratio, feed composition, etc. In order to make the simulated results in close agreement with the experimental results, it is necessary to choose certain variables to be adjusted. The important input variables required for the simulation model are the feed flowrate (F), liquid split (R_L), vapor split (R_V), side stream (S), distillate (D_2), and reflux ratio (R_2).

The reflux ratio (R_2) and liquid split (R_L) are controlled automatically by a controlled timer and reflux ratio and liquid split are variables used to optimize the energy use of the reboiler. Therefore they should not be chosen to be adjusted. The feed, top, side, and bottom flowrate are chosen as adjusted variables in the simulation process. The vapor split is not controlled. It depends on the inner diameter of the feed and side section and the pressure drop inside the

Chapter 4: Pilot plant and experimental verification Application for non-reactive mixture

packed section. In our pilot plant the vapor split is around 0.5. Therefore, it also should be chosen to be adjusted.

Figure 4.7 shows the step-by-step adjusted variables in order to make the simulation results as close as possible close to the actual experiment behavior.

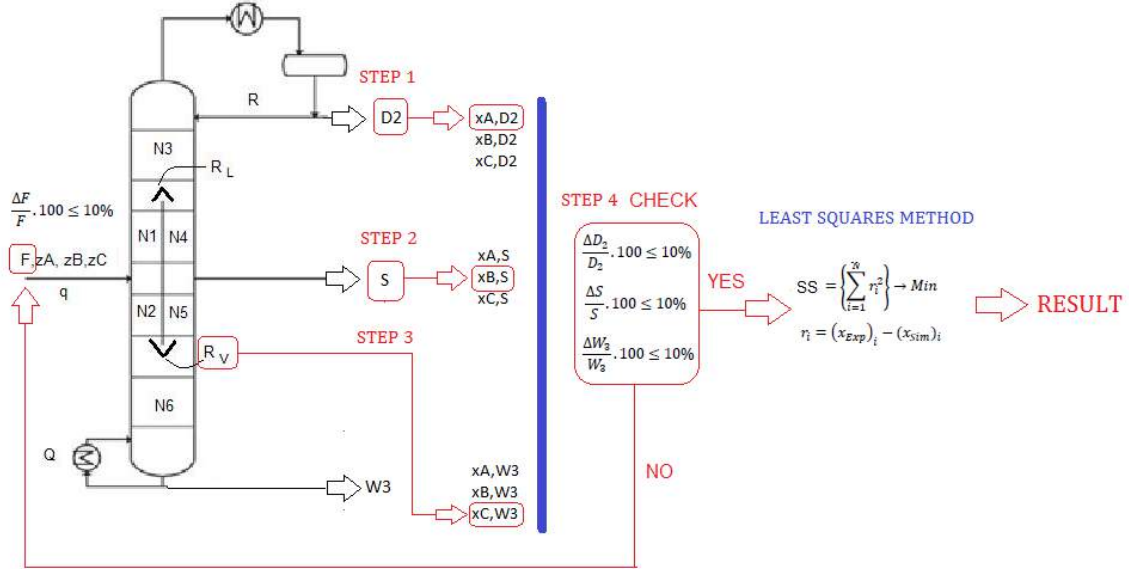


FIGURE 4.7 Step-to-step to adjust variables for simulation process

1. Distillate flowrate (D_2) is adjusted to obtain a purity of component A in the distillate product that is the same as in the experimental result.
2. Side flowrate (S) is adjusted to obtain a purity of component B in the side product that is the same as in the experimental result.
3. The vapor split (R_v) is adjusted to obtain a purity of component C in the bottom product that is the same as in the experiment result.
4. The relative error (%) between the values set in the simulation and values in the actual experiment data are calculated. If it is in agreement that relative errors are less than 10% then the least squares error for all points along the column is calculated. If it is not, the feed flowrate (F) is adjusted and the sequence starts again from step 1. The best-fit curve of a given type is the curve that has the minimal least square error from a given set of data.

The least square error can be determined by the least square method:

$$\text{Least square error} = \left\{ \sum (x_{\text{experiment}} - x_{\text{simulation}})^2 \right\} \rightarrow \min$$

And relative error of key component:

Chapter 4: Pilot plant and experimental verification
Application for non-reactive mixture

$$\text{Relative error} = \left(\frac{x_{\text{simulation}} - x_{\text{experiment}}}{x_{\text{experiment}}} \right)_{\text{key component}}$$

4.4.1 Ternary mixture

4.4.1.1 Results

DECHEMA recommended that for a mixture including methanol, 1-propanol, and 1-butanol, NRTL model should be used in the simulation. The parameters of the thermodynamic model are presented in Appendix [2B].

Based on Figure 4.7, the simulation process is carried out in ProSim^{plus} software. The least square error and the relative error of the key components of the case studied are calculated in Table 4.4. From the calculation, it is possible to conclude that the experimental data and simulated results are in good agreement.

TABLE 4.4 Least square error and relative error of key component

Experimental runs	Least square error			Relative error of key component		
	MeOH	1-ProOH	1-BuOH	MeOH	1-ProOH	1-BuOH
Case 1	0.00082	0.01583	0.01193	-0.00038	-0.00058	-0.00600
Case 2	0.00305	0.00503	0.00193	0.00378	-0.00721	-0.00318
Case 3	0.00464	0.01362	0.00801	-0.05264	-0.04465	0.00490
Case 4	0.02141	0.03221	0.01458	0.00721	0.00822	0.07890

Table 4.5 reported the comparison between experimental operating parameters at steady-state conditions and simulated results of case 1 in which feed, distillate, side, bottom streams, and vapor splits are adjusted while reflux ratio and liquid split are fixed to the same as the values of the experiment. These results indicate that the feed stream increases +2.96%, the distillate stream increase +3.01%, the side stream increases +8.57%, and the bottom stream decreases -8.81%. The differences are based on the fact that the errors occur during the experimental run and analysis of the composition of each component by chromatography. The vapor split is also not controlled in our pilot plant. It depends on the resistance of middle section. Theoretically, the liquid split is 0.5 and the cross-sectional areas of each section in middle section are the same hence vapor split should be around 0.5. However the internal liquid stream increases in the feed section because of added liquid by feed stream and the internal liquid stream decreases in the side section because of the liquid removed by side product

Chapter 4: Pilot plant and experimental verification
Application for non-reactive mixture

stream. Hence the vapor split is smaller than 0.5. The result shows that the vapor split is 0.413 as determined by a process to the fit data. Based on the result, only 41.3 % of the vapor reached the prefractionator, whereas the majority of the main vapor stream, 58.7 %, moved through the side section.

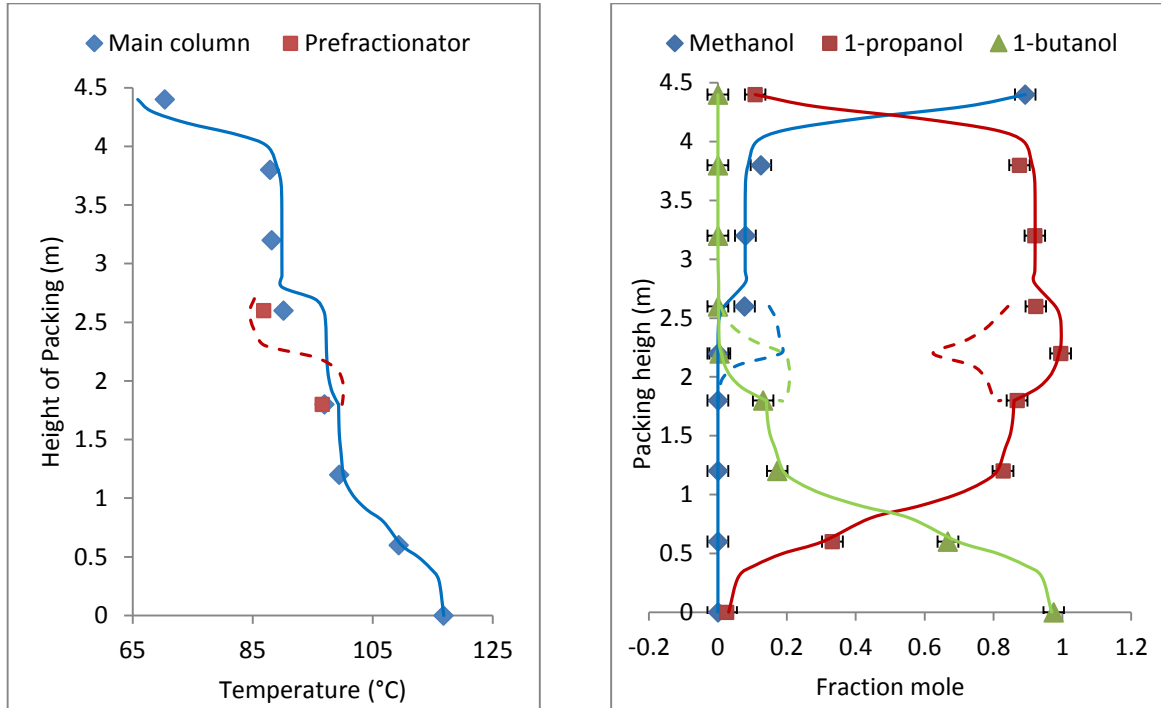
TABLE 4.5 Detail comparisons between experimental data and simulated results of case 1

Parameters	Experiment	Simulation	Relative error (%)
Feed stream (kg ^h ⁻¹)	5.41	5.57	+2.96
Distillate stream (kg ^h ⁻¹)	2.66	2.736	+3.01
Methanol (wt. %)	0.814	0.814	0.00
Side stream (kg ^h ⁻¹)	1.038	1.127	+8.57
1-Propanol (wt. %)	0.995	0.993	-0.20
Bottom stream (kg ^h ⁻¹)	1.872	1.707	-8.81
1-Butanol (wt. %)	0.979	0.974	-0.51
Liquid split R _L (-)	0.5	0.5	+0.00
Vapor split R _V (-)	-	0.413	-
Heat consumption (kW)	2.67	3.21	+ 20.22

In the simulation, we assume that the heat losses from the column walls are negligible. Therefore the heat duty of the condenser in the experiment is used to compare, instead of the heat duty of reboiler as shown in table 4.5. The relative error is +20.22%. The detailed comparison between experimental data and simulated results of cases 2, 3, and 4 are represented in the Appendix [4]. Figure 4.8 illustrates two typical temperature profiles for case 1, 2, 3 and 4. While the temperature in the prefractionator of case 1, 2, and 3 are lower than that temperature of the main column at the top part from 2.2 to 2.6 m and are higher at the bottom part from 1.8 to 2.2 m, the temperature in the prefractionator of case 4 is always lower than in both the top and bottom parts of the main column. The graphs depend on the composition of the mixture between the dividing walls. As shown in Figure 4.8, in cases 1, 2, and 3, the upper section of the prefractionator has significant amounts of methanol, a part of 1-propanol and a little 1-butanol. Therefore, the boiling point of the mixture is lower than that in a side section where a significant quantity of 1-propanol is present. On the other hand, the lower section of the prefractionator has a significant amount of 1-butanol, a part of 1-propanol and a little methanol. Therefore, the boiling point of the mixture is higher than that in the side section where 1-propanol is significant. However, in case 4, the methanol appears both in the upper and lower part of the prefractionator. This means that the temperature of the prefractionator is always lower than that in the main column. The purification of the methanol (lightest boiling component) in the upper part of the main column leads to a temperature reduction until the boiling temperature of pure methanol was reached. In

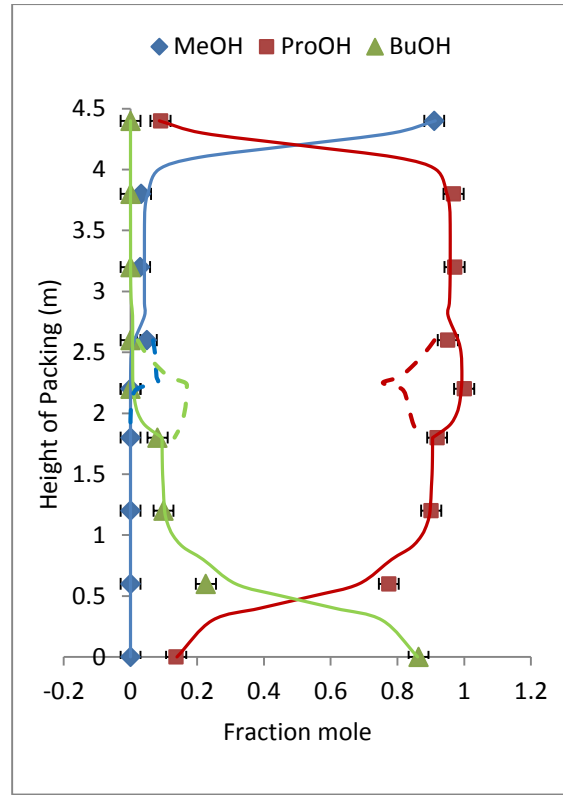
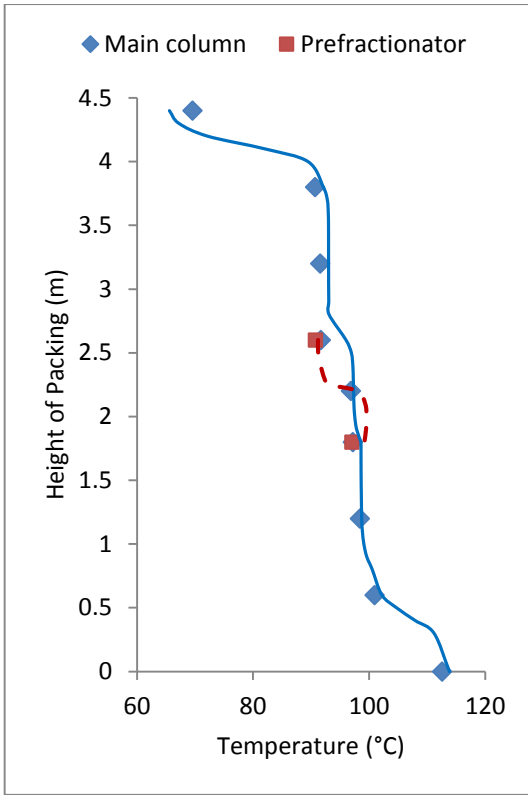
Chapter 4: Pilot plant and experimental verification Application for non-reactive mixture

contrast, the purification of 1-butanol (heavy boiling component) in the lower part of the main column leads to rising temperatures. Figure 4.8 indicated that the product purities show very good agreement between the experiments and the simulation not only for key component products but also for the composition in the whole column.

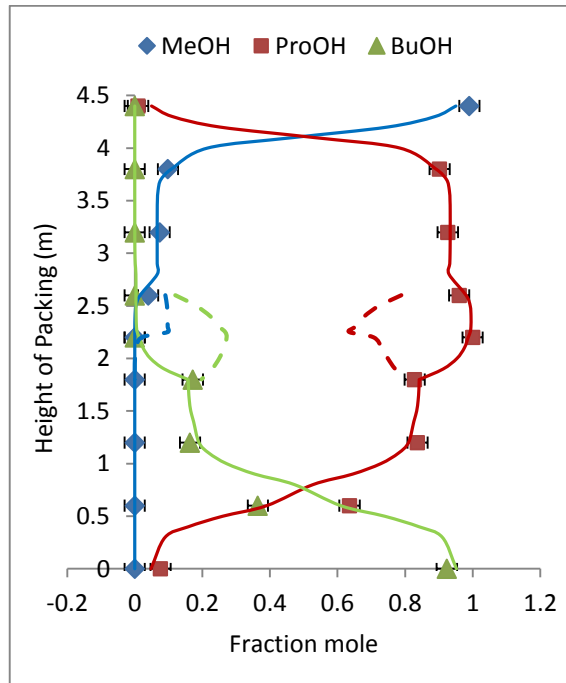
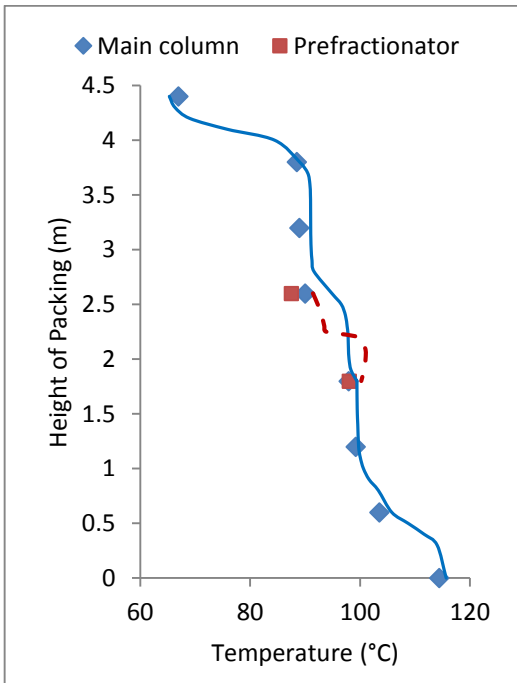


Case 1

Chapter 4: Pilot plant and experimental verification
Application for non-reactive mixture

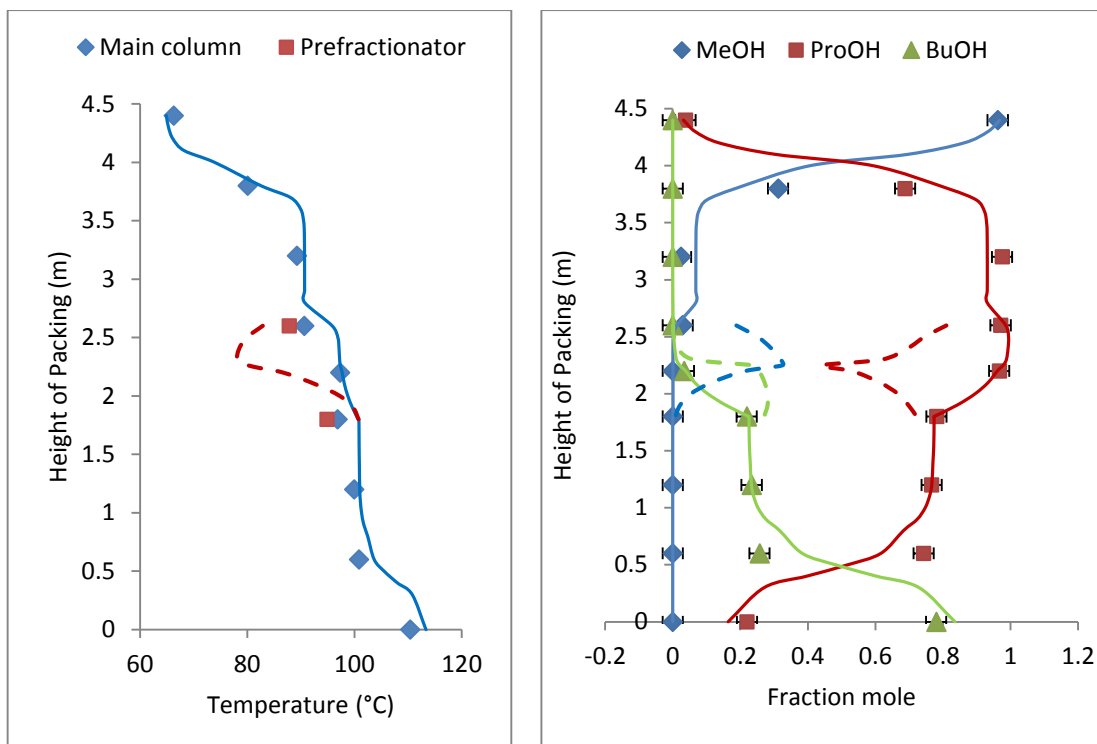


Case 2



Case 3

Chapter 4: Pilot plant and experimental verification
Application for non-reactive mixture



Case 4

FIGURE 4.8 Temperature and composition profile of experimental data and simulation results for the case studied

4.4.1.3 Difference in temperature between dividing wall

The maximum temperature difference between the prefractionator and the main column of cases 1, 2, 3, and 4 are around 12°C, 6°C, 4°C and 19°C, respectively. The results indicate that cases 2 and 3 have a lower temperature difference in which the composition of the intermediate component is equal to or higher than other component while cases 1 and 4 have lower composition of intermediate component. Based on this analysis, it is concluded that the feed composition has an effect on the operation of the divided wall column. If the amount of intermediate component in the mixture is less than the other component, the temperature difference is significant. Hence the effect of heat transfer across the dividing wall should be considered. However, if the amount of the intermediate component of the mixture is higher than other components in the mixture, the temperature difference across the dividing wall is neglected. Figure 4.9 shows the relationship between the temperature difference and the amount of intermediate component in the feed stream.

Chapter 4: Pilot plant and experimental verification
Application for non-reactive mixture

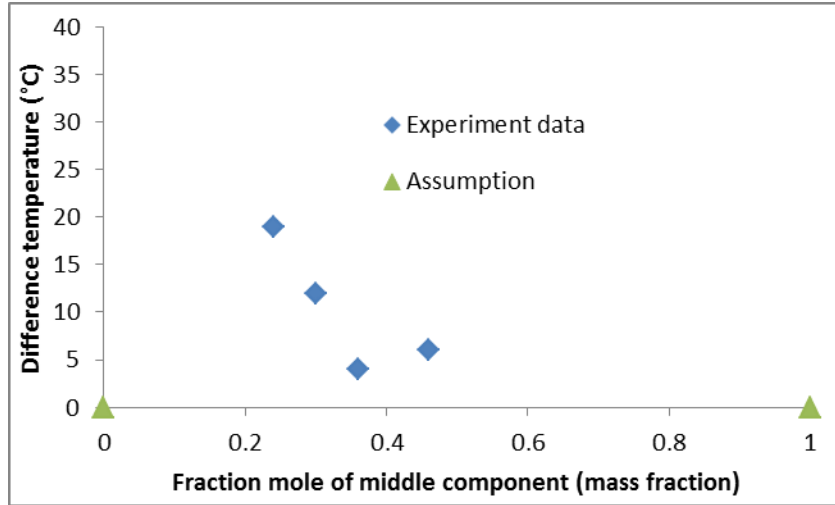


FIGURE 4.9 Difference temperature between the prefractionator and the main column depended on the feed composition

We can assume that if a mixture has 100% or 0% 1-propanol, the temperature difference across the dividing wall is zero as shown in Figure 4.9.

4.4.1.3 Relationship between liquid and vapor split

The vapor split is also considered as a manipulated parameter to obtain good agreement between experimental data and simulated results. The vapor split adjustment is determined by simulations of the process as per figure 4.7. Figure 4.10 shows that although the cross-sectional areas of the prefractionator and the side section were the same, the vapor split values changed from 0.39 to 0.52 with liquid split values changing from 0.4 to 0.6.

Figure 4.10 shows the relationship between the liquid split and the vapor split. When the liquid split is 0.5, as in cases 1 and 2, the internal liquid stream fed to the upper part of the prefractionator is the same as to the upper part of the side section. However, the internal liquid stream increases in the lower part of the prefractionator and decreases in the lower part of the side section because of the feed stream and side product stream. Therefore the vapor splits of cases 1 and 2 are 0.414 and 0.44 (less than 0.5), respectively. The trend shows that when the liquid split is more or less than 0.5, the vapor split value decreases or increases, respectively. When the liquid split is 0.4 or 0.6, the vapor split is 0.516 and 0.39, respectively.

Chapter 4: Pilot plant and experimental verification
Application for non-reactive mixture

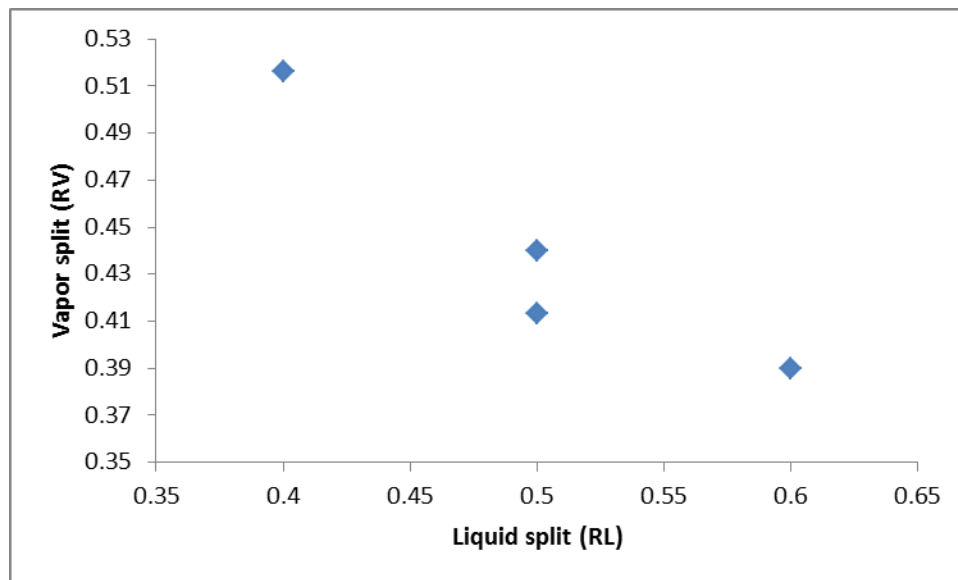


FIGURE 4.10 Vapor split (R_V) depends on the liquid split (R_L)

It is important the note that vapor split is an important adjusted variable to give good agreement between experimental and simulated data.

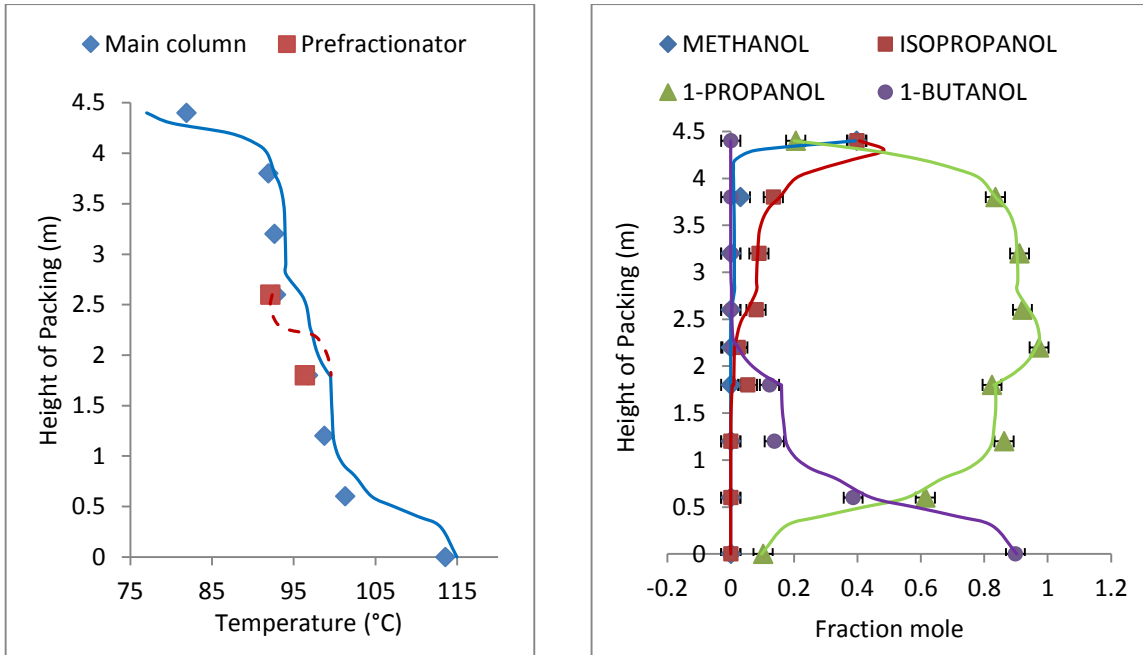
4.4.2 Four-component mixture

For the mixture containing methanol, isopropanol, 1-propanol, and 1-butanol the NRTL model as used in the simulation. The parameters of the thermodynamic model are presented in Appendix [2C]. Figure 4.11 illustrates the temperature and composition profile compared between the experimental data and simulated results while table 4.6 shows the results of the least square error and relative error of the key components.

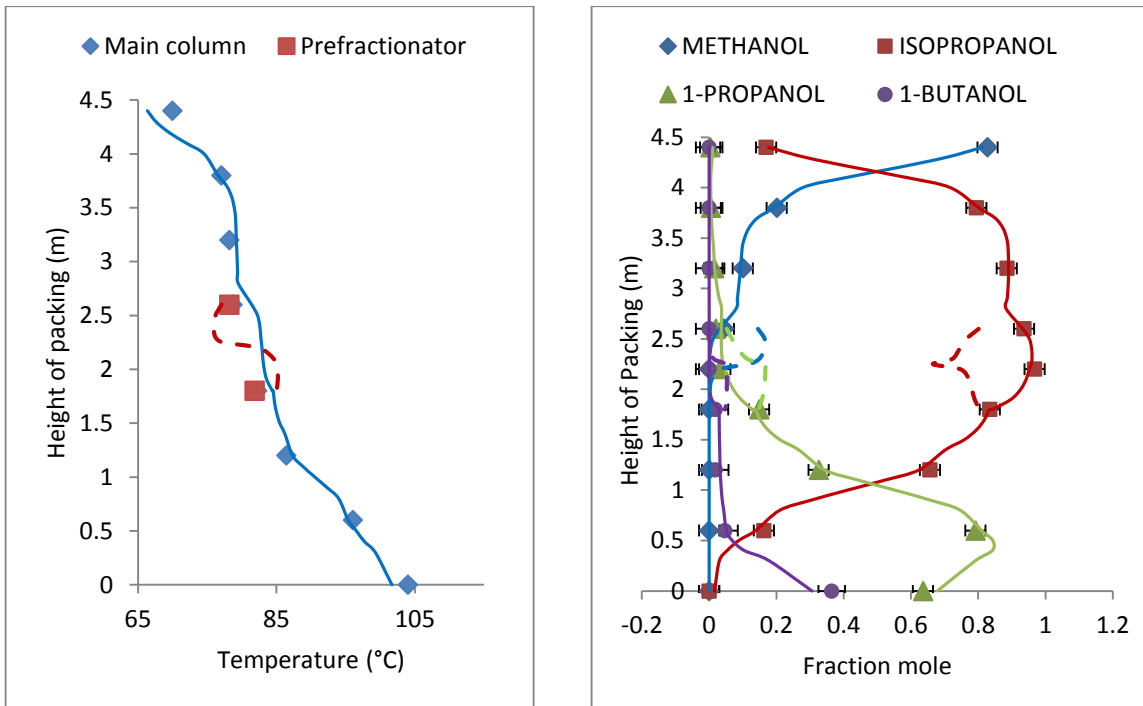
TABLE 4.6 Least square error and relative error of key component

Runs	Least square error				Relative error of key component			
	MeOH	Iso ProOH	1-ProOH	1-BuOH	MeOH	Iso ProOH	1-ProOH	1-BuOH
Case 5	0.0006	0.0045	0.0098	0.0115	-0.0071	0.0197	-0.0088	0.0051
Case 6	0.0015	0.0083	0.0183	0.0152	-0.0181	-0.0155	0.0671	-0.1605

Chapter 4: Pilot plant and experimental verification
Application for non-reactive mixture



Case 5



Case 6

FIGURE 4.11 Temperature and composition profile compared between the experimental data and simulation of case 5 and case 6

Chapter 4: Pilot plant and experimental verification

Application for non-reactive mixture

In the fifth case studied, a mixture of methanol and isopropanol was obtained as the top product; 1-propanol as the side product with 97 % mass fraction; and 1-butanol as the bottom product with 92% mass fraction. In the sixth case studied, methanol is the top product with 72 % mass fraction; isopropanol is the side product with 96.7% mass fraction and a mixture of 1-propanol and 1- butanol is the bottom product. The results indicated that a high purity of key components in the side product is obtained. The maximum relative error of the key component obtained was less than 10% except for 1-BuOH in case 6 as shown in table 4.6. Thus it is possible to note that the simulation results and experimental data are in agreement with each another. The vapor splits of all the cases studied are less than 0.5 as per the trend discussed in section 4.11 when the liquid split is 0.5. The vapor split of cases 5 and 6 are 0.46 and 0.45, respectively.

4.5 CONCLUSION OF CHAPTER 4

The implementation, startup and operation of a dividing wall column to carry out an alcohol mixture separation were achieved in this chapter. Based on the structural parameters of the pilot plant column, the simulation was carried out in ProSim software. The simulated results were found to be in agreement with the data from the experimental runs.

The maximum temperature difference across the dividing wall is considered. The result shows that the maximum temperature difference depended on the amount of middle component in the feed stream. If amount of middle component in the feed stream is lower, the temperature difference between the dividing wall increases.

It is noted that when the structural parameters of the divided wall column and liquid split are fixed, the vapor split (RL) is the most significant factor to affect the separation efficiency especially in terms of the purity of key components in products. The relationship between the liquid and vapor split is also established. Because of the effect of the internal liquid stream across the dividing wall, the vapor split is not equal 0.5. When the liquid split increases, the vapor split decreases. Contrarily, when the liquid split decreases, the vapor split increases.

A four-component mixture containing methanol, isopropanol, 1-propanol, and 1-butanol is also separated in the pilot plant column. The high purity of the key component in the side product is still achieved.

Chapter 5

DESIGN OF REACTIVE DIVIDED WALL COLUMN

5.1 INTRODUCTION

Reactive distillation is a type of process intensification. It is a combination of reaction and separation in one column. Its advantages include increased yield due to overcoming chemical and thermodynamic equilibrium limitations, avoidance of hot spots by liquid evaporation and ability to separate close boiling components.

Both divided wall columns and reactive distillation systems are known and if they are carried out in a single column by integration of the two processes the unit is called a reactive divided wall column as shown in Figure 5.1.

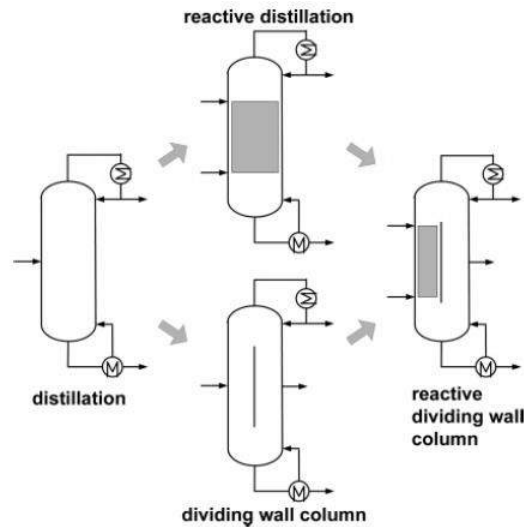


FIGURE 5.1 Processes integration of reactive distillation and divided wall column

As shown in the literature review in chapter 2, some papers have proposed methods for design of reactive divided wall columns, including those of Guido et al., (2006), I. Mueller et al., (2007), and Anton A. Kiss (2007, 2010, and 2012). However, the design, simulation and modelling of reactive divided wall columns is still a comparatively new research area (Guido et al., (2006)).

In this chapter, a proposed conceptual design method for reactive divided wall columns is presented. First, the predesign method developed in our laboratory by R. They et al., (2005) is applied. Then, a modified shortcut method for reactive divided wall columns based on the classical shortcut method adapted to a non-reactive divided wall column by C. Triantafyllou and R. Smith (1992), is proposed.

Chapter 5: Design of reactive divided wall column

To verify the conceptual design method, a simulation process and an experiment in the reactive divided wall column pilot plant in our laboratory are considered. The methodology will be illustrated for the synthesis of methyl acetate from methanol and acetic acid.

5.2 PROCEDURE FOR DESIGN OF A REACTIVE DIVIDED WALL COLUMN

5.2.1 Model and assumptions for a reactive divided wall column

5.2.1.1 Model of reactive divided wall column

Mueller I et al. (2007) suggested that a reactive divided wall column is a highly integrated setup that can be used for reactive systems with more than two products which should be obtained as a pure fraction each; or reactive systems with inert component and with desired separation of both products and inert components; or reactive systems with an excess of a reagent which should be separated to high purity before being recycled. For the design of the reactive divided wall column considered in this thesis, the column is restricted as illustrated in Figure 5.2.

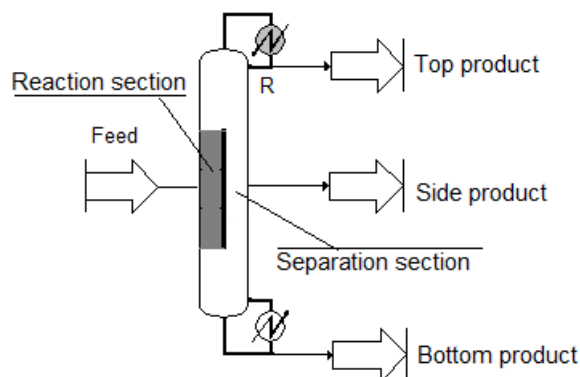


FIGURE 5.2 Restriction of the model for reactive divided wall column

As per Figure 5.2, several restrictions are proposed: (1) the reaction section is considered to be confined to the prefractionator; and (2) the main column is used to separate the reaction products; the reactive divided wall column is considered with (3) single feed; and (4) one reversible equilibrium reaction.

5.2.1.2 Assumptions

To design reactive divided wall columns, both the assumptions for the design of reactive distillation and for the design of divided wall columns have to be considered. For reactive distillation, Barbosa D and Michael F. Doherty (1988) presented several assumptions for design reactive distillation.

- (1) The heat losses from the column walls are negligible.
- (2) The molar heat of vaporization of the mixture is constant.
- (3) The heat of mixing in the both the vapor and liquid is negligible.
- (4) The increase in sensible heat with increase in temperature through the column is negligible.
- (5) The heat of reaction is negligible compared to the enthalpy of the vapor phase.
- (6) Vapor – liquid equilibrium is achieved on each plate.
- (7) The column operates with a partial condenser.

For a divided wall column, the assumptions also are applied as shown in Chapter 3. Moreover, the predesign method of They et al., (2005) mainly relied on the Static Analysis (SA) method of S. Giessler (1999, 2001). Therefore, the principal assumptions of the SA method also are considered:

- (8) The vapor and liquid flowrates in the column are infinite.
- (9) The capacity of the reaction part in the column is large enough to carry out a given conversion rate, and the reaction part is located at a certain place in the column.
- (10) The plant is operated at steady state, and theoretical stages are chosen.
- (11) One reversible equilibrium reaction is considered.

In the chapter, we propose a conceptual design method comprising of three steps to design the reactive divided wall column as illustrated in Figure 5.3.

Firstly, the decomposed method for a reactive divided wall column is applied (Mueller I et al., (2007)). The authors show how the reactive divided wall column is decomposed step-by-step into single non-reactive and reactive columns in which the prefractionator is the reactive

Chapter 5: Design of reactive divided wall column

column where the reaction occurs and the main column is a non-reactive column where separation occurs.

Secondly, the predesign method of They et al., (2005) is applied for the classification of feed composition. The feed composition x^F is converted to the pseudo initial x^* by using a certain conversion of reaction ξ .

Thirdly, based on assumption (8), the composition change, caused by the reaction on each tray, can be neglected. Therefore, the pseudo mixture is separated by a non - reactive divided wall column. A modified shortcut method for reactive divided wall columns that is based on the classical shortcut method adapted to a non-reactive divided wall column by C. Triantafyllou and R. Smith (1992) is applied.

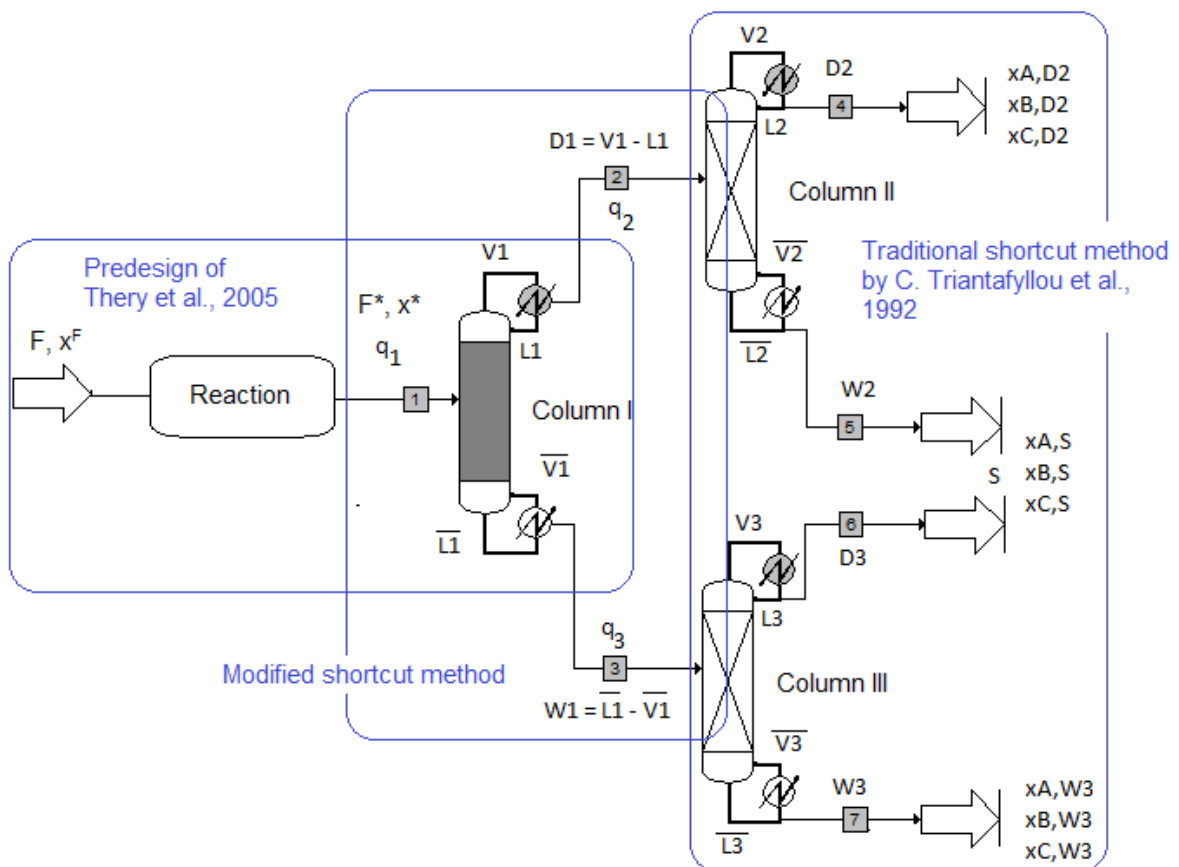


FIGURE 5.3 Decomposed the reactive divided wall column into reactive distillation (column I) and two conventional distillations (column II and III)

5.2.2 Classification of feed composition region by predesign method

The predesign of R. They et al., (2005) relies on the work of S. Giessler et al., (1998) that uses minimal information about the physicochemical properties of the reaction mixture, to calculate the maximum degree of conversion, the reactive zone location and its quantitative length.

Firstly, the feed composition of the reactive mixture x^F is converted to the pseudo initial mixture x^* by giving a certain conversion of the reactant. Then, the pseudo initial mixture x^* is separated in the prefractionator. The composition of one product in the prefractionator is fixed and the composition of the other product is restricted by the material balance. The composition of two products and the pseudo initial mixture x^* must lie on the same line in the distillation diagram. The analysis enables to get the maximum conversion yield, the distillate and bottom composition, and flowrates of the products. Clearly, by applying this step, it is possible to classify the entire feed composition of the reactive system x^F to give the composition of products, flowrate of products, and maximum conversion yield are known.

Details of the procedure, described below for one reaction, are: (1) feed composition; (2) phase equilibrium model parameters; (3) chemical equilibrium model parameters, and (4) the stoichiometry of the reaction.

Step 1: Initialize the conversion of the reagent ξ to its maximal value, that is:

$$\xi = \xi_{\max} = 100\%.$$

Step 2: Compute the pseudo - initial composition x^* by mass balance. The composition x^* has to lie on the stoichiometric line.

We have:

F – feed flowrate (kmolh^{-1}).

x_i^F – Composition of the component i in the feed stream x^F (mole fraction).

v_i – Stoichiometric coefficient of component i .

$$v_T = \sum v_i$$

The pseudo-initial composition mixture x_i^* can be determined after assuming a conversion of the reagent ξ :

$$x_i^* = (1 - v_T \cdot \alpha) \cdot x_i^F + v_i \cdot \alpha$$

Where:

Chapter 5: Design of reactive divided wall column

$$\alpha = \frac{\xi}{F + v_T \cdot \xi}$$

Step 3: Located the stable and unstable nodes.

Step 4: One of the product compositions is fixed. There are two possibilities that the composition of the distillate product is fixed for the direct separation or the composition of the bottom product is fixed for the indirect separation.

Step 5: For direct separation, initialize the ratio $K_D = \frac{D_1}{W_1}$ to its maximal value $K_{D,max}$. Then compute the composition of the bottom product:

$$\left\{ \begin{array}{l} K_{D,max} = \max(K_D) \\ \text{and} \\ 0 \leq x_{i,W_1} = (K_D + 1) \cdot x_i^* - K_D \cdot x_{i,D_1} \leq 1; i = 1 - N_c \end{array} \right\}$$

For the indirect separation, initialize the ratio $K_I = \frac{W_1}{D_1}$ to its maximal value ($K_{I,max}$). Then, compute the composition of the distillate product:

$$\left\{ \begin{array}{l} K_{I,max} = \max(K_I) \\ \text{and} \\ 0 \leq x_{i,D_1} = (K_I + 1) \cdot x_i^* - K_I \cdot x_{i,W_1} \leq 1; i = 1 - N_c \end{array} \right\}$$

Where:

D_1 – distillate product flowrate (kmolh⁻¹)

W_1 – bottom product flowrate (kmolh⁻¹)

x_{i,D_1} – Composition of the distillate product D_1 (mole fraction)

x_{i,W_1} – Composition of the bottom product W_1 (mole fraction)

Step 6: If the composition of the distillate and bottom product does not sit on the same distillation line, then we can conclude that they do not belong to the same distillation region. Thus, these products cannot be obtained in the same reactive distillation column. In that case, decrease the K_D or K_I ratio and go back to Step 5. If no recovery ratio value (K_D or K_I) is feasible, decrease the reaction extent and go back Step 2. If no reaction extent can be found, the feed composition x^F is not feasible, choose another one and come back to Step 1. If both K_D (K_I) and ξ are feasible, compute a new set of feed compositions and go back to Step 1. If the entire feed composition is considered, the procedure is finished.

The results of the procedure give a feasible feed composition, distillate, and bottom compositions, distillate and bottom flowrates, and also reaction extents.

5.2.3 Modified shortcut design method for reactive divided wall column

C. Triantafyllou et al. (1992) presented a method to decompose divided wall columns into three traditional distillation columns in which the columns I, II and III are only used for separation. However, for reactive divided wall columns, I. Mueller et al. (2007) also applied the method to decompose into a single reactive distillation column (column I) and two non-reactive distillation columns (column II and III) as shown in Figure 5.3.

From the first step, we have:

F^* – pseudo feed flowrate (kmolh^{-1}).

x^* – pseudo composition in the feed (mole fraction).

This mixture will be separated in the divided wall column.

5.2.3.1 Minimum vapor flowrate for column I

To determine the minimum vapor flowrate for column I, both the minimum vapor flowrate for the pure separation mixture and for the reactive mixture must be considered. For pure separation, at the minimum reflux condition, the minimum vapor flowrate can be calculated by the Underwood equation as in Chapter 3 for column I:

$$V_{1,\min}^{\text{pure}} = \sum_{i=A}^C \frac{\alpha_i \cdot x_{i,D_1} \cdot D_1}{\alpha_i - \theta}$$

For the reactive mixture, Doherty et al., (1988) presented an algorithm to find the minimum reflux ratio for reactive mixtures. For systems with a reaction, Barbosa and Doherty (1988) defined the transformed composition variables:

$$X_i = \frac{v_k x_i - v_i x_k}{v_k - v_T x_k}$$

And

$$Y_i = \frac{v_k y_i - v_i y_k}{v_k - v_T y_k}$$

Where:

x_i, y_i – Mole fraction of component i in the liquid and vapor phase.

x_k, y_k – Mole fraction of reference component in the liquid and vapor phase.

X_i, Y_i – Transformed composition variables.

Chapter 5: Design of reactive divided wall column

Step 1: Given X_F , specify Y_{D1} and X_{W1} in such a way that X_F , Y_{D1} , and X_{W1} lie on a straight line.

Step 2: Guess a value for minimum reflux ratio r_1 for column I

Step 3: Calculate reboiler ratio s_1

$$s_1 = \frac{(1 + r_1)(v_k - v_T X_{k,W1})}{(v_k - v_T Y_{k,N-1})} \frac{X_{i,W1} - X_{i,F}}{X_{i,F} - Y_{i,D1}}$$

With $i = 1, \dots, c - 1$ and $i \neq k$

If $v_T = 0$, based on the equation, reboiler ratio s_1 can be calculated as:

$$s_1 = \frac{D_1}{W_1} (1 + r_1)$$

Step 4: Solve equations for pinch composition (feed pinch and saddle pinch points):

$$s_1 Y_i^s - (s_1 + 1) X_i^s + X_{i,W1} = 0$$

$$r_1 X_i^r - (r_1 + 1) Y_i^r + Y_{i,D1} = 0$$

Where: X_i^r, Y_i^r, X_i^s , and Y_i^s - Transformed composition of feed pinch and saddle pinch points of component $i = 1$ and 2 .

Step 5: Check whether X^r, X^s , and X_F are collinear. That is, check whether:

$$(X_2^s - X_{2,F})(X_1^r - X_{1,F}) - (X_2^r - X_{2,F})(X_1^s - X_{1,F}) = 0$$

Step 6: If step 5 is satisfied, the chosen value of r_1 is equal to $r_{1,\min}$, so stop. Otherwise, go to step 2 and repeat this procedure.

From the procedure we can calculate the minimum external reboiler ratio s_1 and minimum vapor flowrate $V_{1,\min}^{\text{reac}}$ for reactive mixtures:

$$V_{1,\min}^{\text{reac}} = s_1 \cdot W_1$$

Therefore, the minimum vapor flowrate for the column I should be chosen:

$$V_{1,\min} = \max\{V_{1,\min}^{\text{pure}}(\theta); V_{1,\min}^{\text{reac}}\}$$

5.2.3.2 Minimum vapor flow-rate for column II and III

Following the restrictions, in columns II and III only separation occurs. Thus, the minimum vapor flowrates are determined by the Underwood equation as in the shortcut method of C. Triantafyllou et al. (1992) as presented in Chapter 3.

5.2.3.3 Minimum vapor flow-rate for column II and III

The minimum vapor flow of the DWC system should be chosen by Halvorsen et al (2003):

Chapter 5: Design of reactive divided wall column

$$V_{\min, \text{DWCs}} = \max\{V_{2, \min}, \bar{V}_{3, \min} + (1 - q_1) \cdot F^*\}$$

5.2.3.4 Number of stage for each section of DWC system

Starting from the structure in Figure 5.3 an evaluation of the NTS for each section and reflux ratio for each column are computed based on a shortcut method of Fenske, Underwood and Gilliland and Kirkbride equations (Henry Z. Kister 1992).

5.2.4 Simulation

5.2.4.1 Model of simulation for reactive divided wall column

The model for simulation of a reactive divided wall column is presented in Figure 5.4 as a two-column model sequence. The first column is the prefractionator where reaction takes place and the second column is the main column where the reaction products are separated. Other information is the same as the model used for simulation of the divided wall column as shown the Chapter 3.

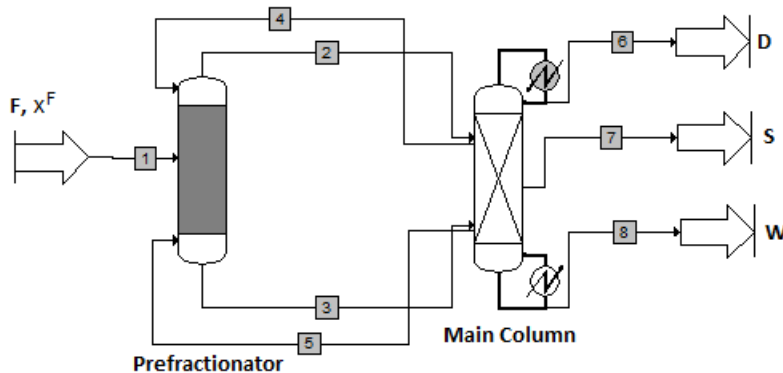


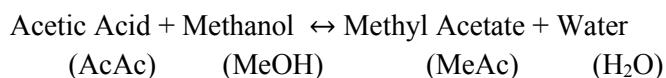
FIGURE 5.4 The model for simulation of reactive divided wall column by ProSim^{plus}

The initial parameters for simulation are the same as the divided wall column as shown in Chapter 3. However, it is note that prefractionator carried out reaction. Therefore, we have to consider the chemical reaction definition. If using an equilibrium model, we have to set the equilibrium constants. If using a kinetic model, we have to set the frequency factor and the holdup in each stage.

5.3 CASE STUDY FOR METHYL ACETATE SYNTHESIS

5.4.1 Introduction

Methyl acetate is used as an intermediate in the manufacture of a variety of polyesters. The reaction for methyl acetate production is operated at standard pressure and temperature between 76°C to 117°C. The methyl acetate was difficult to purify because of the formation of an azeotrope between methyl acetate and methanol, and also between methyl acetate and water. The reaction scheme is as follows:



The conventional processes used multiple reactors in which a large excess of one of the reactants is used to achieve high conversion of the other reactant and a series of vacuum and atmospheric distillation columns are used to obtain purity of methyl acetate (Agreda et al., 1990).

Barbosa and Doherty (1988a, b) presented a method to design a single feed reactive distillation for methyl acetate production. The feed stream is a binary mixture of methanol 60 % mole fraction and acetic acid 40 % mole fraction. The minimum reflux ratio is 0.58. In the column, the methyl acetate and methanol azeotrope is the distillate product and the bottom product is water and a little acetic acid.

Huss, Song, Malone, and Doherty, 1997 presented a reaction equilibrium device with double feeds, where acetic acid is fed near the top of the column and methanol near the bottom of the column. The top product is methyl acetate and bottom product is water.

R. They et al., 2005 also presented a method for the design of a two feed reactive distillation for methyl acetate production. The feed composition is equimolar. This configuration is a column made up of 39 plates to obtain a distillate composed of 98% mole of methyl acetate. The acetic acid feed is located on the third plate (starting from the top) and the methanol feed is introduced on the plate 36. The reflux ratio is equal to 1.7.

Based on several reviews for methyl acetate synthesis with reactive distillation and traditional processes, depending on the single or double feed stream and feed composition, a reactive

Chapter 5: Design of reactive divided wall column

divided wall column can be chosen for the reactive distillation or a reactive divided wall column. In the case with double feed and equimolar feed composition, the reactive distillation should be used because purity of methyl acetate can be obtained as the distillate product and the conversion of reactants is almost 100% (R. They et al., 2005). However, in the case with single feed and a large excess of one of the reactants, a reactive divided wall column should be used because reaction products and methanol (or acetic acid) need to be separated.

5.4.2 Kinetic and equilibrium equations and thermodynamic model

5.4.2.1 Equilibrium equation

Methyl acetate can be made by the liquid phase reaction of acetic acid and methanol catalyzed by sulfuric acid or a sulfonic acid ion-exchange resin in the temperature range of 310 – 325K and at a pressure of 1 atm.

The liquid phase activity coefficients for each point were obtained using the Wilson model with parameters given in Appendix [2D] (Song et al., (1998)).

The thermodynamic equilibrium constant is a function of temperature. The equilibrium constant for the esterification reaction is (Song et al. 1998):

$$\ln(K) = -0.8226 + \frac{1309.8}{T}$$

5.4.2.2 Kinetic of reaction

The reaction of methanol and acetic acid to give methyl acetate has equilibrium limitations. Agreda et al., (1990) proposed the rate equation of the reaction:

$$r = k_0 \exp\left(\frac{-E_a}{RT}\right) \left(C_{MeAc} C_{H_2O} - \frac{C_{AcAc} C_{MeOH}}{K_e} \right)$$

Where: K_e is the liquid equilibrium constant and is equal as 5.2 (Agreda (1990));

E_a - Activation energy is equal 10,000 (calmol⁻¹) by Smith, H.A (1939).

Smith, H. A (1939) also proposed rate constant $k_0 = 1.2 \cdot 10^6$ (l mole⁻¹ s).

5.4.3 Design Procedure

Chapter 5: Design of reactive divided wall column

In this case, only direct separation is considered because the methyl acetate is collected in the distillate product. Therefore, the entire feed composition of the reactive system can be classified for direct separation in which the distillate composition of the product is fixed. Table 5.1 shows the temperature of the azeotropic point and the pure component. It is noted that the azeotrope of methyl acetate 66 % mole and methanol 34 % mole has the lowest boiling temperature. Therefore it is fixed as the distillate product in the direct separation.

TABLE 5.1 Ranking of azeotrope temperature and pure component normal boiling point temperature

Component and azeotrope point	Boiling point (°C)
Azeotrope of MeAc and MeOH	53.65
Azeotrope of MeAc and H ₂ O	56.43
MeAc	57.03
MeOH	64.53
AcAc	118.01

Table 5.2 presents the results of classification as obtained by predesign of They et al., (2005). We assumed that the feed flowrate is equal to 100kmolh⁻¹. The results of table 5.2 show that if the quantity of methanol in the feed composition is less than or equal 60 % mole the bottom product of the mixture includes water and acetic acid. If the quantity of methanol in the feed composition is more than 70% mole, the bottom product of the mixture includes methanol and water.

TABLE 5.2 Classification of feed composition for direct separation

Feed molar liquid composition		Distillate molar liquid composition				Bottom molar liquid composition				ξ	K_D
MeOH	AcAc	MeOH	AcAc	MeAc	H ₂ O	MeOH	AcAc	MeAc	H ₂ O		
0.1	0.9	0.34	0.00	0.66	0.00	0.00	0.93	0.00	0.07	0.066	0.11
0.2	0.8	0.34	0.00	0.66	0.00	0.00	0.83	0.00	0.17	0.154	0.25
0.3	0.7	0.34	0.00	0.66	0.00	0.00	0.72	0.00	0.28	0.198	0.43
0.4	0.6	0.34	0.00	0.66	0.00	0.00	0.56	0.00	0.44	0.264	0.66
0.5	0.5	0.34	0.00	0.66	0.00	0.00	0.34	0.00	0.66	0.330	1.00
0.6	0.4	0.34	0.00	0.66	0.00	0.00	0.01	0.00	0.99	0.396	1.50
0.7	0.3	0.34	0.00	0.66	0.00	0.45	0.00	0.00	0.55	0.3	0.83
0.8	0.2	0.34	0.00	0.66	0.00	0.71	0.00	0.00	0.29	0.2	0.43
0.9	0.1	0.34	0.00	0.66	0.00	0.88	0.00	0.00	0.12	0.1	0.19

If the amount of methanol in the feed composition is 10 % mole fraction, then the bottom product is mainly acetic acid 93 % mole and a little water 7 % mole fraction. If the amount of

Chapter 5: Design of reactive divided wall column

methanol in the feed composition is 60%, then the bottom product is mainly water 99% mole fraction and a little acetic acid 1% mole fraction. In these cases, we should use reactive distillation instead of a reactive divided wall column because the pure separation of bottom products is not needed.

However, if the amount of methanol in the feed composition is between 10% and 50% mole fraction, then the distillate product is as azeotrope of methyl acetate and methanol, and the bottom product includes acetic acid and water. Therefore, one should use the reactive divided wall column to separate the water and acetic acid from the mixture to obtain pure acetic acid.

If the amount of methanol in the feed composition is more than 70% mole fraction, then the distillate product is an azeotrope of methyl acetate and methanol, and the bottom product is a mixture of methanol and water. Therefore, a reactive divided wall column should be used to obtain pure methanol.

In this section, two feed compositions are chosen to be investigated. In the first case, the feed mixture is composed of methanol 80% mole fraction and acetic acid 20% mole fraction. Therefore, in this case, the azeotrope of methyl acetate and methanol is the distillate product, methanol is the side product and water is the bottom product. In the second case, the feed mixture is composed of methanol 20% mole fraction and acetic acid 80% mole fraction. In this case, the azeotrope of methyl acetate and methanol is also the distillate product, water is the side product and acetic acid is the bottom product. The operating pressure is 1 atm, the feed flowrate is 100 kmol/h and the separation type is direct separation.

5.4.3.1 First case

The figure 5.5 shows the feed composition and specification of the products for case 1.

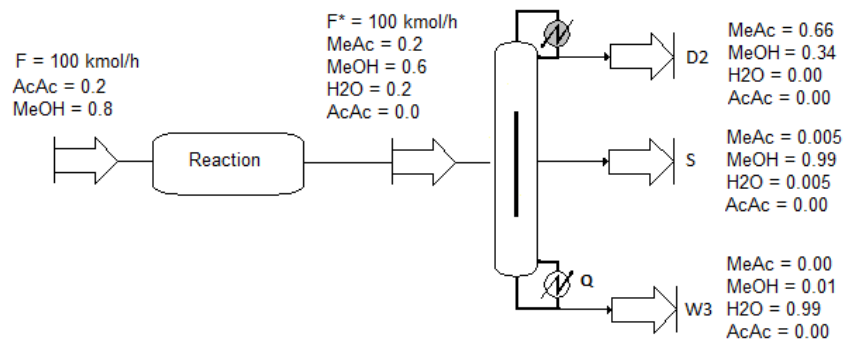


FIGURE 5.5 Feed composition and specifications of the products for case 1

Chapter 5: Design of reactive divided wall column

Based on the procedure of They et al., (2005), the pseudo-initial composition can be determined as in Figure 5.5. Acetic acid does not occur in the pseudo-initial mixture because of its 100% conversion to methyl acetate. Therefore, the feed composition for the shortcut procedure is methyl acetate at 20 % mole, methanol at 60 % mole, water at 20 % mole and acetic acid at 0 % mole. The specification of the key component in the product is also presented in figure 5.5 in which the methyl acetate in the top product is 66 % mole and methanol 34 % mole as the azeotrope point, the methanol in the side product is 99% mole and the water in the bottom product is 99% mole. Figure 5.6 shows the results obtained from the shortcut design method in which the detailed structure and operating variables of the reactive divided wall column are listed.

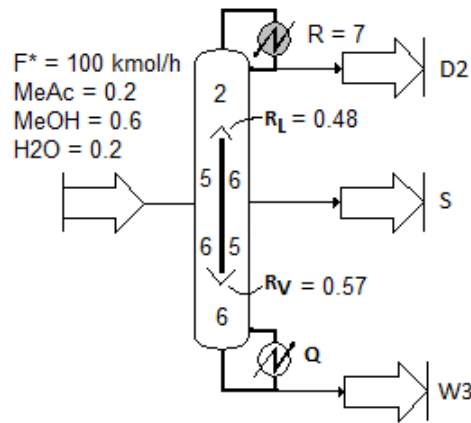


FIGURE 5.6 Structure parameters of reactive divided wall column

The structure of the reactive divided wall column consisted of 19-stages, with 11-stages in the prefractionator located between stages 2 and 13, the feed location is at stage 7, the side stream at stage 8, liquid and vapor split are 0.48 and 0.57, respectively, the reflux ratio is 7 and the reboiler duty of 2116 kW.

The reactive divided wall column is simulated by ProSim^{plus} software with structural and operational parameters the same as in Figure 5.6. In this case, the equilibrium model is used with the Wilson model and thermodynamic parameters as indicated previously (Song et al., (1998)).

The composition profiles for the liquid phase in the reactive divided wall column of Figure 5.6 are displayed in Figure 5.7. According to the figure, the top product is a mixture of methyl acetate and methanol. The methanol is the distributed component and is collected as a side product (97.1% mole). The bottom product contains water as it is heaviest component (97% mole). The figure shows that the content of acetic acid in the prefractionator and main

column are almost zero. It is in agreement with table 5.2 where acetic acid reacts with methanol and converts almost 100% into methyl acetate in the prefractionator, immediately.

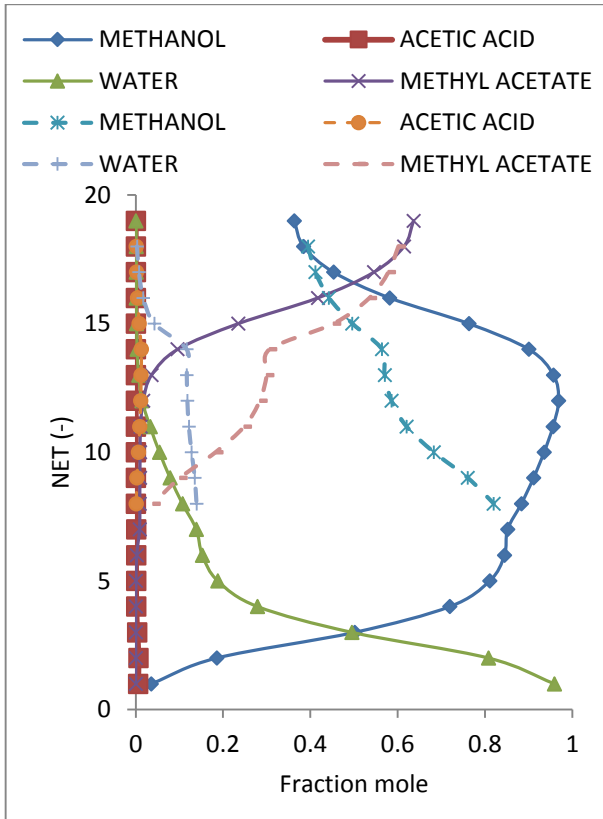


FIGURE 5.7 Composition profile in the reactive divided wall column

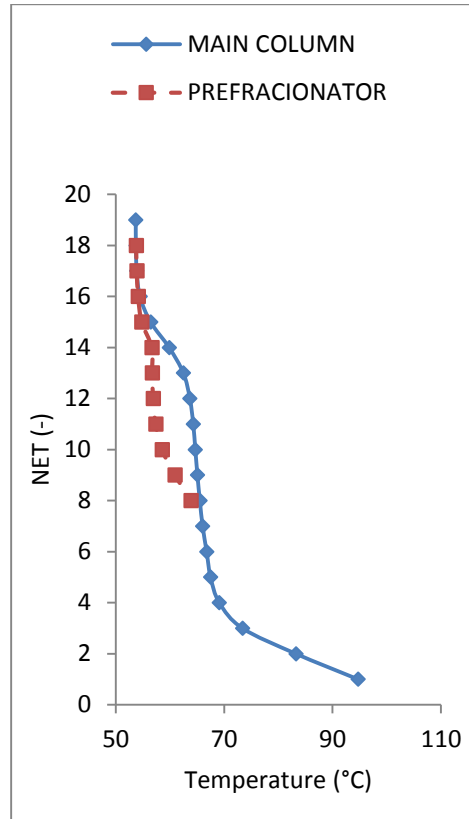


FIGURE 5.8 Temperature profile in the reactive divided wall column

Figure 5.8 shows the temperature profile in the prefractionator and main column. The temperature gradient is almost zero from stage 17 to stage 19. It is noted that at the top of the column for the pure separation not many stages are required.

The temperature of prefractionator is lower than temperature of the side section because the feed section has a mixture of methyl acetate, methanol, a little acetic acid and water while the side section contains mainly methanol. The maximum temperature difference between them is 7°C.

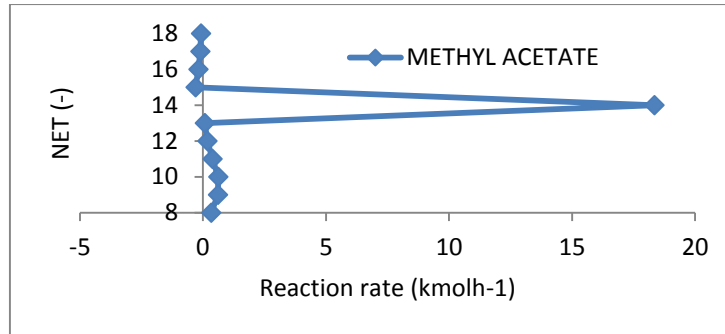


FIGURE 5.9 Reaction profiles in the prefractionator (Case 1)

Figure 5.9 presents the reaction profiles and it can be seen that most of reaction takes place around stage 7 where the methanol and acetic acid are introduced to the reactive zone.

TABLE 5.3 Relative errors between simulation and specification of key component (Case 1)

Parameters	Shortcut data	Simulation	Relative error (%)
Distillate			
Methyl acetate (% mole fraction)	0.66	0.640	-3.03
Methanol (% mole fraction)	0.34	0.359	+5.59
Water (% mole fraction)	0.00	0.001	-
Acetic acid (% mole fraction)	0.00	0.000	-
Side stream			
Methyl acetate (% mole fraction)	0.005	0.016	-
Methanol (% mole fraction)	0.99	0.971	-1.92
Water (% mole fraction)	0.005	0.013	-
Acetic acid (% mole fraction)	0.00	0.000	-
Bottom stream			
Methyl acetate (% mole fraction)	0.00	0.000	-
Methanol (% mole fraction)	0.01	0.030	-
Water (% mole fraction)	0.99	0.970	-2.02
Acetic acid (% mole fraction)	0.00	0.000	-
Reflux ratio (R)	6.97	6.97	-
Liquid split (R_L)	0.48	0.48	-
Vapor split (R_V)	0.58	0.52	-10.37
Energy consumption Q_b (kW)	2116	2091	-1.18

The relative error results compare the simulation and specification of several important parameters as shown in the table 5.3. The results show that the relative errors of key components are less than 6 %. It is possible to note that the simulation results and specification are in good agreement. The mole fraction purity of 97.1 % mole for methanol is reached as the side product. Therefore, it is possible to obtain a very high purity of methanol. It is important note that the reactive divided wall column can still separate it as a high purity side product.

5.4.3.2 Second case

Figure 5.10 shows the mixture including acetic acid 80 % mole and methanol 20 % mole. The separation type is also direct separation. Table 5.3 shows the conversion of reaction is $\xi = 0.154$. That means the feed composition x^F is converted to the pseudo-initial composition x^* including four components: methyl acetate at 15.4 % mole, methanol at 4.6 % mole, water at 15.4 % mole and acetic acid at 64.6 % mole. In this case, the azeotrope of methyl acetate and methanol is the top product, water is the side product, and acetic acid is the bottom product.

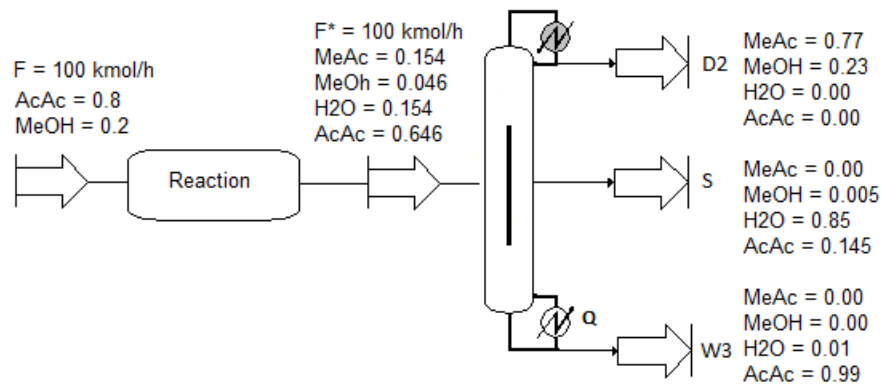


FIGURE 5.10 Feed composition and specification of the products for case 2

In this case, first we choose the composition of the distillate as the stable node composition, that being the azeotrope of methyl acetate and methanol. Then, the calculation can be made again for a specified distillate product. We have to do that because the distillate composition obtained in a reactive section must satisfy the chemical equilibrium and then must lie on the chemical equilibrium manifold which is a set of liquid phase compositions for which the rate of chemical reaction is equal to zero.

TABLE 5.4 Corrected the composition of the distillate product

Composition	Specification of distillate product of reactive section		
	Trial 1	Trial 2	Trial 3
MeAc	0.66	0.798	0.770
MeOH	0.34	0.201	0.229
H2O	0	0.001	0.001
AcAc	0	0	0

Chapter 5: Design of reactive divided wall column

In table 5.4, first, the azeotrope of methyl acetate and methanol is chosen as the distillate composition of product however the compositions of the top product in the prefractionator do not lie in the chemical equilibrium manifold. It is not feasible. Therefore, we have to choose again the composition of the top product. Table 5.4 shows that we should choose the methyl acetate at 77 % mole and methanol at 23 % mole as the distillate product. Figure 5.10 shows the feed composition and specification of products.

Even if the acetic acid and water system does not form an azeotrope at atmospheric pressure, the separation of the binary mixture water and acetic acid by direct distillation is not suitable for industrial applications because of the presence of a tangent pinch on the pure water end (Carlo Pirola, 2013). Therefore, in figure 5.9 the composition of water is specified as 85 % mole and acetic acid is 1.45 % mole.

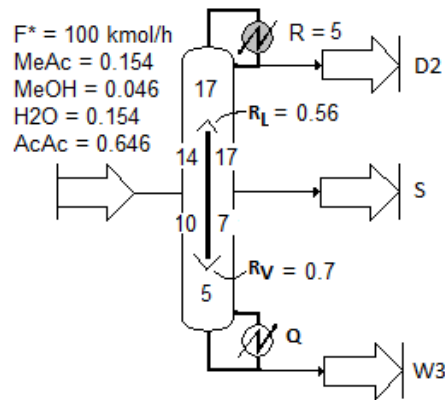


FIGURE 5.11 Structure parameters result of the reactive divided wall column

Figure 5.11 shows the results obtained from the shortcut design method in which the detailed structure and operating variables of the reactive divided wall column are listed. The structure of the reactive divided wall column consisted of 46-stages, with 24-stages in the prefractionator located between stages 17 and 41, the feed location at stage 31, the side stream at stage 34, liquid and vapor split of 0.56 and 0.7, respectively, the reflux ratio is 5 and the reboiler duty is 1125 kW. It can be seen that the total number of reactive divided wall columns for case 2 is more than that of case 1. Clearly the mixture of case 2 needs more pure separation stages than case 1.

The structural parameters from the shortcut method re inputted into the simulation tool. The relative error results are compared between the simulation and the specification of key components as shown in table 5.5.

Chapter 5: Design of reactive divided wall column

The composition profiles for the liquid phase in the reactive divided wall column are displayed in figure 5.12. According to the figure, the top product obtains a mixture including three components: methyl acetate 78 % mole, methanol 18 % mole and water 4 % mole. The side product contains a little methanol, 3.7 % mole, water at 79.6 % mole and a little acetic acid, 15.8 % mole. The bottom product produces almost 97.9 % mole acetic acid and 2.1% mole water. It is noted that acetic acid can be recovered back to the feed of the column. It is noted that at stage 27 where the interconnecting stream is located the compositions of components of each side between dividing wall are not the same because at this stage, the reaction for hydrolysis of methyl acetate occurs. That means that methyl acetate reacts with water to produce acetic acid and methanol as shown in Figure 5.14.

TABLE 5.5 Relative errors between simulation and specification of key component (case 2)

Parameters	Specification	Simulation	Relative error (%)
Distillate			
Methyl acetate (% mole)	0.77	0.78	+1.29
Methanol (% mole)	0.23	0.18	-21.7
Water (% mole)	0.00	0.04	-
Acetic acid (% mole)	0.00	0	-
Side stream			
Methyl acetate (% mole)	0	0.009	-
Methanol (% mole)	0.005	0.037	-
Water (% mole)	0.85	0.796	-6.35
Acetic acid (% mole)	0.145	0.158	+8.96
Bottom stream			
Methyl acetate (% mole)	0	0	-
Methanol (% mole)	0	0	-
Water (% mole)	0.01	0.021	-
Acetic acid (% mole)	0.99	0.979	-1.11
Reflux ratio (R)	5	5	-
Liquid split (R_L)	0.56	0.50	-10.71
Vapor split (R_V)	0.70	0.70	-
Energy consumption Q_b (kW)	1125	1078	-4.17

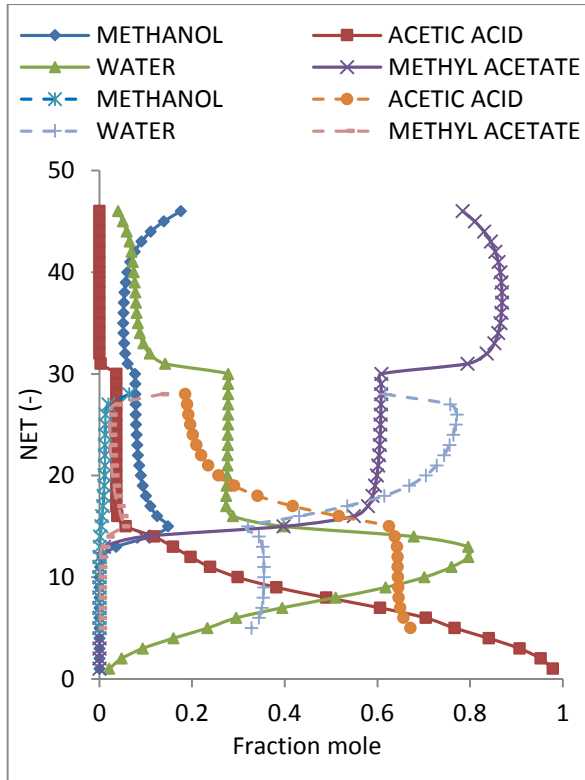


FIGURE 5.12 Composition profile in the reactive divided wall column (Case 2)

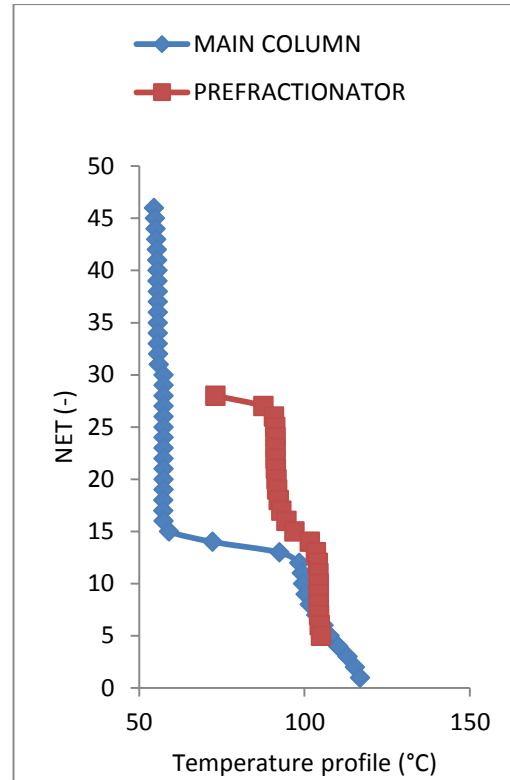


FIGURE 5.13 Temperature profile in the reactive divided wall column (Case 2)

The temperature profiles of the prefractionator and main column are displayed in Figure 5.13. The temperature profile of the main column located from stage 10 to stage 15 changes largely because the amount of water and acetic acid in the mixture increases very fast as shown in Figure 5.12. Therefore the temperature increases from 60°C to 100°C within three stages. While the temperature profile of the prefractionator also increases quickly from stage 25 to 27 because it is affected by the hydrolysis reaction of methyl acetate.

Figure 5.14 presents the reaction profiles in the prefractionator and it can be seen that most of reaction takes place around stage 15 where the methanol and acetic acid are introduced in to the reactive zone. However, the methyl acetate hydrolysis reaction occurs in the top of prefractionator because, in this case, the water is a distributed component thus a part of the water will move to the top of the prefractionator with large amount of methyl acetate. Therefore a part of the methyl acetate and water are converted into methanol and acetic acid.

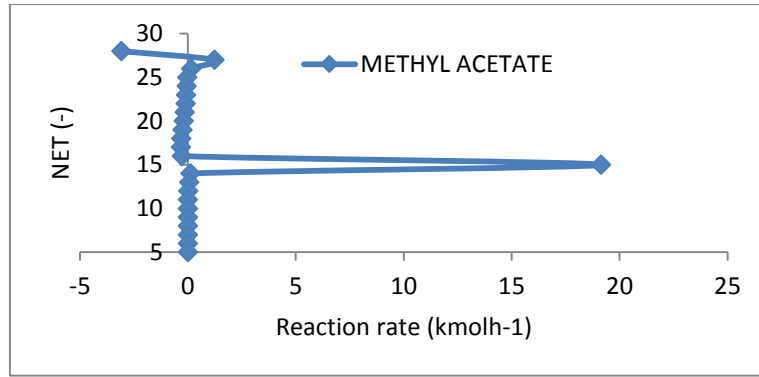


FIGURE 5.14 Reaction profiles in the prefractionator

5.4.4 Conclusion

The conceptual design and simulation of methyl acetate synthesis carried out in a reactive divided wall column were achieved. The results of the simulation are in agreement with the specifications of the design. These results validated the process simulation studies about the design of the system. The analysis of two cases of methyl acetate synthesis show that the case of excess of methanol has a smaller number of stages, greater conversion and no methyl acetate hydrolysis reaction when compared with the case of excess acetic acid.

Based on the analysis, we choose the mixture of excess of methanol for experiment in the reactive divided wall column plot plant.

5.5 EXPERIMENT VERIFICATION FOR REACTIVE MIXTURE IN DIVIDED WALL COLUMN

5.5.1 Introduction

The structure of the pilot plant for the non-reactive divided wall column in our laboratory is changed in order to be used for a reactive mixture in which the prefractionator has 4 reactive packing elements (Katapak packing) and 2 non-reactive packing elements (Sulzer DX packing); the side section has 6 non-reactive packing elements (Sulzer DX packing); the top column has 4 elements with non-reactive packing and the bottom section has 6 elements with non-reactive packing.

Chapter 5: Design of reactive divided wall column

Based on the structure of the pilot plant for the reactive divided wall column, the structure of the simulation model is modified to apply for the reactive divided wall column. It is noted that because the packing used in the prefractionator and side section are different (Katapak and Sulzer DX packing) therefore the number of stages in the prefractionator is not the same as the number of stages in side section. In this case, the prefractionator has 6 stages in which there are 2 reactive stages and 4 separation stages while the side section has 15 stages for separation. The top part of the column has 10 stages while the bottom part of the column has 15 stages in the separation zone. Feed location is 13-stage and the side stream is at stage 17. The structural parameters of the pilot plant for the reactive divided wall column are presented in Figure 5.15.

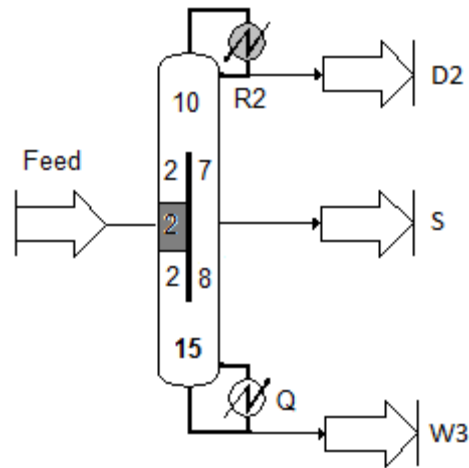


FIGURE 5.15 Structure parameters of reactive divided wall column in simulation model

5.5.2 Experiment results

The feed flowrate is $5.79\text{kg}\cdot\text{h}^{-1}$. Feed composition is methanol 62.8 % mass fraction, acetic acid 29.4 % mass fraction, and water 7.8 % mass fraction. Water is present in the feed stream because we use a mixture of acetic acid (80% mass fraction) and water (20% mass fraction). The feed composition was chosen to ensure that the mole ratio of Methanol and Acetic acid is equal to 4:1. In this case, methanol is the excess component therefore the top product is an azeotrope of methyl acetate and methanol, the side product is methanol and the bottom product is water and acetic acid. Operating pressure is atmospheric pressure $P = 1\text{ atm}$.

Chapter 5: Design of reactive divided wall column

Based on the simulated results for the reactive divided wall column, the predicted parameters are applied for an actual experimental run in which the reflux ratio (R) is set to 7, and the liquid split (R_L) is set 0.5. Table 5.6 shows the material balance results of an experimental run in our pilot plant.

TABLE 5.6 Mass balance of total and each component

Component	Feed stream (kg/h)	Top product (kg/h)	Side product (kg/h)	Bottom product (kg/h)	OUT - IN	Mole of reaction
Methanol	3.696	0.933	1.572	0.643	-0.548	-0.017
Acetic acid	1.730	0.000	0.000	0.637	-1.093	-0.018
Methyl acetate	0.000	1.192	0.078	0.014	1.270	0.017
Water	0.459	0.000	0.000	0.768	0.309	0.017 ^(*)
Total	5.886	2.125	1.650	2.062	0.049	-

(*) Assumption that amount of water has only at bottom product.

The samples that were collected from experimental run obtained methanol, methyl acetate, acetic acid, and water. They are analyzed by a chromatography method. Chromatography can analyse the methanol, methyl acetate, and acetic acid in the samples but cannot detect water in the samples. Therefore the amount of methyl acetate, methanol, and acetic acid in the samples can be determined but the amount of water in the mixture cannot be determined. In order to solve this problem, we assume that the water is only collected in the bottom product. The stoichiometric ratio of reactants and products found from the balanced chemical equation show that it requires 1 mole of methanol and 1 mole of acetic acid to produce 1 mole of methyl acetate and 1 mole of water. Therefore the material balance is in agreement if the ratio of mole of each component is 1:1:1:1.

Table 5.6 shows the actual ratio of moles of components is $0.017:0.018:0.017:0.017 = 1:1.06:1:1$. It is possible to conclude that the material balance of the experimental run is in agreement. The details of this calculation are presented in Appendix [5].

Table 5.7 shows the experimental data compared with the simulated results while Figure 5.15 shows the temperature profile in the prefractionator and main column. Because we do not know the amount of water in the mixture therefore the compositions of samples are transformed into “dry” samples (not including the water). The detailed procedure to transform the composition is shown in Appendix [6].

It is noted that the procedure in Figure 4.7 does not need to be applied for this case because the information from experimental run is good for the simulation.

TABLE 5.7 Experimental results at steady-state run compare with simulation result

Parameters	Experiment ^(*)	Simulation ^(*)	Relative error (%)
Feed (kgh⁻¹)	5.837	5.837	-
Methanol (% mass)	0.628	0.628	-
Acetic acid (% mass)	0.294	0.294	-
Methyl acetate (% mass)	0.000	0.000	-
Water (% mass)	0.078	0.078	-
Distillate (kgh⁻¹)	2.125	2.125	-
Methanol (% mass)	0.439	0.431	-1.93
Acetic acid (% mass)	0.000	0.000	-
Methyl acetate (% mass)	0.561	0.569	+1.51
Water (% mass)	-	-	-
Side stream (kgh⁻¹)	1.650	1.650	-
Methanol (% mass)	0.953	0.968	+1.69
Acetic acid (% mass)	0.000	0.022	-
Methyl acetate (% mass)	0.047	0.010	-
Water (% mass)	-	-	-
Bottom stream (kgh⁻¹)	2.062	2.062	-
Methanol (% mass)	0.497	0.512	+3.02
Acetic acid (% mass)	0.492	0.488	-0.81
Methyl acetate (% mass)	0.011	0.000	-
Water (% mass)	-	-	-
Liquid split (-)	0.5	0.53	+6.00
Vapor split (-)	-	0.48	-
Reflux ratio (-)	7	7	-
Heat duty (kW)	2.9	3.2	+10.3

(*) The composition of samples is transformed into “dry” samples.

The results show that relative errors of key components of all products are less than 5%. The relative error of the heat duty is more than 10 %. It is noted that the energy consumption of the condenser in the experimental run is used to compare with the heat duty of the reboiler in the simulation because in the simulation process, we assume that heat loss through the wall is neglected.

The experimental and simulated temperature profiles for experimental runs are depicted in Figure 5.16. The maximum temperature difference between experimental and simulation results is around 2 °C. It is noted that the temperatures of the prefractionator are lower than that of the main column. Moreover, the vertical double S-shape of the temperature profiles of the main column indicate that the upper part of main column is used to separate methyl acetate and methanol while the lower part of the main column is used to separate methanol and water. The results are in good agreement with each other.

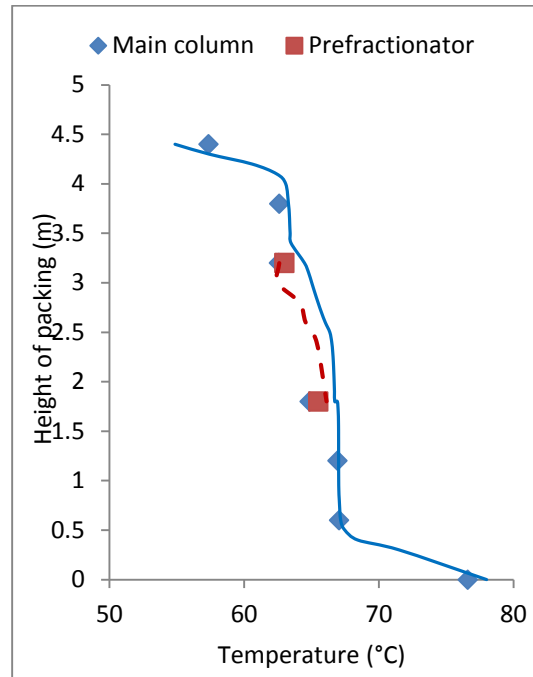


FIGURE 5.16 Temperature profile compare between the experiment and simulation result

The result is important because it allows us to validate the results found by simulation. The experimental test allows us to validate the simulations of the system with the reactive divided wall column.

5.6 CONCLUSION OF THE CHAPTER 5

A procedure for the design of reactive divided wall columns is presented. It based on the predesign method of They et al., (2005) and a modified shortcut method based on the method of C. Triantafyllou et al., (1992). To validate our procedure, methyl acetate production is carried out in the reactive divided wall column. The results of the study indicate that the approach works well and provides both the basis for preliminary optimization and a good initialization for rigorous simulation in the ProSim^{plus} software. It is the first time a reactive divided wall column has be simulated in the ProSim software in

Chapter 5: Design of reactive divided wall column

which the two-column model sequence is applied. A pilot plant for the reactive divided wall column is also built and is used for methyl acetate production. The experimental results are in good correspondence with the simulated results. Therefore it can be expected that improvements achieved in a simulation will also be found in an industrial scale column. The results provide good proof that can help to increase the acceptance of reactive divided wall column in industrial processes.

Chapter 6

GENERAL CONCLUSIONS AND FUTURE WORK

6.1 THE MAIN CONTRIBUTIONS OF THE THESIS

First of all, the thesis has reviewed several papers that were published addressing divided wall columns and reactive divided wall columns. The review shows that the design of divided wall columns is more complex than for conventional columns because of the increasing number of degrees of freedom, i.e. design parameters. There are several proposed design methodologies for divided wall columns but most notably the method of C. Triantafyllou and Smith (1992) which is based on the Fenske-Underwood-Gilliland-Kirkbride equation. The model combines the individual equations to establish the minimum number of equilibrium stages (Fenske), minimum reflux (Underwood), the number of stages at the chosen operating reflux ratio (Gilliland), and the feed location (Kirkbride). Process simulators still do not have a standard model for a divided wall column in commercial software packages such as ASPEN^{plus}, Chemcad or ProSim^{plus}. It is important to note that simulation processes in the papers published have not yet used ProSim^{plus} to simulate a divided wall column or reactive divided wall column. The review also shows that design, simulation, control, and experimental data of a reactive divided wall column are still a new research area.

Secondly, the thesis proposed a procedure for optimal design of a divided wall column, based on the FUGK model. The structural and operational parameters of the system can easily and rapidly be determined. It is important to note that both technological and hydrodynamic aspects of the divided wall column are considered in the procedure. For application of the technology, it is easier if the number of stages or HETP in the prefractionator is the same as in the side section. The value of the liquid splits must be found to get this condition because liquid split affects to internal reflux ratios in each section of the column. In terms of hydrodynamics, the side product quality can be manipulated to give the optimal performance of the divided wall column in order to keep the F-factor constant in all sections. Then, the design parameters are used for rigorous simulation and optimization in the ProSim^{plus} software. In order to validate our procedure, both ideal and non-ideal ternary mixtures are investigated in the divided wall column. The results show that the procedure can give a good initialization for a rigorous simulation. The energy usage of the conventional distillation configurations and the divided wall columns are also compared. It is noted that the divided wall column can save energy consumption by up to 33 %. However, the divided wall column is not always the best compared with the conventional distillation columns. This selection depends on the feed composition and the ESI value of the mixture.

Chapter 6: General conclusion and future work

Thirdly, a pilot plant is built in our laboratory (LGC, Toulouse, France, 2013) for non-reactive and reactive divided wall columns. It is noted that the pilot plant will provide necessary experimental evidence to further develop and validate work on divided wall columns. A ternary mixture (methanol, 1-propanol, and 1-butanol) and four-component mixture (methanol, isopropanol, 1-propanol, and 1-butanol) have been examined in our pilot plant at steady state conditions. The results show that not only the composition of products but also composition and temperature profile along the column are in very good agreement with experimental data and simulated results.

Finally, a proposed conceptual design method for a reactive divided wall column is presented. The reactive divided wall column is decomposed step-by-step into single non-reactive and reactive columns in which the prefractionator represents a reactive column where reaction occurs and the main column is a non-reactive column where the separation takes place. Then, the predesign method of R. They et al., (2005) is applied to classify the feed composition. The feed composition is converted to the pseudo initial composition by using the reaction conversion. The pseudo mixture will be separated by the non-reactive divided wall column. A modified shortcut method for the reactive divided wall column based on the classical shortcut method adapted to a non-reactive divided wall column by C. Triantafyllou and R. Smith (1992) is applied. To verify the conceptual design method, rigorous simulations and experiment runs in the reactive divided wall column pilot plant in our laboratory are carried out. The methodology will be illustrated for the synthesis of Methyl Acetate from Methanol and Acetic Acid. The experimental results are in good agreement with the simulated results. Therefore the results provide good evidence to increase the acceptance of reactive divided wall columns in industrial processes.

6.2 PERSPECTIVES

In order to design divided wall columns, constant relative volatilities, constant molar flows, and constant operating pressures are assumed. However they are not necessarily constant along the column. Additionally the divided wall column is decomposed into three columns, therefore the interconnecting streams are considered as the feed flowrates for column II and

Chapter 6: General conclusion and future work

III with superheated vapor and sub-cooled liquid conditions. This issue calls for further studies.

The thesis focuses only on the design of middle dividing walls in the column. In future work, a procedure should be developed that can be applied to both upper dividing walls and lower dividing walls.

In chapter 3 and 4, a four-component mixture is considered in the divided wall column. This mixture can be separated into two high pure products and one product which is as a mixture of two components. The divided wall column can be expanded for four or more products; the separation can be performed in one divided wall column such as a Kaibel column or multiple dividing wall columns in which four high pure products can be achieved. Multiple-dividing wall columns have not yet been attempted in industrial practice. Therefore, based on the procedure, a design of a complex divided wall column requires further study in the future.

Chapter 3 assumes that heat transfer through the dividing wall is neglected. Thus the procedure does not consider the effect of heat transfer across the dividing wall. However, the results show that the temperature difference between the prefractionator and side section increases as the amount of middle component in the feed stream decreases. In future work, the effect of heat transfer through the dividing wall should be considered in the design, control and operation of the divided wall column.

In Chapter 3, a non-ideal mixture is considered but the method is still based on the procedure with ideal mixture assumptions. Therefore, the extensions to non-ideal and azeotropic mixtures in divided wall columns also require further study.

The thesis focuses on the conceptual design of divided wall columns and reactive divided wall columns. In Chapter 2, a review of controllability is considered and has shown that for control problems it is very important to adjust the degrees of freedom in order to obtain the required composition and minimum energy consumption. However the thesis has not carried out any controllability studies. Therefore future work should deal with the control approaches for divided wall columns and reactive divided wall columns.

The shortcut method for design of reactive divided wall columns in the thesis is restricted to a single feed, a single equilibrium reaction, and a reactive zone located in the prefractionator.

Chapter 6: General conclusion and future work

In future work, a double feed, two or more equilibrium reactions, and a reactive zone occurring outside of the prefractionator or in the main column should be studied.

The reactive mixture has only one experimental run in the thesis. Clearly the experimental data is too poor to validate our approach. Therefore more experimental data are needed to provide important insights into the behavior of reactive divided wall columns and to confirm our design method.

APPENDIX

Appendix 1: Equation of Stichmair (1998)

Concerning a ternary mixture A, B, and C, in which A is the lightest component and C is the heaviest component. We assume that recovery of component A in the top of prefractionator is 1, recovery of component B in the top of prefractionator β_P and recovery of component C in the top of prefractionator is zero.

We have: The minimum vapor flow in the prefractionator:

$$V_{1,\min} = \sum_{i=A}^C \frac{\alpha_i \cdot x_{i,D_1} \cdot D_1}{\alpha_i - \theta}$$

For ternary mixture, we have two roots of Underwood equation.

θ_1, θ_2 - are two roots of Underwood's equation at the minimum reflux condition. They must be following ranges: $\alpha_A > \theta_1 > \alpha_B > \theta_2 > \alpha_C$

$$(1 - q_1) = \sum_{i=A}^C \frac{\alpha_i \cdot z_i}{\alpha_i - \theta}$$

In order to obtain minimum vapor flowrate in the prefractionator: $V_{1,\min}(\theta_1)$ must equal to $V_{1,\min}(\theta_2)$. Therefore we have:

$$\begin{aligned} \frac{\alpha_A \cdot x_{A,D_1} \cdot D_1}{\alpha_A - \theta(1)} + \frac{\alpha_B \cdot x_{B,D_1} \cdot D_1}{\alpha_B - \theta(1)} + \frac{\alpha_C \cdot x_{C,D_1} \cdot D_1}{\alpha_C - \theta(1)} \\ = \frac{\alpha_A \cdot x_{A,D_1} \cdot D_1}{\alpha_A - \theta(2)} + \frac{\alpha_B \cdot x_{B,D_1} \cdot D_1}{\alpha_B - \theta(2)} + \frac{\alpha_C \cdot x_{C,D_1} \cdot D_1}{\alpha_C - \theta(2)} \\ \frac{\alpha_A \cdot x_{A,D_1} \cdot D_1}{\alpha_A - \theta(1)} \frac{z_A^F}{z_A^F} + \frac{\alpha_B \cdot x_{B,D_1} \cdot D_1}{\alpha_B - \theta(1)} \frac{z_B^F}{z_B^F} + \frac{\alpha_C \cdot x_{C,D_1} \cdot D_1}{\alpha_C - \theta(1)} \frac{z_C^F}{z_C^F} \\ = \frac{\alpha_A \cdot x_{A,D_1} \cdot D_1}{\alpha_A - \theta(2)} \frac{z_A^F}{z_A^F} + \frac{\alpha_B \cdot x_{B,D_1} \cdot D_1}{\alpha_B - \theta(2)} \frac{z_B^F}{z_B^F} + \frac{\alpha_C \cdot x_{C,D_1} \cdot D_1}{\alpha_C - \theta(2)} \frac{z_C^F}{z_C^F} \end{aligned}$$

Because $\tau_{A,T} = \frac{x_{A,D_1} \cdot D_1}{z_A^F} = 1$ and $\tau_{C,T} = \frac{x_{C,D_1} \cdot D_1}{z_C^F} = 0$. Therefore we have:

$$\frac{\alpha_A \cdot z_A^F}{\alpha_A - \theta(1)} + \frac{\alpha_B \cdot \beta_P \cdot z_B^F}{\alpha_B - \theta(1)} = \frac{\alpha_A \cdot z_A^F}{\alpha_A - \theta(2)} + \frac{\alpha_B \cdot \beta_P \cdot z_B^F}{\alpha_B - \theta(2)}$$

And we have recovery of component B in the top of prefractionator:

$$\tau_{B,T} = \beta_P = - \frac{\left(\frac{\alpha_A \cdot z_A^F}{\alpha_A - \theta_1} \right) - \left(\frac{\alpha_A \cdot z_A^F}{\alpha_A - \theta_2} \right)}{\left(\frac{\alpha_B \cdot z_B^F}{\alpha_B - \theta_1} \right) - \left(\frac{\alpha_B \cdot z_B^F}{\alpha_B - \theta_2} \right)}$$

Appendix 2: Thermodynamic models

Appendix 2A: Thermodynamic model for non-ideal mixture Methanol - Water

```
. THERMODYNAMIC MODEL..... From activity coefficients
. MIXING RULES..... Standard
. LIQUID MOLAR VOLUME..... Ideal mixture
. EQUATION OF STATE FOR THE GAS PHASE... Perfect gas
. ACTIVITY COEFFICIENTS MODEL..... NRTL
. PURE LIQUID FUGACITY STANDARD STATE... Vapor pressure
. USER-DEFINED THERMODYNAMIC MODEL..... None
. TRANSPORT PROPERTIES:
  - LIQUID VISCOSITY..... Classic methods
  - VAPOR VISCOSITY..... Classic methods
  - LIQUID THERMAL CONDUCTIVITY..... Classic methods
  - VAPOR THERMAL CONDUCTIVITY..... Classic methods
  - SURFACE TENSION..... Classic methods
. ENTHALPY CALCULATION..... H*=0, ideal gas, 25°C, 1 atm
```

BINARY INTERACTIONS PARAMETERS

COEFFICIENTS

I	J	CIJ0	CJI0	AIJ0
1 METHANOL	2 WATER	-253.88	845.21	0.29940

Appendix 2B: Thermodynamic model for mixture methanol – 1-propanol – 1-butanol

```
. THERMODYNAMIC MODEL..... From activity coefficients
. MIXING RULES..... Standard
. LIQUID MOLAR VOLUME..... Ideal mixture
. EQUATION OF STATE FOR THE GAS PHASE... Perfect gas
. ACTIVITY COEFFICIENTS MODEL..... NRTL
. PURE LIQUID FUGACITY STANDARD STATE... Vapor pressure
. USER-DEFINED THERMODYNAMIC MODEL..... None
. TRANSPORT PROPERTIES:
  - LIQUID VISCOSITY..... Classic methods
  - VAPOR VISCOSITY..... Classic methods
  - LIQUID THERMAL CONDUCTIVITY..... Classic methods
  - VAPOR THERMAL CONDUCTIVITY..... Classic methods
  - SURFACE TENSION..... Classic methods
. ENTHALPY CALCULATION..... H*=0, ideal gas, 25°C, 1 atm
```

BINARY INTERACTIONS PARAMETERS

COEFFICIENTS

I	J	CIJ0	CJI0	AIJ0
1 METHANOL	2 1-PROPANOL	12249.	-10432.	7.60000E-03
1 METHANOL	3 1-BUTANOL	43509.	-38251.	2.20000E-03
2 1-PROPANOL	3 1-BUTANOL	-46.904	45.899	0.30460

Appendix 2C: Thermodynamic model for mixture methanol – isopropanol - 1-propanol**– 1-butanol**

- . THERMODYNAMIC MODEL..... From activity coefficients
- . MIXING RULES..... Standard
- . LIQUID MOLAR VOLUME..... Ideal mixture
- . EQUATION OF STATE FOR THE GAS PHASE... Perfect gas
- . ACTIVITY COEFFICIENTS MODEL..... NRTL
- . PURE LIQUID FUGACITY STANDARD STATE... Vapor pressure
- . USER-DEFINED THERMODYNAMIC MODEL..... None
- . TRANSPORT PROPERTIES:
 - LIQUID VISCOSITY..... Classic methods
 - VAPOR VISCOSITY..... Classic methods
 - LIQUID THERMAL CONDUCTIVITY..... Classic methods
 - VAPOR THERMAL CONDUCTIVITY..... Classic methods
 - SURFACE TENSION..... Classic methods
- . ENTHALPY CALCULATION..... H*=0, ideal gas, 25°C, 1 atm

BINARY INTERACTIONS PARAMETERS

COEFFICIENTS

I	J	CIJ0	CJI0	AIJ0
1 METHANOL	2 ISOPROPANOL	482.84	-245.77	0.30280
1 METHANOL	3 1-PROPANOL	12249.	-10432.	7.60000E-03
1 METHANOL	4 1-BUTANOL	43509.	-38251.	2.20000E-03
2 ISOPROPANOL	3 1-PROPANOL	662.45	-488.88	0.34330
2 ISOPROPANOL	4 1-BUTANOL	165.70	-172.29	0.29880
3 1-PROPANOL	4 1-BUTANOL	-46.904	45.899	0.30460

Appendix 2D: Thermodynamic model for mixture methanol – acetic acid – methyl**acetate – water**

- . THERMODYNAMIC MODEL..... From activity coefficients
- . MIXING RULES..... Standard
- . LIQUID MOLAR VOLUME..... Ideal mixture
- . EQUATION OF STATE FOR THE GAS PHASE... Association
- . ACTIVITY COEFFICIENTS MODEL..... Dechema-compatible Wilson
- . PURE LIQUID FUGACITY STANDARD STATE... Vapor pressure
- . USER-DEFINED THERMODYNAMIC MODEL..... None
- . TRANSPORT PROPERTIES:
 - LIQUID VISCOSITY..... Classic methods
 - VAPOR VISCOSITY..... Classic methods
 - LIQUID THERMAL CONDUCTIVITY..... Classic methods
 - VAPOR THERMAL CONDUCTIVITY..... Classic methods
 - SURFACE TENSION..... Classic methods
- . ENTHALPY CALCULATION..... H*=0, ideal gas, 25°C, 1 atm

BINARY INTERACTIONS PARAMETERS

COEFFICIENTS

I	J	AIJ0	AJI0
1 METHANOL	2 ACETIC ACID	-547.52	2535.2
1 METHANOL	3 WATER	107.38	469.55
1 METHANOL	4 METHYL ACETATE	813.18	-31.193
2 ACETIC ACID	3 WATER	237.53	658.03
2 ACETIC ACID	4 METHYL ACETATE	1123.1	-696.50
3 WATER	4 METHYL ACETATE	1918.2	645.72

Appendix 3: Uncertainty calculation

Appendix 3A: Three - component mixture: Methanol – 1-propanol – 1-butanol

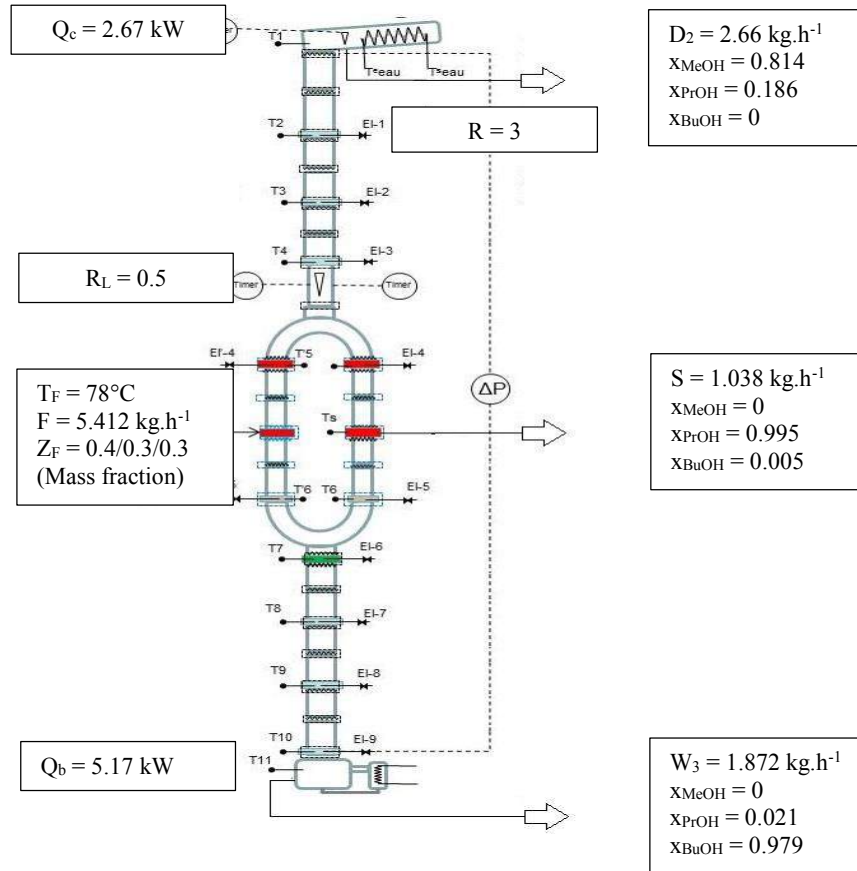
SAMPLES (mass %)			ANALYSIS (mass %)			UNCERTAINTY = ABS (SAMPLE - ANALYSIS)		
MeOH	1-ProOH	1-BuOH	MeOH	1-ProOH	1-BuOH	MeOH	1-ProOH	1-BuOH
0.100	0.200	0.690	0.120	0.250	0.630	0.020	0.050	0.060
0.940	0.030	0.030	0.942	0.039	0.018	0.002	0.009	0.012
0.096	0.810	0.094	0.108	0.802	0.090	0.012	0.008	0.004
0.395	0.318	0.280	0.372	0.326	0.301	0.023	0.008	0.021
0.021	0.027	0.952	0.053	0.060	0.887	0.032	0.033	0.065
0.100	0.200	0.690	0.146	0.198	0.657	0.046	0.002	0.033
0.940	0.030	0.030	0.944	0.050	0.006	0.004	0.020	0.024
0.096	0.810	0.094	0.119	0.850	0.031	0.023	0.040	0.063
0.395	0.318	0.280	0.352	0.355	0.293	0.043	0.037	0.013
0.021	0.027	0.952	0.107	0.039	0.854	0.086	0.012	0.098
0.213	0.389	0.399	0.150	0.443	0.407	0.063	0.054	0.008
0.330	0.206	0.464	0.250	0.300	0.450	0.080	0.094	0.014
0.151	0.196	0.653	0.158	0.209	0.633	0.007	0.013	0.020
0.990	0.010	0.000	0.973	0.027	0.000	0.016	0.016	0.000
0.005	0.989	0.007	0.000	1.000	0.000	0.005	0.011	0.007
0.000	0.008	0.992	0.000	0.019	0.981	0.000	0.011	0.011
MEAN						0.031	0.026	0.030

Appendix 3B: Four - component mixture: Methanol – iso propanol - 1-propanol – 1-butanol

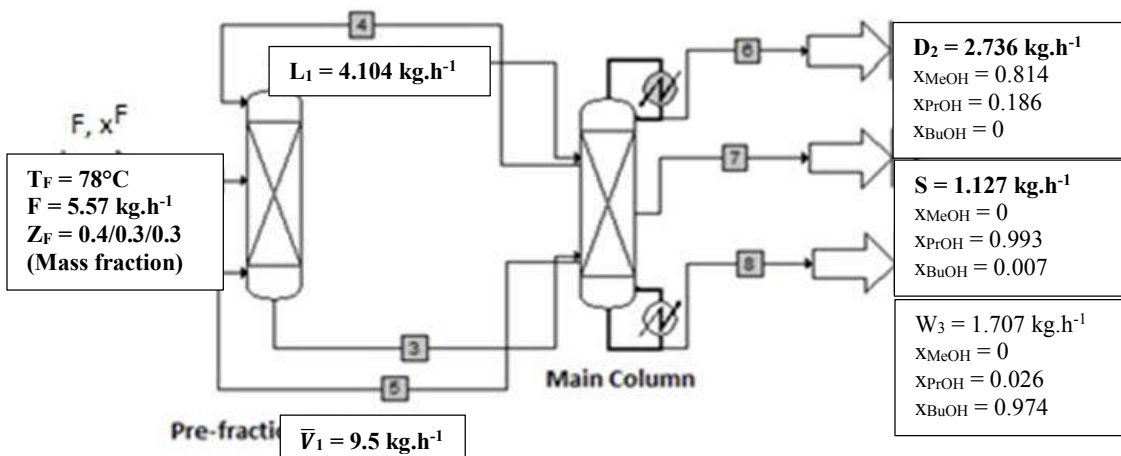
SAMPLES (mass %)				ANALYSIS (mass %)				UNCERTAINTY = ABS (SAMPLES - ANALYSIS)			
MeOH	Iso ProOH	1-ProOH	1-BuOH	MeOH	Iso ProOH	1-ProOH	1-BuOH				
0.105	0.216	0.358	0.321	0.151	0.178	0.360	0.311	0.046	0.038	0.002	0.01
0.105	0.216	0.358	0.321	0.155	0.185	0.365	0.295	0.05	0.031	0.007	0.026
0.105	0.216	0.358	0.321	0.157	0.172	0.369	0.302	0.052	0.044	0.011	0.019
0.910	0.075	0.015	0.000	0.905	0.030	0.065	0.000	0.005	0.045	0.05	0
0.910	0.075	0.015	0.000	0.917	0.040	0.043	0.000	0.007	0.035	0.028	0
0.910	0.075	0.015	0.000	0.908	0.035	0.057	0.000	0.002	0.04	0.042	0
0.000	0.892	0.045	0.063	0.000	0.894	0.020	0.086	0	0.002	0.025	0.023
0.000	0.892	0.045	0.063	0.000	0.889	0.027	0.084	0	0.003	0.018	0.021
0.000	0.892	0.045	0.063	0.000	0.882	0.024	0.094	0	0.01	0.021	0.031
MEAN								0.027	0.028	0.023	0.022

Appendix 4: Experimental and simulated results

Experiment 1: Methanol – 1-propanol – 1-butanol (0.4/0.3/0.3)



Experimental data



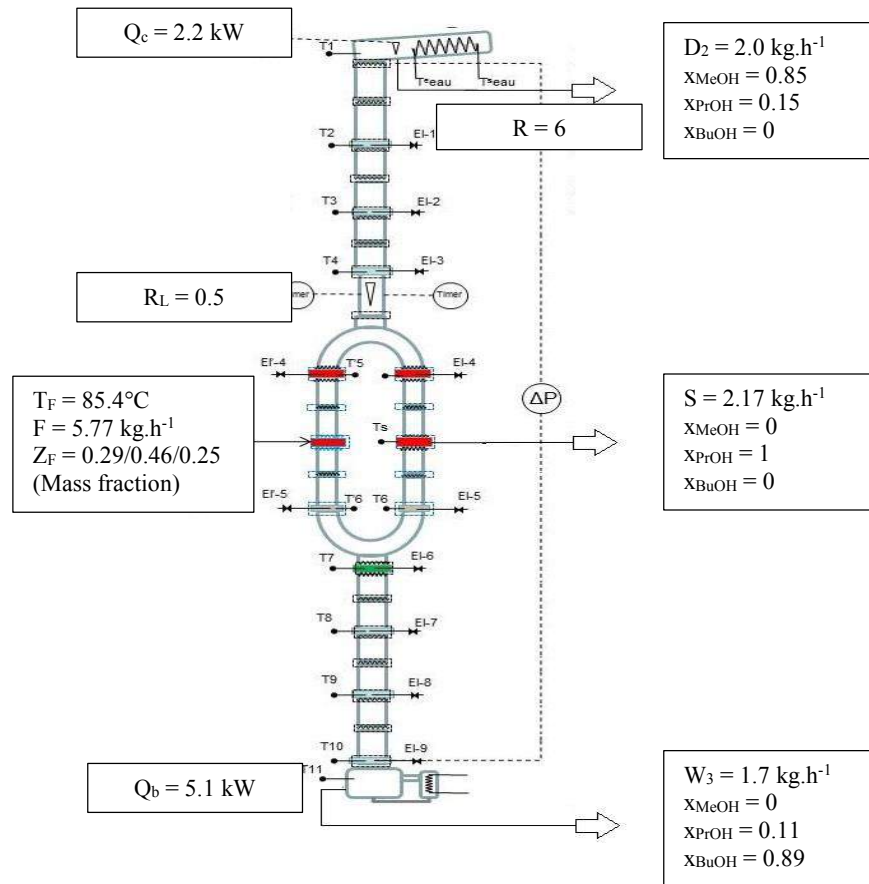
Botd: Data for simulation

Simulated data

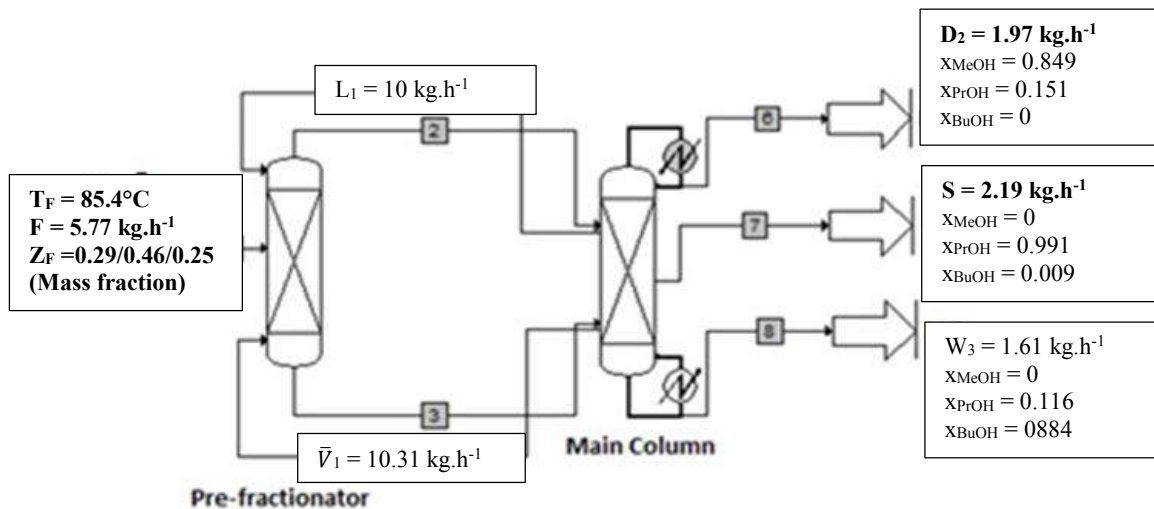
Comparison between experimental and simulated results

Parameters	Experiment	Simulation	Relative error (%)
Feed (kgh⁻¹)	5.41	5.57	+2.96
Distillate stream (kgh⁻¹)	2.66	2.736	+3.01
Methanol (wt. %)	0.814	0.814	0.00
1-Propanol (wt. %)	0.186	0.186	0.00
1-Butanol (wt. %)	0.00	0.00	0.00
Side stream (kgh⁻¹)	1.038	1.127	+8.57
Methanol (wt. %)	0.00	0.00	0.00
1-Propanol (wt. %)	0.995	0.993	-0.20
1-Butanol (wt. %)	0.005	0.007	+ 40.00
Bottom stream (kgh⁻¹)	1.872	1.707	-8.81
Methanol (wt. %)	0.00	0.00	0.00
1-Propanol (wt. %)	0.021	0.026	+23.81
1-Butanol (wt. %)	0.979	0.974	-0.51
Liquid split R_L (-)	0.5	0.5	0.00
Vapor split R_V (-)	-	0.413	-
Heat consumption (kW)	2.67	3.21	+ 20.22

Experiment 2: Methanol – 1-propanol – 1-butanol (0.29/0.46/0.25)



Experimental data



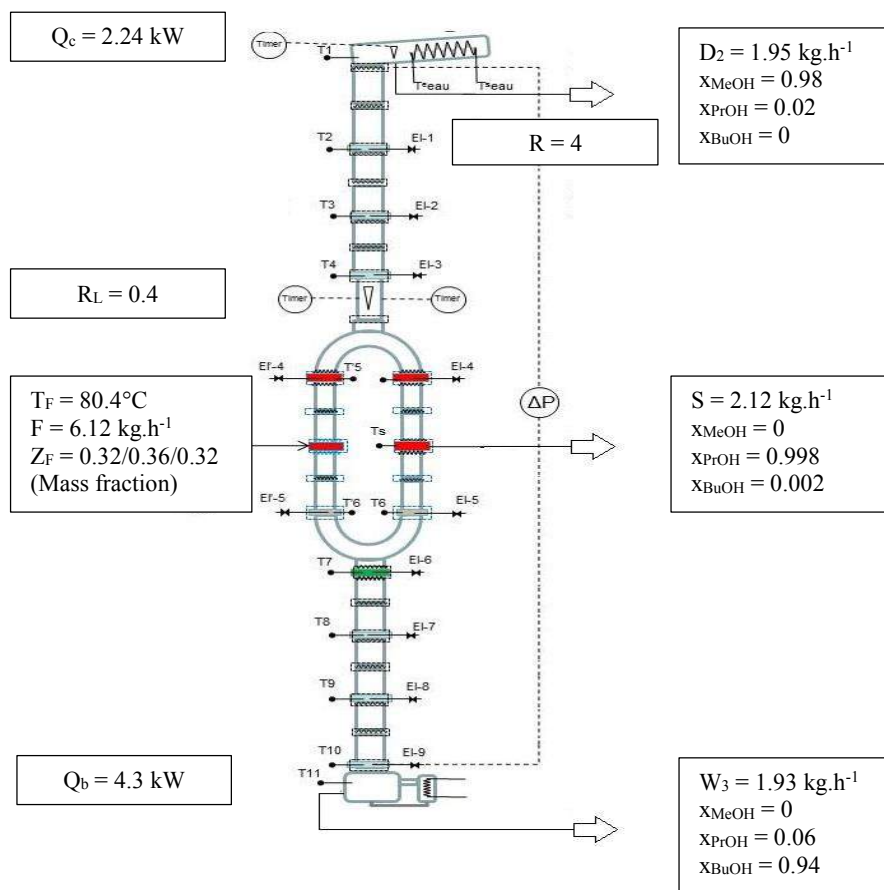
Botd: Data for simulation

Simulated data

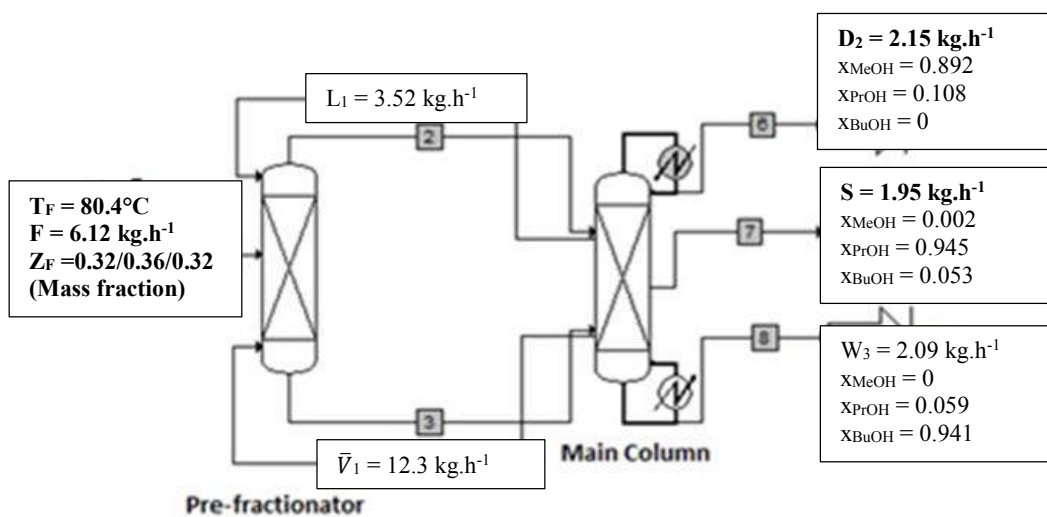
Comparison between experimental and simulated results

Parameters	Experiment Results	Simulation Results	Relative error (%)
Feed (kg/h)	5.77	5.77	0.00
Distillate (kg/h)	2.00	1.97	-1.50
Methanol (wt. %)	0.85	0.849	-0.12
1-Propanol (wt. %)	0.15	0.151	+0.67
1-Butanol (wt. %)	0	0	0.00
Side stream (kg/h)	2.17	2.19	+0.92
Methanol (wt. %)	0	0	0
1-Propanol (wt. %)	1	0.991	-0.90
1-Butanol (wt. %)	0	0.009	-
Bottom stream (kg/h)	1.7	1.61	-5.29
Methanol (wt. %)	0	0	0.00
1-Propanol (wt. %)	0.114	0.116	+1.75
1-Butanol (wt. %)	0.89	0.884	-0.23
Liquid split R_L (-)	0.5	0.5	-
Vapor split R_V (-)	-	0.44	-
Heat consumption (kW)	2.2	4	+81.81

Experiment 3: Methanol – 1-propanol – 1-butanol (0.32/0.36/0.32)



Experimental data



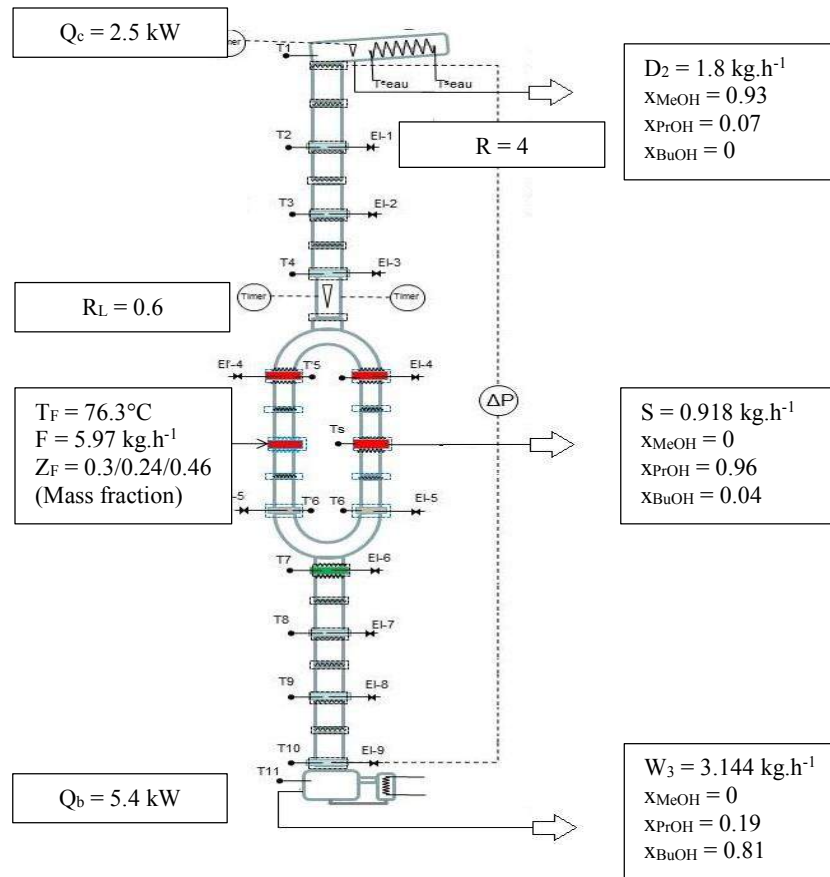
Botd: Data for simulation

Simulated data

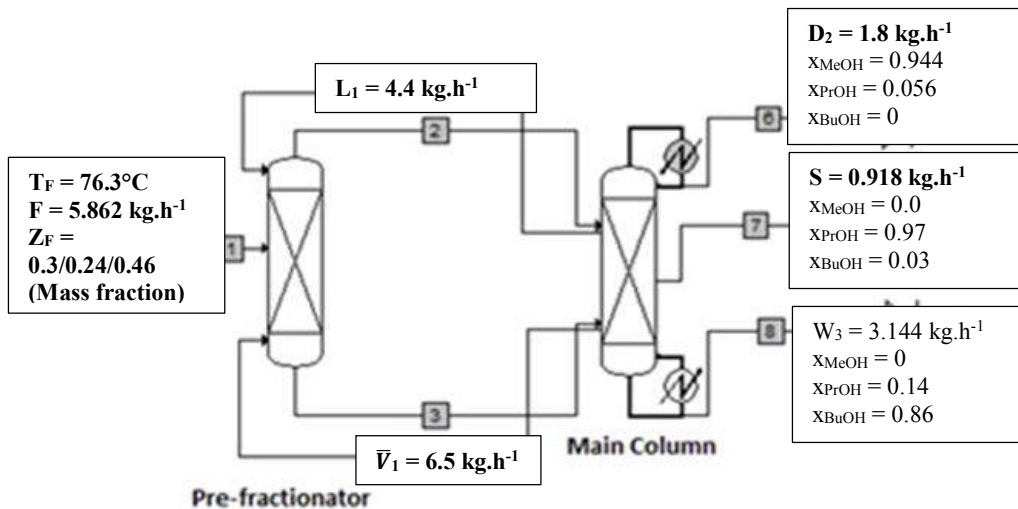
Comparison between experimental and simulated results

Parameters	Experiment Results	Simulation Results	Relative error (%)
Feed (kg/h)	6.12	6.12	0
Distillate (kg/h)	1.95	2.15	+10.25
Methanol (wt. %)	0.98	0.892	-8.98
1-Propanol (wt. %)	0.02	0.108	+440.00
1-Butanol (wt. %)	0	0	0
Side stream (kg/h)	2.12	1.95	-8.02
Methanol (wt. %)	0	0.002	-
1-Propanol (wt. %)	0.998	0.945	-5.31
1-Butanol (wt. %)	0.002	0.053	+2550.00
Bottom stream (kg/h)	1.93	2.09	+8.29
Methanol (wt. %)	0	0	0
1-Propanol (wt. %)	0.06	0.059	-1.67
1-Butanol (wt. %)	0.94	0.941	+0.11
Liquid split R_L (-)	0.4	0.4	-
Vapor split R_V (-)	-	0.516	-
Heat consumption (kW)	2.24	3.32	+ 48.21

Experiment 4: Methanol – 1-propanol – 1-butanol (0.3/0.24/0.46)



Experimental data



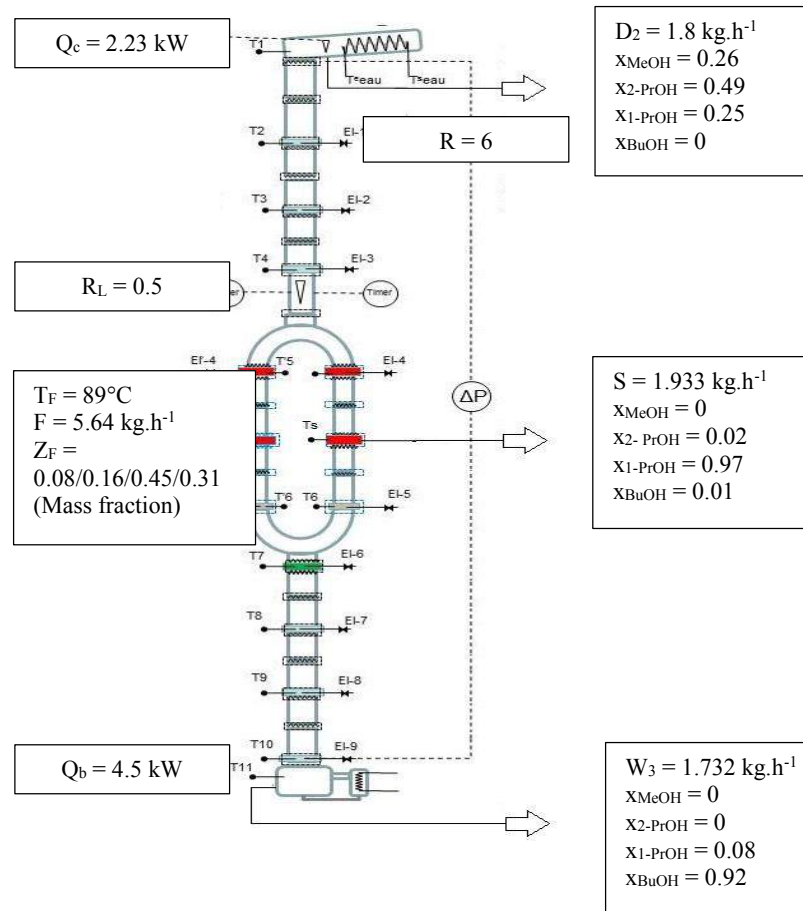
Botd: Data for simulation

Simulated data

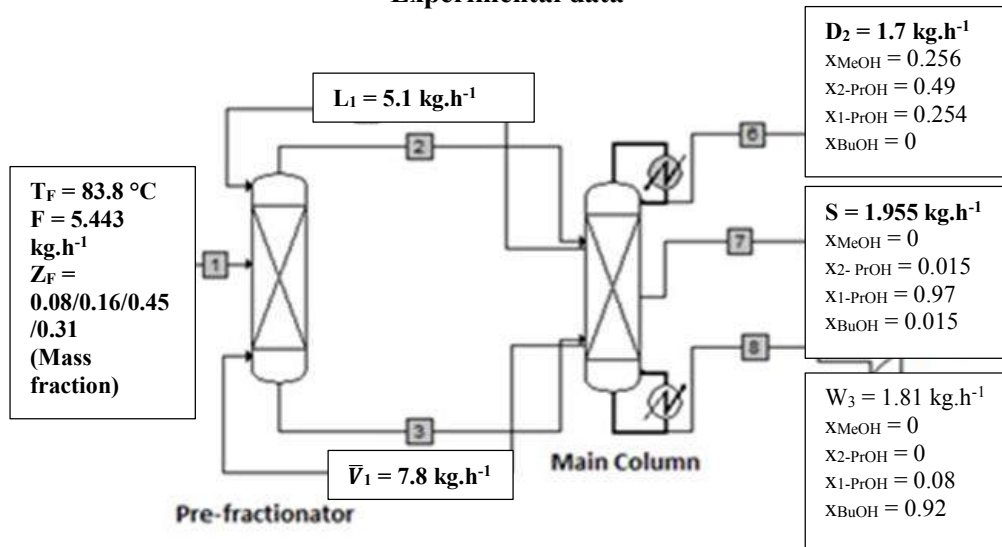
Comparison between experimental and simulated results

Parameters	Experiment Results	Simulation Results	Relative error (%)
Feed (kg/h)	5.97	5.862	-1.81
Distillate (kg/h)	1.8	1.8	0
Methanol (wt. %)	0.93	0.944	+1.51
1-Propanol (wt. %)	0.07	0.056	-20.00
1-Butanol (wt. %)	0	0	0
Side stream (kg/h)	0.918	0.918	0
Methanol (wt. %)	0	0	0
1-Propanol (wt. %)	0.96	0.97	+1.04
1-Butanol (wt. %)	0.04	0.03	-25.00
Bottom stream (kg/h)	3.144	3.144	0
Methanol (wt. %)	0	0	0
1-Propanol (wt. %)	0.19	0.14	-26.32
1-Butanol (wt. %)	0.81	0.86	+6.17
Liquid split R_L (-)	0.6	0.6	-
Vapor split R_V (-)	-	0.39	-
Heat consumption (kW)	2.5	2.79	+11.6

Experiment 5: Methanol – isopropanol – 1-propanol – 1-butanol (0.08/0.16/0.45/0.31)



Experimental data



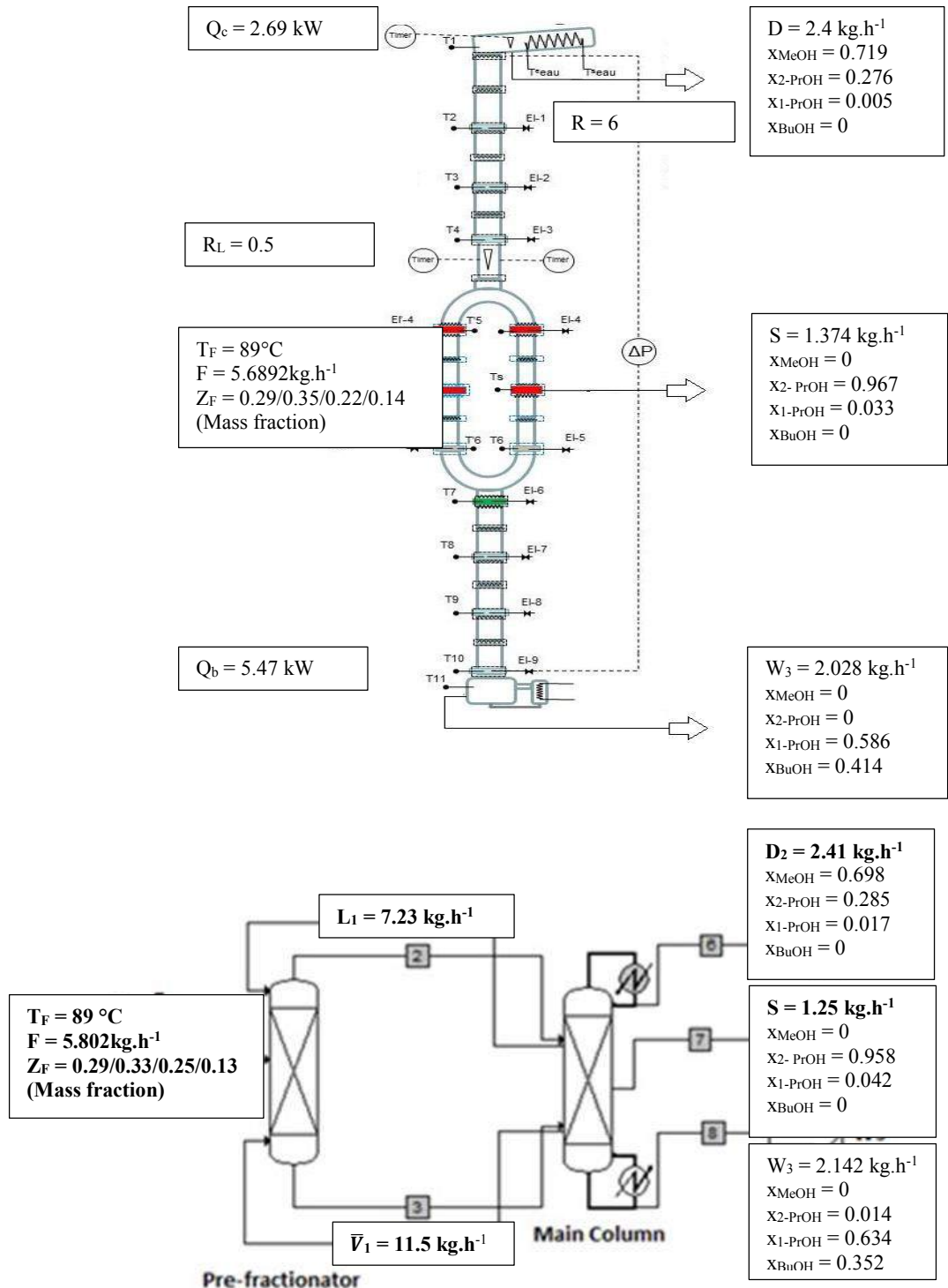
Botd: Data for simulation

Simulated data

Comparison between experimental and simulated results

Parameters	Experiment Results	Simulation Results	Relative error (%)
Feed (kg/h)	5.640	5.443	-3.49
Distillate (kg/h)	1.800	1.700	-5.55
Methanol (wt. %)	0.26	0.257	-1.15
Isopropanol (wt. %)	0.49	0.497	+1.43
1-Propanol (wt. %)	0.25	0.246	-1.60
1-Butanol (wt. %)	0.00	0.00	0.00
Side stream (kg/h)	1.933	1.933	0.00
Methanol (wt. %)	0.00	0.00	0.00
Isopropanol (wt. %)	0.02	0.015	-25.00
1-Propanol (wt. %)	0.97	0.97	0.00
1-Butanol (wt. %)	0.01	0.015	+50.00
Bottom stream (kg/h)	1.732	1.81	+4.50
Methanol (wt. %)	0.00	0.00	0.00
Isopropanol (wt. %)	0.00	0.00	0.00
1-Propanol (wt. %)	0.08	0.08	0.00
1-Butanol (wt. %)	0.92	0.92	0.00
Liquid split R_L (-)	0.5	0.5	-
Vapor split R_V (-)	-	0.46	-
Heat consumption (kW)	2.23	2.72	+21.97

Experiment 6: Methanol – isopropanol – 1-propanol – 1-butanol (0.08/0.16/0.45/0.31)



Botd: Data for simulation

Simulated data

Comparison between experimental and simulated results

Parameters	Experiment Results	Simulation Results	Relative error (%)
Feed (kg/h)	5.892	5.802	-1.53
Distillate (kg/h)	2.400	2.41	+0.42
Methanol (wt. %)	0.719	0.698	-2.92
Isopropanol (wt. %)	0.276	0.285	+3.26
1-Propanol (wt. %)	0.005	0.017	+240
1-Butanol (wt. %)	0.000	0.00	0.00
Side stream (kg/h)	1.374	1.25	-9.02
Methanol (wt. %)	0.000	0.00	0.00
Isopropanol (wt. %)	0.967	0.958	-0.93
1-Propanol (wt. %)	0.033	0.042	+27.27
1-Butanol (wt. %)	0.000	0.00	0.00
Bottom stream (kg/h)	2.028	2.142	+5.62
Methanol (wt. %)	0.000	0.00	0.00
Isopropanol (wt. %)	0.000	0.014	-
1-Propanol (wt. %)	0.586	0.634	+8.19
1-Butanol (wt. %)	0.414	0.352	-14.97
Liquid split R_L (-)	0.5	0.5	-
Vapor split R_V (-)	-	0.45	-
Heat consumption (kW)	2.69	4.62	+71

Appendix 5: Step to step to solve mass balance equation for reactive mixture

We have the reaction:

	Methanol	+	Acetic acid	↔	Methyl acetate	+	Water
IN (kgh ⁻¹)	3.696		1.730		0.000		0.459
OUT (kgh ⁻¹)	3.148		0.637		1.270		?
OUT - IN	-0.548		-1.093		1.270		
Molar mass (g/mole)	32.04		60.05		74.08		18.01
kmole of reaction	-0.017		-0.018		+ 0.017		?

Because the stoichiometric ratio of reactants and products is 1:1:1:1, mole of reaction of water that is equal mole of reaction of methyl acetate is 0.017. Therefore the mass of water due to reaction is $0.017 \times 18.01 = 0.306$. Thus total mass of water: $x = 0.306 + 0.459 = 0.765$ kgh⁻¹.

Based on assumption that water has only in the bottom product we can estimate amount of components in the products.

Parameters	Experiment	Mass (kgh⁻¹)
Distillate (kgh⁻¹)	2.125	
Methanol (% mass)	0.439	0.933
Acetic acid (% mass)	0.000	0.000
Methyl acetate (% mass)	0.561	1.192
Water (% mass)	-	
Side stream (kgh⁻¹)	1.650	
Methanol (% mass)	0.953	1.572
Acetic acid (% mass)	0.000	0.000
Methyl acetate (% mass)	0.047	0.078
Water (% mass)	-	
Bottom stream (kgh⁻¹)	2.062	
Methanol (% mass)	0.497	0.644
Acetic acid (% mass)	0.492	0.638
Methyl acetate (% mass)	0.011	0.015
Water (% mass)	-	0.765

Appendix 6: Transformation composition

This explanation is best illustrated using an example.

For example, in the 100 kg h^{-1} of the mixture, the composition of the mixture is 40% mass of methyl acetate, 30% mass of methanol, 20% mass of acetic acid, and 10% mass of water.

That means we have:

40 kg h^{-1} methyl acetate

30 kg h^{-1} methanol

20 kg h^{-1} acetic acid

10 kg h^{-1} water

Therefore, the transformation compositions of component in “dry” mixture are:

$$x_{\text{MeAc}} = \frac{m_{\text{MeAc}}}{M} = \frac{40}{40 + 30 + 20} = \frac{40}{90} = 0.444 \text{ (wt. \%)}$$

$$x_{\text{MeOH}} = \frac{m_{\text{MeOH}}}{M} = \frac{30}{40 + 30 + 20} = \frac{30}{90} = 0.333 \text{ (wt. \%)}$$

$$x_{\text{AcAc}} = \frac{m_{\text{AcAc}}}{M} = \frac{20}{40 + 30 + 20} = \frac{20}{90} = 0.223 \text{ (wt. \%)}$$

Appendix 7: Analysis by Gas Chromatography

GC condition for non-reactive mixture:

Zone temperatures:

Column: Initial: 40°C for 5 min
Ramp 1: 10°C/min to 70°C
Ramp 2: 80°C/min to 210°C
Injector: Temperature: 210°C
Split flow (ml/min): 10
Detector: 240°C

Gas flows:

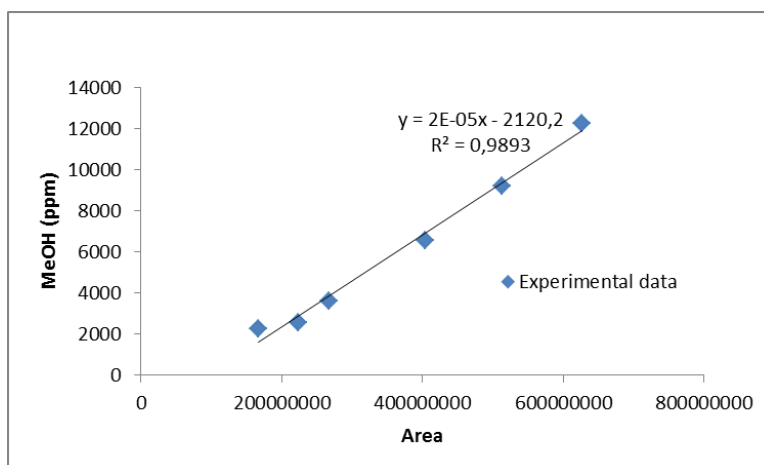
Hydrogen: 35(ml/min)
Makeup: 35 ml/min
Air: 350 (ml/min)

Injection volume: 3 (µl)

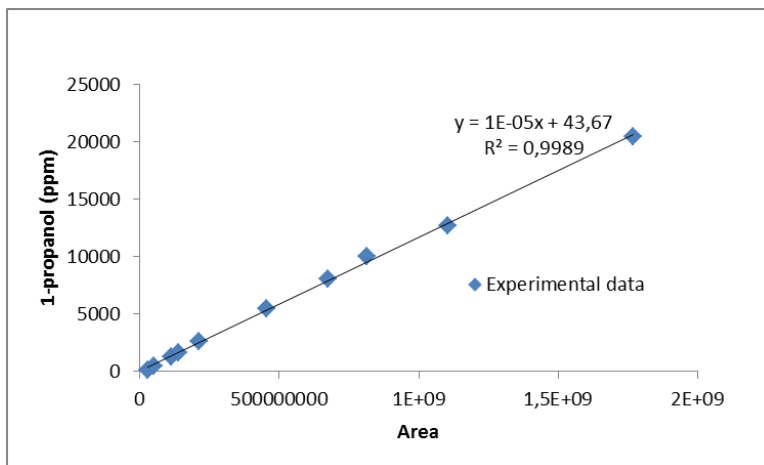
Column: WCOT FUSED SILICA 25MX0.25MM ID; COATING CP-WAX 52CB; DF = 0.2

Retention times (min):

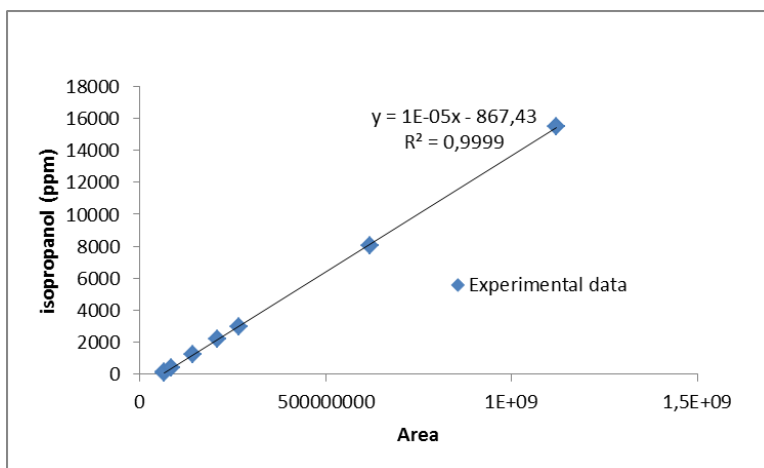
Methanol: 2.9323 min
Isopropanol: 3.332 min
1-propanol: 5.603 min
1-Butanol: 8.053 min



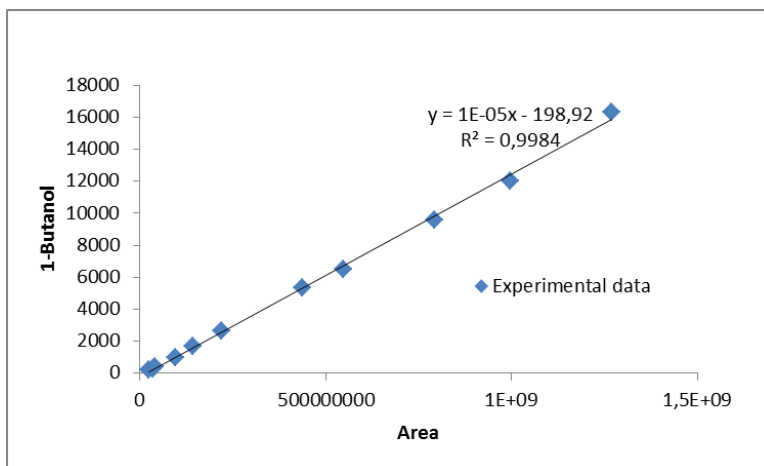
Calibration GC for Methanol



Calibration GC for 1-Propanol



Calibration GC for Isopropanol



Calibration GC for 1-Butanol

GC condition for reactive mixture:

Zone temperatures:

Column: Initial: 40°C for 5 min
Ramp 1: 15°C/min to 80°C
Ramp 2: 80°C/min to 250°C
Injector: Temperature: 250°C
Split flow (ml/min): 125
Detector: 240°C

Gas flows:

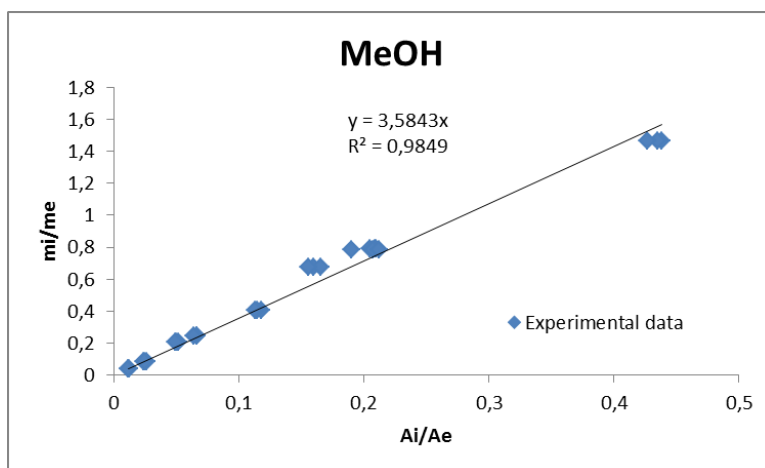
Hydrogen: 35(ml/min)
Makeup: 35 ml/min
Air: 350 (ml/min)

Injection volume: 3 (µl)

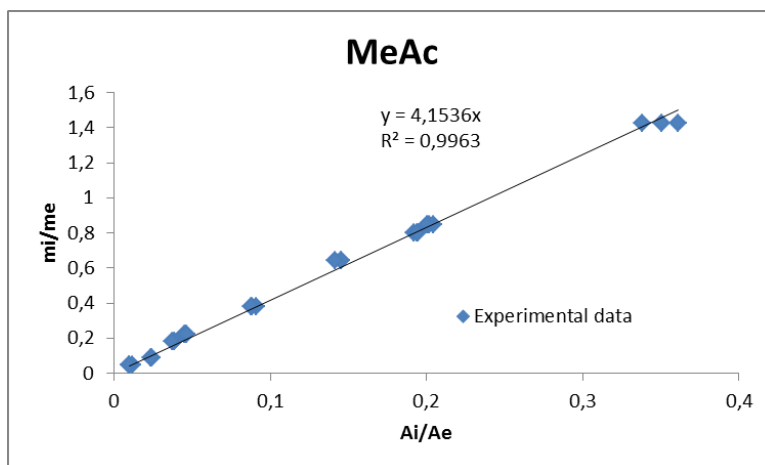
Column: WCOT FUSED SILICA 25MX0.25MM ID; COATING CP-WAX 52CB; DF = 0.2

Retention times (min):

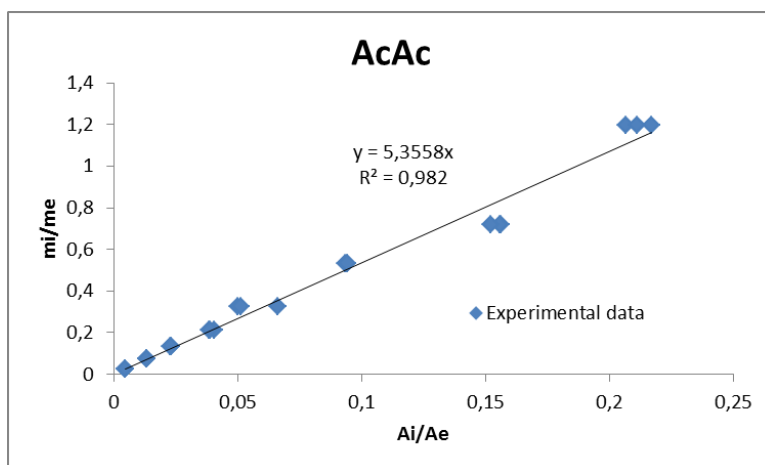
Methyl Acetate: 1.158 min
Methanol: 1.408 min
1-Butanol: 5.426 min
Acetic acid: 8.870 min



Calibration GC for Methanol



Calibration GC for Methyl Acetate



Calibration GC for Acetic acid

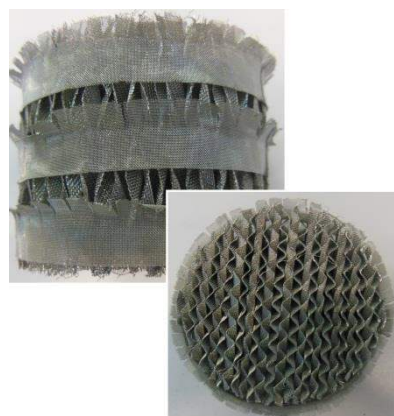
Appendix 8: Several pictures of pilot plant in our laboratory



Pilot plant



Liquid splitter



Packing



Boiler

NOMENCLATURE

A, B, C - ternary mixture (A is the most volatile component and C is the least volatile component).

A_b, A_c, A_d, A_e [-] – cross-sectional area of each section between dividing wall

C_p [$J \cdot mol^{-1} \cdot K^{-1}$] – Molar heat capacity

D [$kmol \cdot h^{-1}$] - Top product flowrate

E_a [$cal \cdot mol^{-1}$] - Activation energy

El [-] – Liquid sample position

ESI – Easy separation index

F [$kmol \cdot h^{-1}$] - feed flowrate

F^* [$kmol \cdot h^{-1}$] - The pseudo feed flowrate

F – factor [$\frac{m}{s} \cdot \sqrt{\frac{kg}{m^3}}$] - The factor is defined by Kaibel: “is as the product of the gas velocity multiplied by the square root of gas density”

H_L [$kJ \cdot mol^{-1}$] – Liquid enthalpy

H_V [$kJ \cdot mol^{-1}$] – Latent heat of vaporization

HETP [m] - Height equivalent to a theoretical plant

K [-] - Volatility of component

K_e [-] - Liquid equilibrium constant.

K_D [-] – Ratio of flowrate of top prefractionator to flowrate of bottom prefractionator

K_I [-] - Ratio of flowrate of bottom prefractionator to flowrate of top prefractionator

k_0 [$l \cdot mole^{-1} \cdot s$] – Reaction rate constant

L [$kmol \cdot h^{-1}$] - liquid flowrate in the rectifying

\bar{L} [$kmol \cdot h^{-1}$] - liquid flowrate in the stripping

$N_1, N_2, N_3, N_4, N_5, N_6$ [-] - Number of stage of each section

N_C [-] – Number of components

P [at] – Operation pressure

Q_B [kWh] – Heat duty of Reboiler

Q_D [kWh] – Heat duty of Condenser

q [-] – Quantity of the stream

R [-] - Reflux ratio

R_L [-] - Liquid split between prefractionator and main column

R_V [-] - Vapor split between pre-fractionator and main column

S [$kmol \cdot h^{-1}$] - Side product flowrate

s [-] – Reboiler ratio
SS [-] – Least square error
T [K], t [°C] – Temperature
TC – Temperature control
TAC – Total annual cost
 u_G [m. s⁻¹] – Gas velocity
v [-] – Vapor boilup
V [kmol.h⁻¹] - vapor flowrate in the rectifying
 \bar{V} [kmol.h⁻¹] - vapor flow rate in the stripping
 $X_i^f, Y_i^f, X_i^s,$ and Y_i^s - Transformed composition of feed pinch and saddle pinch points of component i
x [-] – Liquid mole or mass fraction
 x^* [-] - The pseudo composition
X [-] – Liquid transformed composition
y [-] – Vapor mole or mass fraction
Y [-] – Vapor transformed composition
z [-] - Mole or mass fraction at the feed flowrate
W [kmol.h⁻¹] - Bottom product flowrate

SUBCRIPS

1, 2, 3 – Column I, II, and III
b, c, d, e – sections are separated by dividing wall
F, f – Feed
BP – Bubble point
DP – Dew point
T – Top of the prefractionator
B – Bottom of the prefractionator
R - Rectifying section
S - Stripping section
HK – Heaviest key component
LK – Lightest key component
k – reference component
Min – Minimum

Max – Maximum

av - Average

GREEK SYMBOLS

α [-] – Relative volatility of component

β_p [-] – Preferred split

τ [-] – Recovery of the component

ξ [kmol.h⁻¹]– Conversion of the reagent

ν [-] - Stoichiometric coefficient of component

ν_T [-] – as define by Barbosa D and Michael F. Doherty (1988). $\nu_T = \sum \nu_i$

$\theta, \theta', \theta''$ [-] - Roots of Underwood equation

ρ_G [kg. m⁻³] – Gas density

REFERENCES

A

Agrawal. (1999). More operable fully thermally coupled distillation column configuration for multicomponent distillation. *Trans IChemE*, Volume 77.

Agreda, V. H., Partin, L. R. and Heise, W. H. (1990). High-purity methyl acetate via reactive distillation. *Chem.Eng.Prog*, (2), 40-46.

Amiya K. Jana. (2010). Heat integrated distillation operation. *Applied Energy*, 87, 1477-1494.

Amminudin, K. A., Smith, R., Thong, D. C., & Towler, G. P. (2001). Design and optimization of fully thermally coupled distillation columns: Part 1: Preliminary design and optimization methodology. *Chemical Engineering Research and Design*, 79(7), 701-715.

Amminudin, K. A., & Smith, R. (2001). Design and optimization of fully thermally coupled distillation columns: part 2: application of dividing wall columns in retrofit. *Chemical Engineering Research and Design*, 79(7), 716-724.

Asprion, N., Kaibel, G. (2010). Dividing wall columns: Fundamentals and recent advances. *Chemical Engineering and Processing: Process Intensification*, 49, 2, 139-146.

B

Barbel Kolbe et al. (2004). Novel distillation concepts using one-shell columns. *Chemical engineering and processing*, Issue 43, pp. 339-346.

Barbosa, D., & Doherty, M. F. (1988). Design and minimum-reflux calculations for single-feed multicomponent reactive distillation columns. *Chemical Engineering Science*, 43(7), 1523-1537.

Nomenclature and references

Barroso-Muñoz, F. O., López-Ramírez, M. D., Díaz-Muñoz, J. G., Hernández, S., Segovia-Hernández, J. G., Hernández-Escoto, H., & Torres, R. H. C. (2009). Thermodynamic analysis and hydrodynamic behavior of a reactive dividing wall distillation column. *Chemical Engineering*, *17*, 1263.

Becker, H., Godorr, S., Kreis, H., (2001). Partitioned distillation columns—why, when and how, *Chemical Engineering*, *108* (1), 68–74.

Brugma J. A. (1942). Process and device for fractional distillation of liquid mixtures, more particularly petroleum, *Patent US2295256 A*.

Buck, C., Hiller, C., & Fieg, G. (2011). Applying model predictive control to dividing wall columns. *Chemical Engineering & Technology*, *34*(5), 663-672.

Bumbac, G., Elena Pleșu, A., & Pleșu, V. (2007). Reactive distillation process analysis in a divided wall column. *Computer Aided Chemical Engineering*, *24*, 443-448.

Bumbac, G., Ene, A., Isopescu, R., & Toma, A. (2009). Process simulation of reactive distillation in dividing wall column for ETBE synthesis process. *Chemical Engineering*, *18*(4), 7.

C

C. Triantafyllou and R. Smith. (1992). The design and optimization of fully thermally coupled distillation columns. *Institution of chemical engineering*, *70*, A2, March, 118-132.

Calzon-McConville, C. J., Rosales-Zamora, M. B., Segovia-Hernandez, J. G., Hernandez, S., & Rico-Ramírez, V. (2006). Design and optimization of thermally coupled distillation schemes for the separation of multicomponent mixtures. *Industrial & engineering chemistry research*, *45*(2), 724-732.

Chu, K. T., Cadoret, L., Yu, C. C., & Ward, J. D. (2011). A new shortcut design method and economic analysis of divided wall columns. *Industrial & Engineering Chemistry Research*, *50*(15), 9221-9235.

Cheng, K., Wang, S. J., & Wong, D. S. (2013). Steady-state design of thermally coupled reactive distillation process for the synthesis of diphenyl carbonate. *Computers & Chemical Engineering*, 52, 262-271.

Cossio-Vargas, E., Hernandez, S., Segovia-Hernandez, J. G., & Cano-Rodriguez, M. I. (2011). Simulation study of the production of biodiesel using feedstock mixtures of fatty acids in complex reactive distillation columns. *Energy*, 36(11), 6289-6297.

Cho, Y., Kim, B., Kim, D., & Han, M. (2008, October). Recovery of lactic acid by reactive dividing wall column. In *Control, Automation and Systems, 2008. ICCAS 2008. International Conference on* (pp. 2596-2599). IEEE.

D

Dejanović, I., Matijašević, L., & Olujić, Ž. (2010). Dividing wall column—a breakthrough towards sustainable distilling. *Chemical Engineering and Processing: Process Intensification*, 49(6), 559-580.

Dejanovic, I., Matijašević, L., Jansen, H., & Olujić, Z. (2011). Designing a packed dividing wall column for an aromatics processing plant. *Industrial & engineering chemistry research*, 50(9), 5680-5692.

Delgado-Delgado, R., Hernández, S., Barroso-Muñoz, F. O., Segovia-Hernández, J. G., & Castro-Montoya, A. J. (2012). From simulation studies to experimental tests in a reactive dividing wall distillation column. *Chemical Engineering Research and Design*, 90(7), 855-862.

Dwivedi, D., Strandberg, J. P., Halvorsen, I. J., Preisig, H. A., & Skogestad, S. (2012). Active vapor split control for dividing-wall columns. *Industrial & Engineering Chemistry Research*, 51(46), 15176-15183.

Dwivedi, D., Strandberg, J. P., Halvorsen, I. J., & Skogestad, S. (2012). Steady state and dynamic operation of four-product dividing-wall (Kaibel) columns: experimental verification. *Industrial & Engineering Chemistry Research*, 51(48), 15696-15709.

E

Erik A. Wolff and Sigurd Skogestad. (1995). Operation of Integrated three-product (Petlyuk) Distillation columns, *Ind. Eng. Res*, 34, 6, 2094-2103.

G

Ghadrdan, M., Halvorsen, I. J., & Skogestad, S. (2011). Optimal operation of Kaibel distillation columns. *Chemical Engineering Research and Design*, 89(8), 1382-1391.

Giessler, S., Danilov, R. Y., Pisarenko, R. Y., Serafimov, L. A., Hasebe, S., & Hashimoto, I. (1999). Feasible separation modes for various reactive distillation systems. *Industrial & engineering chemistry research*, 38(10), 4060-4067.

Giessler, S., Danilov, R. Y., Pisarenko, R. Y., Serafimov, L. A., Hasebe, S., & Hashimoto, I. (2001). Systematic structure generation for reactive distillation processes. *Computers & Chemical Engineering*, 25(1), 49-60.

Gomez-Castro, F. I., Rico-Ramirez, V., Segovia-Hernandez, J. G., & Hernandez, S. (2010). Feasibility study of a thermally coupled reactive distillation process for biodiesel production. *Chemical Engineering and Processing: Process Intensification*, 49(3), 262-269.

Gómez-Castro, F. I., Rico-Ramírez, V., Segovia-Hernández, J. G., & Hernández-Castro, S. (2011). Esterification of fatty acids in a thermally coupled reactive distillation column by the two-step supercritical methanol method. *Chemical Engineering Research and Design*, 89(4), 480-490.

Gómez-Castro, F. I., Rico-Ramírez, V., Segovia-Hernández, J. G., Hernández-Castro, S., González-Alatorre, G., & El-Halwagi, M. M. (2012). Simplified methodology for the design and optimization

of thermally coupled reactive distillation systems. *Industrial & Engineering Chemistry Research*, 51(36), 11717-11730.

Guido Daniel, et al. (2006). Conceptual design of reactive dividing wall column. *ICHEME*, Issue 152.

H

Halvorsen, I. J., & Skogestad, S. (2011). Energy efficient distillation. *Journal of Natural Gas Science and Engineering*, 3(4), 571-580.

Halvorsen, I. J., & Sigurd Skogestad. (1997). Optimizing control of Petlyuk distillation: Understanding the steady-state behavior, *Computer and Chemical Engineering*, 21, Supplement, S249-S254.

Halvorsen, I. J., & Sigurd Skogestad. (1999). Optimal operation of Petlyuk distillation: steady-state behavior, *Journal of Process Control*, 9, 5, 407-424.

Halvorsen, I. J., & Skogestad, S. (2003). Minimum energy consumption in multicomponent distillation. 1. V min diagram for a two-product column. *Industrial & engineering chemistry research*, 42(3), 596-604.

Halvorsen, I. J., & Skogestad, S. (2003). Minimum energy consumption in multicomponent distillation. 2. Three-product Petlyuk arrangements. *Industrial & engineering chemistry research*, 42(3), 605-615.

Halvorsen, I. J., & Skogestad, S. (2003). Minimum energy consumption in multicomponent distillation. 3. More than three products and generalized Petlyuk arrangements. *Industrial & Engineering Chemistry Research*, 42(3), 616-629.

Hao Ling and William L. Luyben. (2009). New control structure for divided wall columns, *Ind. Eng. Chem. Res*, 48, 13, 6034-6049.

Hao Ling, Luyben, W. L. (2010). Temperature control of the BTX divided-wall column, *Industrial & Engineering Chemistry Research*, 49, 189–203.

Henry Z. Kister., 1992. Distillation design, McGraw-Hill.

Hernández, S., Sandoval-Vergara, R., Barroso-Muñoz, F. O., Murrieta-Dueñas, R., Hernández-Escoto, H., Segovia-Hernández, J. G., & Rico-Ramirez, V. (2009). Reactive dividing wall distillation columns: simulation and implementation in a pilot plant. *Chemical Engineering and Processing: Process Intensification*, 48(1), 250-258.

Huss, R. S., Chen, F., Malone, M. F., & Doherty, M. F. (2003). Reactive distillation for methyl acetate production. *Computers & chemical engineering*, 27(12), 1855-1866.

J

J Stichlmair., 1988. Ullmann's Encyclopedia of Industrial Chemistry, Wiley Online Library

K

Kaibel, B., Jansen, H., Zich, E., & Olujic, Z. (2006). Unfixed dividing wall technology for packed and tray distillation columns. *Distillation Absorption*, 152, 252e66.

Kaibel, G. and Miller, C. (2005) In WCCE 7, Glasgow, July 11 – 14.

Kaibel et al. (2006). U.S. Patent No 7909748 B2.

Kiss, A. A., & van Diggelen, R. C. (2010). Advanced Control Strategies for Dividing-Wall Columns. *Computer Aided Chemical Engineering*, 28, 511-516.

Kiss, A. A., & Rewagad, R. R. (2011). Energy efficient control of a BTX dividing-wall column. *Computers & Chemical Engineering*, 35(12), 2896-2904.

Nomenclature and references

Kiss, A.A., Hans Pragt, Cornald van Strien. (2007). Overcoming equilibrium limitations in reactive dividing wall columns, 17th European symposium on computer aided process engineering.

Kiss, A.A., J. J. Pragt. C. J. van Strien. (2010). Reactive dividing wall column: towards enhanced process integration, *Distillation Absorption*, pp. 253-258.

Kiss, A.A., Rohit R. Rewagad. (2011). Control and dynamic optimization of a BTX dividing wall column, *21st European symposium on computer aided process engineering – ESCAPE 21*.

Kiss, A.A., D.J-P.C. Suszwalak. (2012). Enhanced dimethyl ether synthesis by reactive distillation in a dividing wall column, *Procedia Engineering*, Issue 42, pp. 581-587.

Kiss, D. J.-P. C. Suszwalak. (2012). Innovative dimethyl ether synthesis in a reactive dividing wall column, *Computers and Chemical Engineering*, Issue 38, pp. 74-81.

Kiss, A. A., Flores Landaeta, S. J., & Infante Ferreira, C. A. (2012). Towards energy efficient distillation technologies—Making the right choice. *Energy*, 47(1), 531-542.

Kim, Y. H. (2002). Structural design and operation of a fully thermally coupled distillation column. *Chemical Engineering Journal*, 85(2), 289-301.

Kolbe, B., Wenzel, S. (2004). Novel distillation concepts using one-shell columns. *Chem. Eng. Process*, 43, 339–346.

M

Maria Serra, Antonio Espuria, Luis Puigjaner. (1999). Control and optimization of the divided wall column, *Chemical Engineering and Processing: Process Intensification*, 38, 4-6, 549-562.

Maria Serra, Michel Perrier, Antonio Espuna, Lluís Puigjaner. (2000). Study of the divided wall column controllability: influence of design and operation, *Computer and Chemical Engineering*, 24, 2-7, 901-907.

Massimiliano Errico et al. (2009). Energy saving and capital cost evaluation in distillation column sequences with a divided wall column, *Chemical engineering research and design*, Issue 87, 1649-1657.

Miranda-Galindo, E. Y., Segovia-Hernández, J. G., Hernandez, S., Gutiérrez-Antonio, C., & Briones-Ramírez, A. (2010). Reactive thermally coupled distillation sequences: Pareto front. *Industrial & Engineering Chemistry Research*, 50(2), 926-938.

Michael A. Schultz, Douglas G. Stewart, Jame M. Harris, Steven P. Rosenblum, Mohammed S. Shakur, and Dennis E. O'Brien. (2002). Reduce costs with dividing wall columns, *Reactions and separations*, 64-71.

Michael A. Schultz, O'Brien, D. E., Hoehn, R. K., Luebke, C. P., & Stewart, D. G. (2006). Innovative flowschemes using dividing wall columns. *Computer Aided Chemical Engineering*, 21, 695-700.

M. Serra, M. Perrier, A. Espuria, L. Puigjaner. (2001). Analysis of different control possibilities for the divided wall column: feedback diagonal and dynamic matrix control, *Computer and Chemical Engineering*, 25, 4-6, 859-866.

M.I. Abdul Mutalib, R. Smith. (1998a). Operation and Control of Dividing Wall Distillation Columns: Part 1: Degrees of Freedom and Dynamic Simulation, *Trans. IChemE*, 76, Part A, 308 – 318.

M.I. Abdul Mutalib, A.O. Zeglam, R. Smith. (1998b). Operation and Control of Dividing Wall Distillation Columns: Part 2: Simulation and Pilot Plant Studies Using Temperature Control, *Trans. IChemE*, 76, Part A, 319 – 334.

Mueller, I., Pech, C., Bhatia, D., & Kenig, E. Y. (2007). Rate-based analysis of reactive distillation sequences with different degrees of integration. *Chemical Engineering Science*, 62(24), 7327-7335.

N

Niggemann, G., Hiller, C., & Fieg, G. (2010). Experimental and theoretical studies of a dividing-wall column used for the recovery of high-purity products. *Industrial & engineering chemistry research*, 49(14), 6566-6577.

O

Olga A. Flores et al. (2003). Thermodynamic Analysis of Thermally Coupled Distillation Sequences, *Ind. Eng. Chem. Res*, Issue 42, 5940-5945.

Olujić, Ž., Jödecke, M., Shilkin, A., Schuch, G., & Kaibel, B. (2009). Equipment improvement trends in distillation. *Chemical Engineering and Processing: Process Intensification*, 48(6), 1089-1104.

P

Parkinson, G. (2005). Distillation: New wrinkles for an age-old technology. *Chemical Engineering Progress*, 101(7), 10-12.

Parkinson, G. (2007). Dividing-wall columns find greater appeal, *Chem. Eng. Process*, 8–11.

Premkumar, R., & Rangaiah, G. P. (2009). Retrofitting conventional column systems to dividing-wall columns, *Chemical Engineering Research and Design*, 87(1), 47-60.

R

Ramírez-Corona, N., Jiménez-Gutiérrez, A., Castro-Agüero, A., & Rico-Ramírez, V. (2010). Optimum design of Petlyuk and divided-wall distillation systems using a shortcut model. *Chemical Engineering Research and Design*, 88(10), 1405-1418.

S

Nomenclature and references

San-Jang Wang and David S.H. Wong. (2007). Controllability and energy efficiency of a high-purity divided wall column, *Chemical Engineering Science*, 62, 4, 1010-1025.

Sander, S., Flisch, C., Geissler, E., Schoenmakers, H., Ryll, O., & Hasse, H. (2007). Methyl acetate hydrolysis in a reactive divided wall column. *Chemical Engineering Research and Design*, 85(1), 149-154.

Slade, B., Stober, B., & Simpson, D. (2006). Dividing wall column revamp optimizes mixed xylenes production. In *ICHEME Symp Ser* (Vol. 152).

Smith, H. A. (1939). Kinetics of the catalyzed esterification of normal aliphatic acids in methyl alcohol. *Journal of the American Chemical Society*, 61(2), 254-260.

Sotudeh, N., & Shahraki, B.H. (2007). A method for the design of divided wall columns. *Chemical Engineering & Technology*, 30(9), 1284-1291.

Sotudeh, N., & Shahraki, B. H. (2008). Extension of a method for the design of divided wall columns. *Chemical engineering & technology*, 31(1), 83-86.

Strandberg, J., & Skogestad, S. (2006, April). Stabilizing operation of a 4-product integrated Kaibel column. In *Institution of Chemical Engineers Symposium Series* (Vol. 152, p. 638). Institution of Chemical Engineers; 1999.

Song, W., Venimadhavan, G., Manning, J. M., Malone, M. F., & Doherty, M. F. (1998). Measurement of residue curve maps and heterogeneous kinetics in methyl acetate synthesis. *Industrial & engineering chemistry research*, 37(5), 1917-1928.

Sun, L., & Bi, X. (2014). Shortcut Method for the Design of Reactive Dividing Wall Column. *Industrial & Engineering Chemistry Research*, 53(6), 2340-2347.

Suphanit, B., A. Bischert, P. Narataruksa. (2007). Exergy loss analysis of heat transfer across the wall of the dividing wall distillation column, *Energy*, 32, 2121-2134.

T

Nomenclature and references

Tedder, D. W., & Rudd, D. F. (1978). Parametric studies in industrial distillation: Part I. Design comparisons. *AIChE Journal*, 24(2), 303-315.

They, R., Meyer, X. M., Joulia, X., & Meyer, M. (2005). Preliminary design of reactive distillation columns. *Chemical Engineering Research and Design*, 83(4), 379-400.

Till Adrian, Hartmut Schoenmakers, Marco Boll. (2004). Model predictive control of integrated unit operations: Control of a divided wall column, *Chemical Engineering and Processing: Process Intensification*, 43, 3, 347-355.

V

Van Dongen, D. B., & Doherty, M. F. (1985). Design and synthesis of homogeneous azeotropic distillations. 1. Problem formulation for a single column. *Industrial & engineering chemistry fundamentals*, 24(4), 454-463.

Y

Yildirim, Ö., Kiss, A. A., & Kenig, E. Y. (2011). Dividing wall columns in chemical process industry: A review on current activities. *Separation and Purification Technology*, 80(3), 403-417.

W

Wright, R.O, 1946, Fractionation Apparatus, US patent No. 2471134, 1949.